BRANCHED COVERS AND BRAIDED EMBEDDINGS

A Dissertation
Presented to
The Academic Faculty

By

Sudipta Kolay

In Partial Fulfillment
of the Requirements for the Degree
Doctor of Philosophy in the
School of Mathematics

Georgia Institute of Technology

August 2021

BRANCHED COVERS AND BRAIDED EMBEDDINGS

Approved by:

Dr. John Etnyre, Advisor
School of Mathematics
Georgia Institute of Technology

Dr. Igor Belegradek
School of Mathematics
Georgia Institute of Technology

Dr. David Gay
Department of Mathematics
University of Georgia

Dr. Jennifer Hom
School of Mathematics
Georgia Institute of Technology

Dr. Dan Margalit
School of Mathematics
Georgia Institute of Technology

Date Approved: May 20, 2021

ACKNOWLEDGEMENTS

I would like to thank my advisor John Etnyre for his guidance, support and patience during my time as a graduate student. I would like to also thank the rest of my committee, Igor Belegradek, David Gay, Jen Hom and Dan Margalit for feedback and helpful discussions.

I am grateful to Jamie Conway for his help and feedback during my first few years at Georgia Tech. I am thankful for the friendship with various other fellow graduate students, especially Marcel Celaya, Surena Hozoori, Andrew McCullough, Hyunki Min, Shane Scott, Justin Lanier, Eric Sabo, Hagop Tossounian, and Chi Ho Yuen.

Finally, I would like to thank my parents for all their support.

TABLE OF CONTENTS

LIST OF FIGURES

SUMMARY

We study braided embeddings, which is a natural generalization of closed braids in three dimensions. Braided embeddings give us an explicit way to construct lots of higher dimensional embeddings; and may turn out to be as instrumental in understanding higher dimensional embeddings as closed braids have been in understanding three and four dimensional topology. We study two natural questions related to braided embeddings, the isotopy and lifting problem.

The isotopy problem is the exact analogue of a classical theorem of Alexander, which lets us study knots and links in three dimensions using the theory of braids. This theorem was generalized in ambient dimension four by Viro and Kamada, and we extend this result in ambient dimension five in the piecewise linear category.

The lifting problem can be thought of as a generalization of the classical Borsuk-Ulam theorem, where we look at the problem of lifting general branched covers instead of two fold covers. In fact, Hansen and Petersen studied this problem for honest branched covers. In this thesis, we develop general criterion to extend braided embeddings over a branch locus; and use it to systematically study branched covers over low dimensional spheres. In fact, we were able to affirmatively answer an open question of lifting honest covers over orientable surfaces using the theory of lifting branched covers.

Finally, we briefly discuss on interactions of braided embeddings and contact geometry, following the work of Etnyre and Furukawa, and show non-existence of certain branched covers.

CHAPTER 1

INTRODUCTION TO BRAIDING

1.1 Closed Braids

A *braid*[1] is a collection of strands in three space going from left to right which are allowed to pass under or over each other.

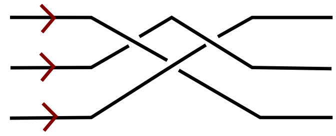

Figure 1.1: A braid

Closing up the ends of a braid gives us a link (as illustrated), which we call a closed braid.

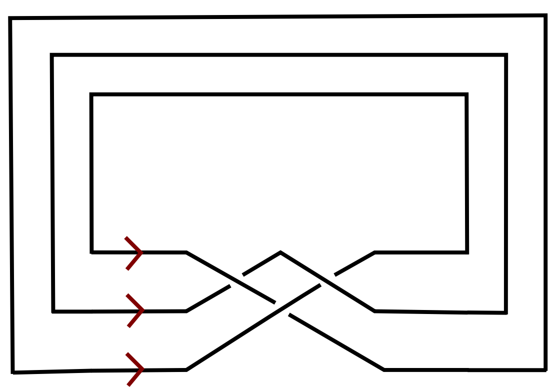

Figure 1.2: Closure of a braid

One might wonder if these closed braids form a proper subset of all links in $\mathbb{R}^3$, or is it always possible to isotope any link to be a closed braid. Remarkably the

[1]We will give a more formal definition in Chapter 3.

latter turns out to be true, by a classical theorem in knot theory due to Alexander. This result (and Markov's theorem) gives us a way of studying knot theory using braids, essentially reducing geometric data to combinatorial (or algebraic) data of braids. This perspective has been useful in the study of knot theory, for instance, the Jones polynomial [42] is a very useful knot invariant originally defined using braids.

The purpose of this thesis is to study higher dimensional braids, with the hope that they will be similarly useful in the study of higher dimensional knots. In this chapter, we will discuss with two examples of how to braid a knot in three space, and a torus in four space.

1.2 An example of braiding in dimension three

A knot in three space is a piecewise linear (or smooth) embedding of S^1 in $\mathbb{R}^3$. To aid in visualization, traditionally we draw project in on the plane, and at each crossing we rememebr the over or under crossing information, and we call this a knot diagram, see for example Figure 1.3. Sometimes we consider oriented knots, by which we mean a choice of direction along which to traverse the knot, and we denote the orientation by an arrow on the knot diagram. We denote the origin in the plane by the green dot in Figure 1.3.

We would like to illustrate a classical theorem of Alexander [3], stating that every knot in three space is isotopic to a closed braid, by showing how to carry out this braiding process in the example of Figure 1.3. Recall that for a closed braid all the strands must go in the same direction without turning back. This turns out to be equivalent to requiring that all the simplices are counterclockwise, when seen from the origin of the knot diagram. In the example of Figure 1.3, there are five edges, exactly three of them are counterclockwise (the ones with the arrows on them) and the other two are clockwise.

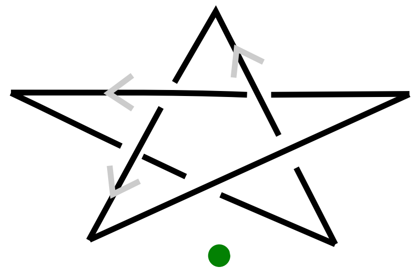

Figure 1.3: A knot diagram in the plane, where the green dot represents the origin.

We note that for the two clockwise edges, all the crossings are of the same type, i.e. all crossings are overcrossings for one of the clockwise edges, and all crossings are undercrossings for the other clockwise edge. Given this information, we can find an embedded triangle in three space, only meeting the knot in a single clockwise edge, and going over (or under) the rest of the knot diagram, so that its projection in the knot diagram contains the origin. We can then push a clockwise edge across this triangle and we see that the clockwise edge is replaced by two other edges, which turns out to be counterclockwise. In Figure 1.4, this is done in a few steps (some intermediate steps show the triangle we are picking), first we select the clockwise edge with only overcrossings, find a triangle going over the rest of the picture, and use this triangle to isotope the clockwise edge to two other edges. We then repeat the process with the clockwise edge with only undercrossings, this time choosing a triangle which goes under the rest of the knot diagram.

The final step shows a planar isotopy so that the resulting knot looks like a closed braid, and we elaborate this step in Figure 1.5.

We have seen so far is doing this triangle move replaces a clockwise edge with two counterclockwise edges as long as the triangle contains the origin. This is true more generally, and we will defer the proof to a later chapter (see Lemma 5.3.2), where we carry out a similar braiding process in slightly higher ambient dimen-

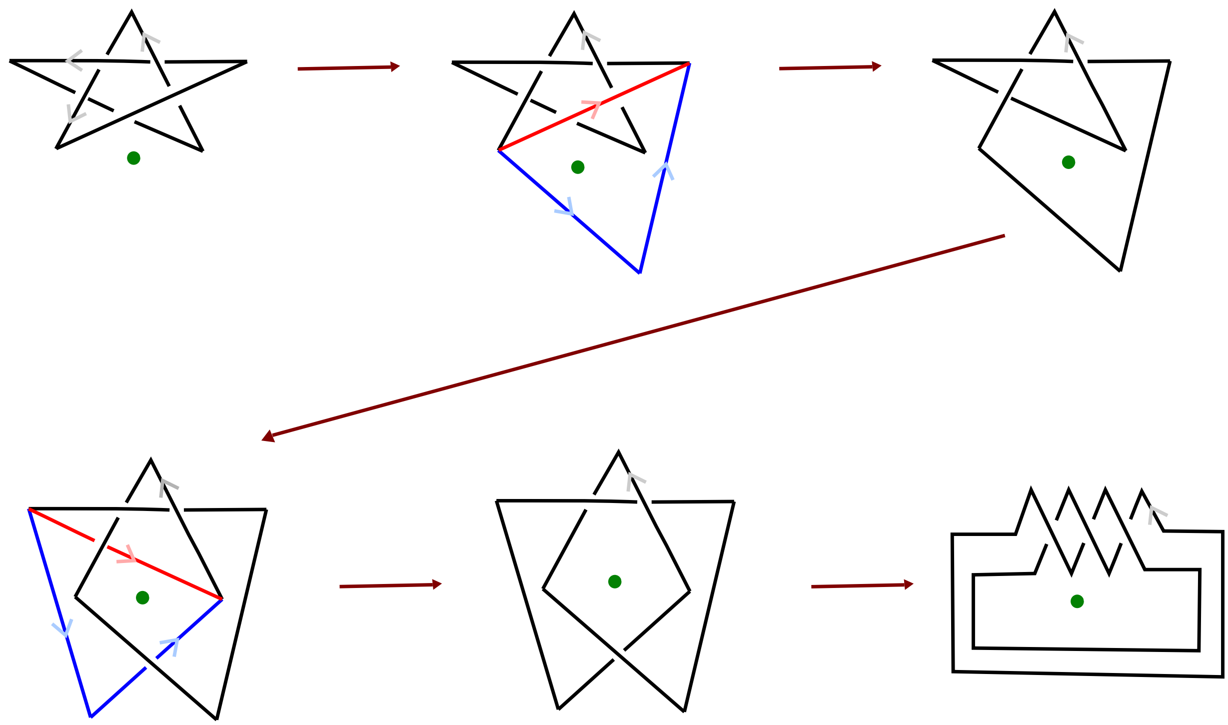

Figure 1.4: An example illustrating how to isotope a knot to a closed braid.

sion.

We would also like to point out that this process is illustrative of a method which isotopes a given knot into a closed braid, and does not tell anything about the minimal number of triangle moves required or what the minimal number of strands is required to express the given knot as a closed braid. The reader may note that by a global translation, we may bring the origin to the center of the knot diagram as shown in Figure 1.6, and then all the simplices are counterclockwise.

1.3 Braiding the standard unknotted torus

As a warm-up to a more general general braiding process, in this section we will describe, by pictures, a process to braid the standard unknotted torus. Each picture in this section will consist of several sub-figures, which are different projec-

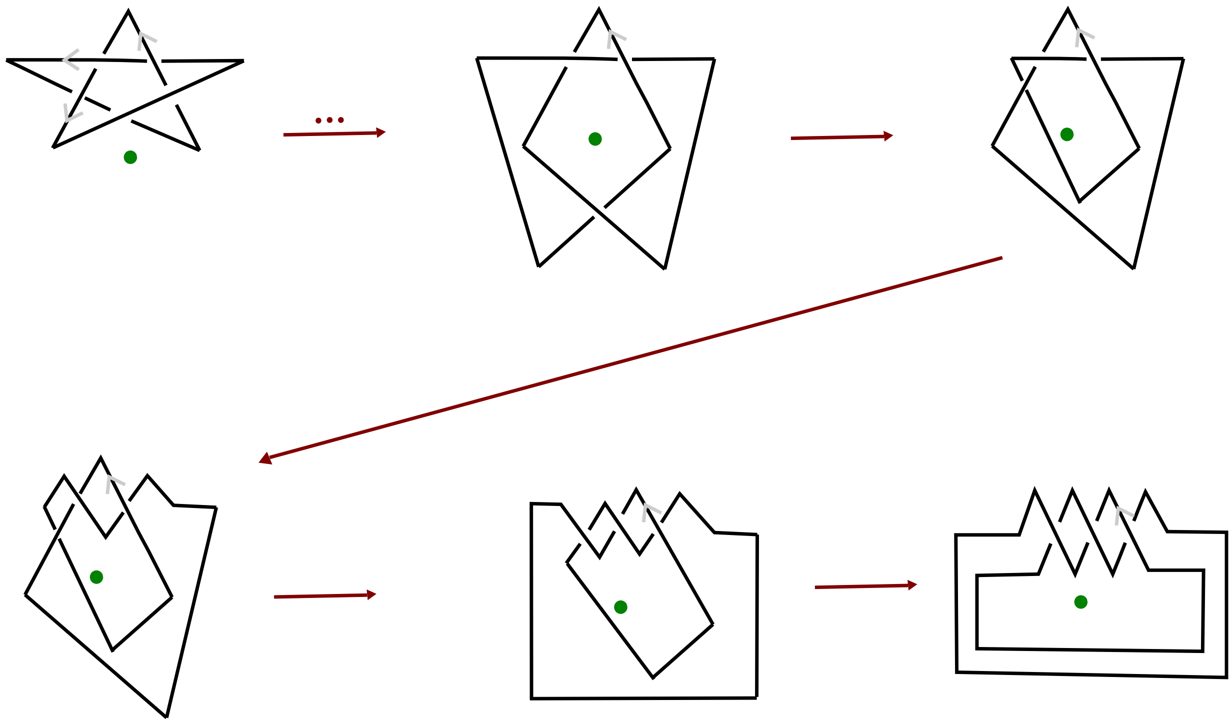

Figure 1.5: An example illustrating how to isotope a knot with only cunterclockwise edges to a closed braid.

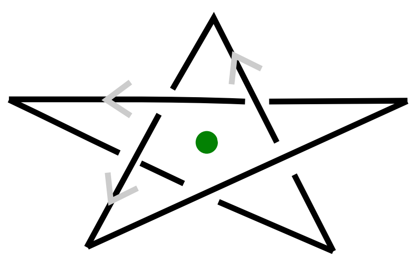

Figure 1.6: Translate of knot diagram in Figure 1.3, so that all the edges are counterclockwise.

tions of the same object in three space. An interested reader may find an interactive demonstration at `people.math.gatech.edu/ skolay3/braidtorus.html`, and the Mathematica code to generate these images in the appendix.

We will begin with an piecewise linear embedded torus in three space, with a cell structure outlined, as shown in Figure 1.7. We explain below how the cells are colored. The black dot represents the origin, and we will determine if a cell of the torus is positive (generalization of counterclockwise) or negative (generalization of clockwise), and color it yellow (respectively blue). We will use the following working definition of positive and negative cells: if we look at a ray starting at the origin, if it intersects a cell on the inside (respectively outside), then the cell is called positive (respectively negative).

Note that in order to talk about outside and inside of the torus we need to choose an orientation on it, just like we had to pick an orientation on the knot for the example of braiding we saw in dimension three. Also, just like in that example in dimension three, in the braiding process of the torus, all the cells will be either positive or negative (the degenerate cases can be avoided).

In Figure 1.7, we see the four cells nearest to the origin are negative, while the remaining twelve cells are positive. We would like to do the equivalent of the triangle move we did in Section 1.2. There is a nice generalization of this move in all dimensions, called *cellular move* (see [RS]), where we find an embedded n-cell Δ intersecting a submanifold in a $(n-1)$-ball B in $\partial\Delta$, and we may use the n-cell to isotope B with its complementary $(n-1)$-ball $\partial\Delta \setminus \mathring{B}$.

For our example, the negative region is an annulus comprising four cells, and we cannot use a single cellular move to make the all the cells positive. To begin with, we would like to isotope one of the four negative cells across the origin. An easy way to visualize this is to translate the entire torus so that the origin passes through one of the negative cells. The result of this operation is shown in Figure 1.8. We note that only one previously negative cell became positive, the cell through which the origin passes. The rest of the cells have the same orientation as before.

Note that after doing the translation, the negative region is a disc comprising three 2-cells. We can now use a single cellular move to push the negative region

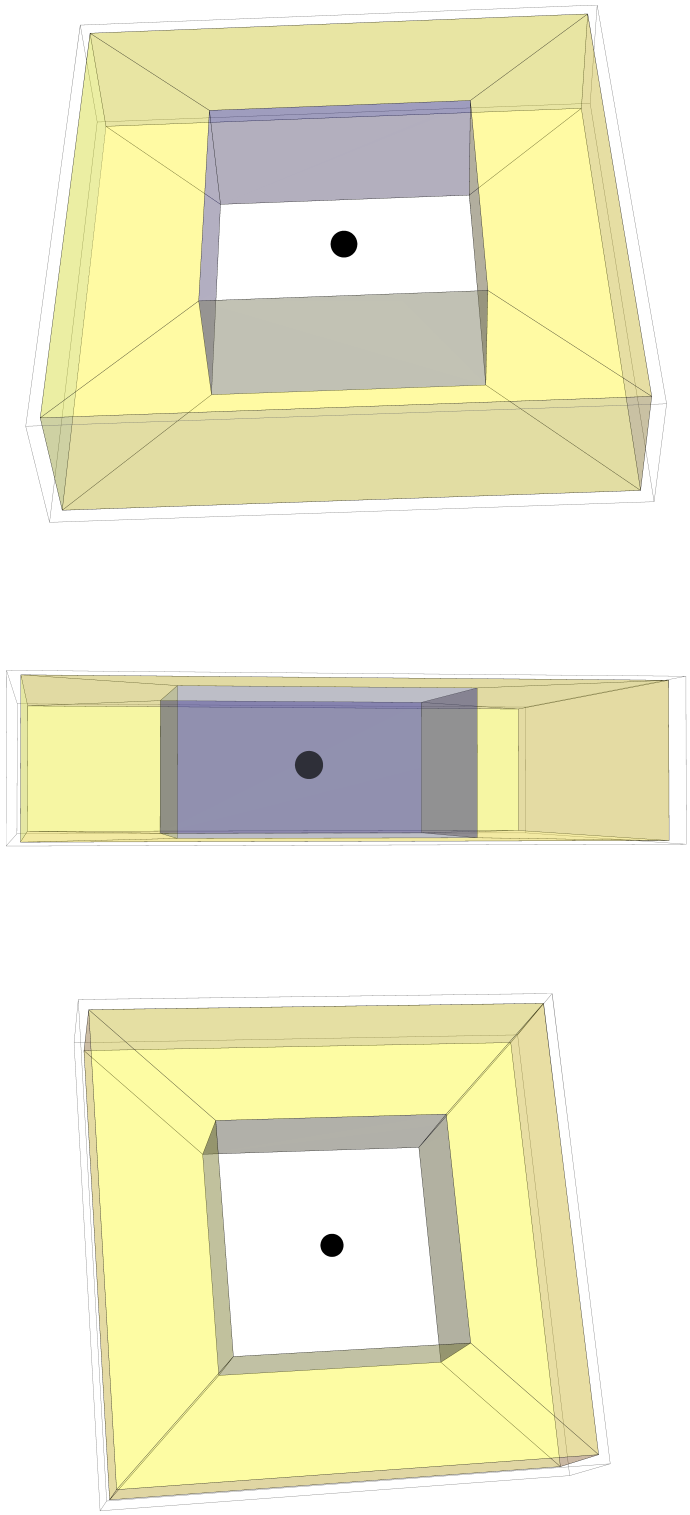

Figure 1.7: The Standard Torus in $\mathbb{R}^3$.

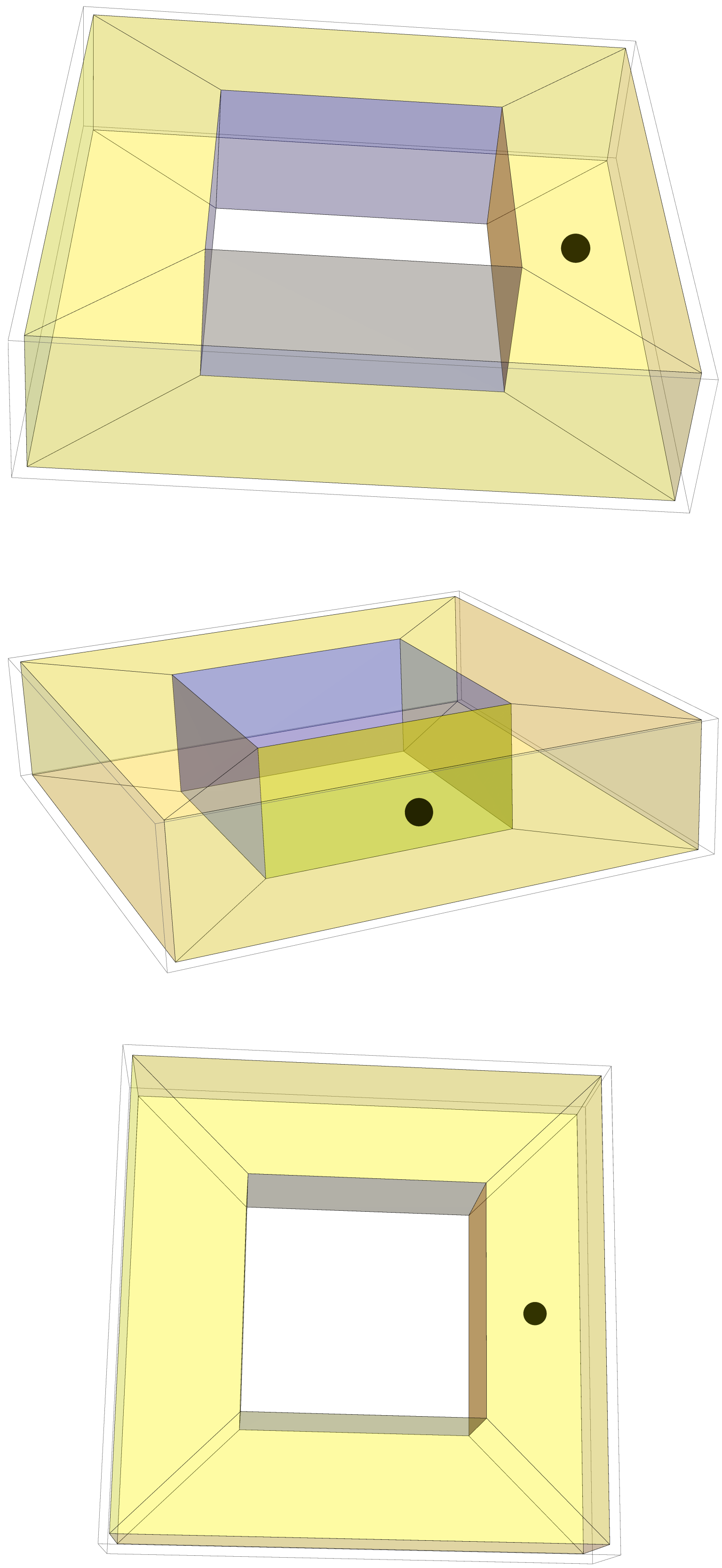

Figure 1.8: Translate the origin.

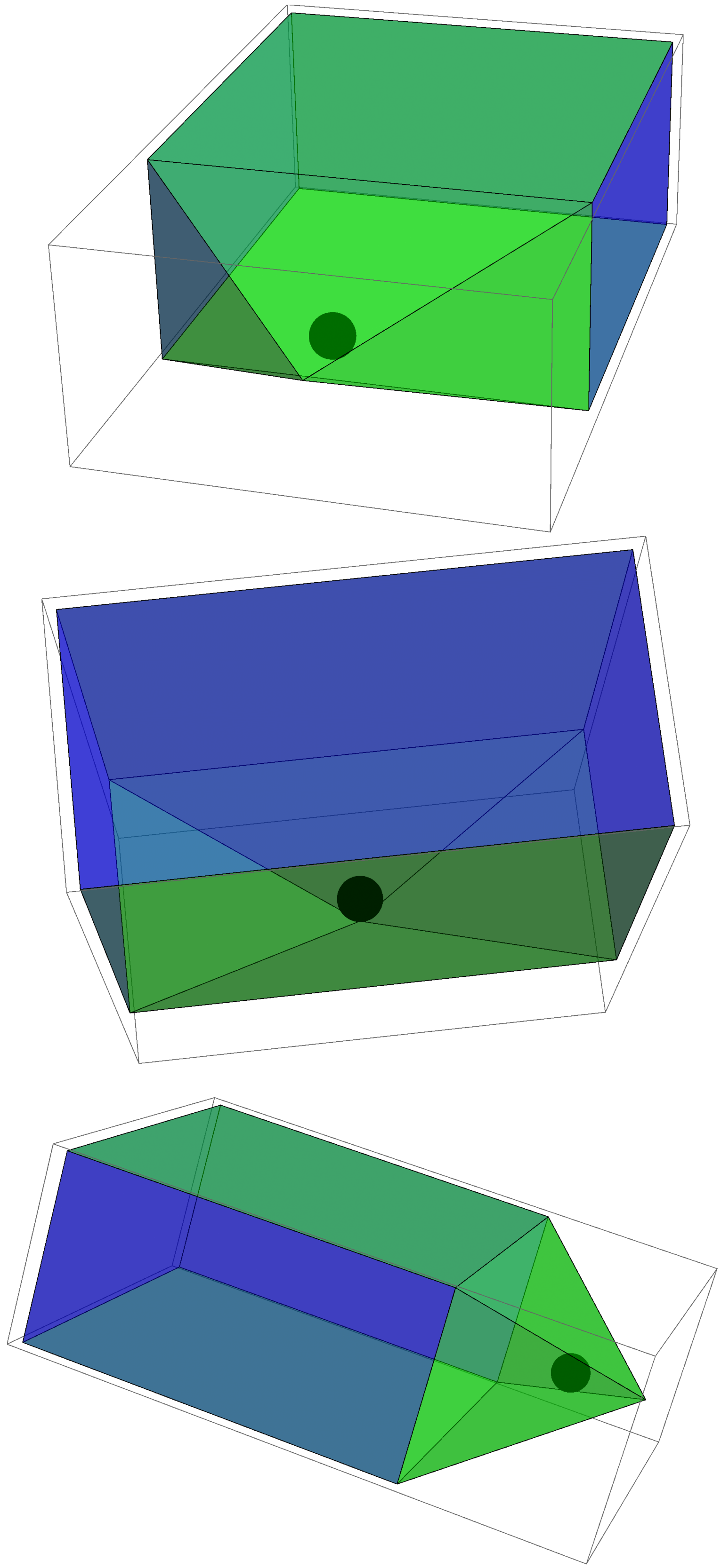

Figure 1.9: The cell along which we will push negative region (in blue) accross to make it positive (in green).

over the origin. To do this we will simply choose a point near the origin inside the torus, and cone the negative region over this point, so as to obtain a 3-ball which contains the origin in its interior. This is illustrated in Figure 1.9.

We observe that this 3-ball intersects the torus in places other than the negative cells. Here is where we will use the fourth dimension. We may choose the fourth coordinate of the cone point to be so large so that the intersection of this 3-ball with the torus is precisely the three negative cells. After performing the cellular move, the three blue cells are replaced by new positive cells, which are shown in green in Figure 1.10, so that it is easy to distinguish with the cells that remained unchanged. The reader will note that any ray starting from the origin hits the torus in at most two points. In fact, with the exception of four such rays, every ray hits the torus on the inside at exactly two points. The four exceptional rays come hit the torus at the four vertices of the yellow cell, which became positive from positive after translation. These four points corresponds to branched points of a branched covering[2] obtained by radial projection in the unit sphere. Any braided embedding of the torus must necessarily have such branch points, as the torus cannot be an honest cover over the two sphere.

[2]We will define coverings and branched coverings in Chapters 2.

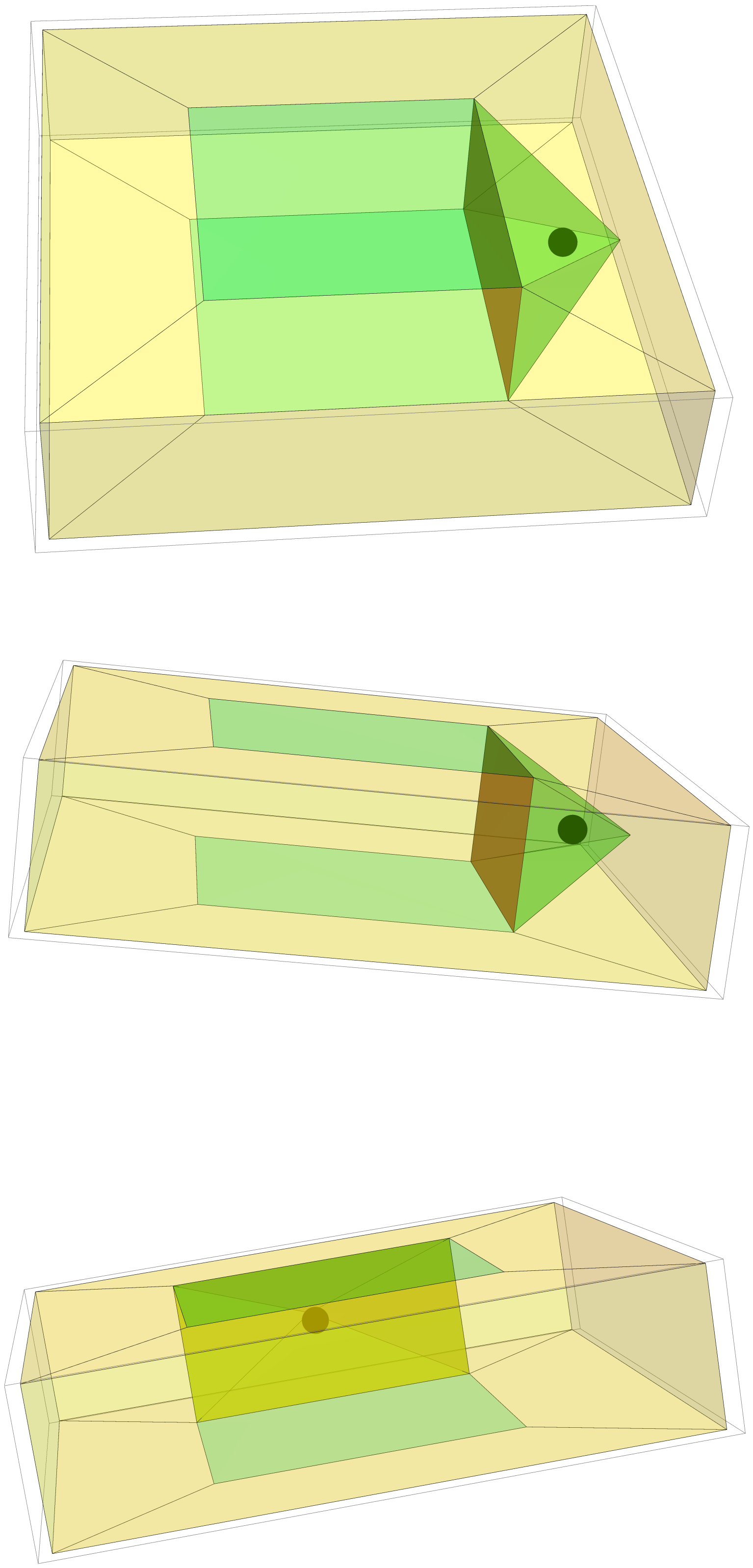

Figure 1.10: Projection of braided torus in $\mathbb{R}^3$.

1.4 Outline of strategy for a more general braiding result

Now that we have discussed examples how to braid a knot in three space, and braid an unknotted torus in four space, let us discuss the points we have to address in order to prove a general braiding result for knotted surfaces in four space.

1. Generalize the notions of positive and negative cells in higher dimensions, when we may not be able to visualize clockwise/ counterclockwise (like we did in Section 1.2) or inside and outside of a cell (like we did in Section 1.3).

2. Show that being a closed braid is equivalent to all cells being positive.

3. We have to address the issue that in general, a negative cell will have crossings in the projection. In our example in Section 1.2 all the crossings on a negative cell were of the same type (i.e. all overcrossings or all undercrossings), and in our discussion in Section 1.3, we did not have any crossings at all.

   In general, we should expect a cell to have both over and undercrossings, and possibly higher order crossings (like triple points, quadruple points etc), depending on the (co)-dimension. The strategy will be to break up negative cells into smaller pieces where there is only one type of crossings, and deal with these crossings individually.

We will discuss how to solve these issues in the Chapter 5.

CHAPTER 2

COVERINGS AND BRANCHED COVERINGS

In this chapter we will discuss covering and branched covering maps, and their monodromies. While we will refer the reader to standard texts in algebraic topology (say for example [33] and [61]) for relations with the fundamental groups and Galois correspondence of covering maps, we will focus on monodromy maps of (branched) coverings and discuss some examples.

2.1 Definition of a covering map

Definition 2.1.1. We say that a continuous map $p : X \to Y$ is a covering map if for any $y \in Y$ has an open neighbourhood U which is evenly covered by p, i.e. $p^{-1}(U)$ is a possibly disconnected open set in X, and p maps each connected component of $p^{-1}(U)$ homeomorphically onto U.

We can also define it more succinctly using the language of fiber bundles.

Definition 2.1.2. A covering map is a fiber bundle where the fiber is discrete.

Example 2.1.3. The exponential map $\exp : \mathbb{R} \to S^1$ is a covering map, where we think of $\mathbb{R}$ and S^1 as the imaginary axis and the unit circle in the complex plane.

Alternately, one can think of this as the quotient map $\mathbb{R} \to \mathbb{R}/\mathbb{Z}$, and this relates to the fact that the fundamental group of the circle is isomorphic to $\mathbb{Z}$, the integers.

Example 2.1.4. For any integer $n \neq 0$, the n-th power map $p_n : S^1 \to S^1$ defined by

$$z \mapsto z^n$$

is a covering map, where we think of S^1 as the unit circle in the complex plane.

Example 2.1.5. For any $n \geq q$, the quotient map $q_k : S^k \to \mathbb{RP}^k$ obtained by quotienting out by the antipodal action is a two fold covering map.

For the purposes of this chapter we will assume all our topological spaces are connected, locally path connected and semi-locally simply connected (these spaces have universal covers). In the rest of the thesis, we will assume all our spaces are manifolds, so this hypothesis will be satisfied.

2.2 Basic propositions about covering maps

It is not hard to check that products of evenly covered neighbourhoods are evenly covered; and hence it follows that:

Proposition 2.2.1. *Products of covering maps are covering maps.*

It follows from the above proposition and Examples 2.1.3 and 2.1.4 that the following are also covering maps.

Example 2.2.2. The Cartesian product of exponential map $exp^d : \mathbb{R}^d \to \mathbb{T}^d$ is a covering map to the d-torus, and we can also think of this map as the quotient map $\mathbb{R}^d \to \mathbb{R}^d/\mathbb{Z}^d$.

Example 2.2.3. For any sequence of non-zero integers $n_1, ..., n_d$; the Cartesian product

$$p_{n_1} \times ... \times p_{n_d} : \mathbb{T}^d \to \mathbb{T}^d$$

is a covering map of the d-torus over itself.

Of course we may combine the above two examples and get the following covering map

Example 2.2.4. For any sequence of non-zero integers $n_1, ..., n_d$; the Cartesian product

$$p_{n_1} \times ... \times p_{n_d} \times \exp^e : \mathbb{T}^d \times \mathbb{R}^e \to \mathbb{T}^{d+e}$$

is a covering map over the $(d+e)$-torus.

In fact, the two above examples completely characterize connected covering spaces over a torus.

Proposition 2.2.5. *Any covering map $p : X \to \mathbb{T}^d$, with X connected, is of the form in Example 2.2.4. Moreover if p is finite sheeted, then it is of the form of Example 2.2.3.*

Proof. We note that $p_*(\pi_1 X)$ is a subgroup of $\pi_1\mathbb{T}^d \cong \mathbb{Z}^d$. We can choose a basis (as a free module over $\mathbb{Z}$) $u_1, \cdots, u_c$ of $\pi_1\mathbb{T}^d$; and a basis $v_1, \cdots, v_c, w_{c+1}, \cdots, w_d$ of $\pi_1\mathbb{T}^d$; so that each u_i is an integer multiple of v_i; and no linear combination of w_j's gives us any u_i. If we use the simple closed curves corresponding to the basis $v_1, \cdots, v_c, w_{c+1}, \cdots, w_d$ to write the torus as a product of circles, we see that we are in the situation of Example 2.2.4. Moreover, in case the covering is finite sheeted it is clear that $c = d$ (as the covering of $\mathbb{R}$ over S^1 is not finite sheeted), and so we are in the situation of Example 2.2.3. □

We will mostly be concerned with finite sheeted covering maps, as general covering maps may not behave well under composition [61, Chapter 9].

Proposition 2.2.6. *Composition of finite sheeted covering maps is a covering map.*

We refer the reader to [61, Chapter 9] for a proof.

Claim 2.2.7. *Pull-backs of covering maps are covering maps.*

Proof. Covering maps are fiber bundles where the fiber is a discrete collection of points. Pull-backs correspond to a base change, and the fibers remain unchanged. So the result follows.
Alternately, it can be checked that the pull back of an evenly covered neighborhood is also evenly covered. □

Proposition 2.2.8. *[33, Proposition 1.33] Given any covering map $p : (X', x_0') \to (X, x_0)$, and a continuous map $f : (Y, y_0) \to (X, x_0)$, then f lifts to $f' : (Y, y_0) \to (X', x_0')$ iff $f_*(\pi_1(Y, y_0)) \subseteq p_*(\pi_1(X', x_0'))$.*

A special case, known as path lifting property, happens when Y is an interval, and in this case the condition $f_*(\pi_1(Y, y_0)) \to p_*(\pi_1(X', x_0'))$ is always true as $\pi_1(Y, y_0)$ is trivial.

We thank Carlo Petronio for outlining the following result to us.

Proposition 2.2.9. *Any branched covering of an orientable manifold over a non orientable manifold must factor through the orientation double cover.*

Proof. Suppose $p : (Y, y_0) \to (X, x_0)$ with Y orientable, and X non-orientable. Let $q : (Z, z_0) \to (X, x_0)$ be the orientation double cover. Consider an arbitrary point $y \in Y$ and some path γ joining y_0 to y. Then we can path lift $p(\gamma)$ with respect to the covering map q, and we set $r(y)$ to be the second endpoint of this lift (the first endpoint being z_0). To see $r : Y \to Z$ is well defined, note that if we had another path δ from y_0 to y, then the concatenation $\gamma * \bar{\delta}$ is loop on Y which is orientation preserving (as Y oriented). Since p is a local homeomorphism, $p(\gamma * \bar{\delta}$ is orientation preserving in X, and so it lifts to a loop in Z. Thus, the second endpoint of the path lifts of $p(\gamma)$ and $p(\delta)$ coincide, so the map $r : Y \to Z$ is well-defined. Now one can check that $p = q \circ r$, and the result follows. $\square$

2.3 Monodromy of a Covering map

Suppose we have a covering map $p : (X, x_1) \to (Y, y_1)$ with n sheets. Then the covering map is determined (up to conjugation) by the monodromy map $\phi : \pi_1(Y, y_1) \to S_n$, described below. Let us suppose the points in the pre-image of y_1 are $x_1, ..., x_n$ (in other words we are labelling the pre-image points with $1, ..., n$, and different such choices give rise to conjugate representations), then for any loop γ in

$\pi_1(Y, y_1)$, if we lift it we get a permutation of $\{1, ..., n\}$ by seeing what the endpoint of the lift starting at m_i is. This defines a group homomorphism $\phi : \pi_1(Y, y_1) \to S_n$ which we will refer to as permutation monodromy.

To go from a monodromy representation $\phi : \pi_1(N, n_1) \to S_n$ to a covering map, we fix some $j \in \{1, ..., n\}$, and look at the subgroup $H := \{\gamma \in \pi_1(N, n_1) | \phi(\gamma)(j) = j\}$. By the correspondence between subgroups of the fundamental group and covering spaces, H gives us a covering space with the required properties.

Let us now discuss the monodromy maps for some of the examples of coverings that we saw in the last section.

1. The monodromy map of the n-th power map $p_n : S^1 \to S^1$ is given by $\pi_1(S^1) \cong \mathbb{Z} \to S_n$ defined by $1 \mapsto (12...n)$.

2. The monodromy map of the double cover $p_n : S^k \to \mathbb{RP}^k$ is the unique non-trivial map $\pi_1(\mathbb{RP}^k) \to S_2$, i.e. it is the identity map when we identify both $\pi_1(\mathbb{RP}^k)$ and S_2 with $\mathbb{Z}/2\mathbb{Z}$.

Let us now discuss how monodromy maps behave for pull-backs of coverings and composition of coverings.

Claim 2.3.1. *If $f : (Y, y_1) \to (X, x_1)$ is a continuous map, and $p : X' \to X$ is a covering map with monodromy $\phi : \pi_1(X, x_1) \to S_n$, then the pullback covering $f^*p : f^*X' \to Y$ has monodromy $\phi \circ f_* : \pi_1(Y, y_1) \to S_n$, where it is assumed that the ordering on the pre-image points over the respective base-points is consistent with the pullback diagram*[1].

Proof. If γ is any closed curve in Y based at y_1, then $f \circ \gamma$ is a closed curve in X based at x_0. If we pick any arc β covering γ (i.e. $f^*p \circ \beta = \gamma$), then the arc $p^*f \circ \beta$ covers $f \circ \gamma$. The result now follows from the consistent choice of numbering the pre-image points over y_1 and x_1. $\square$

[1] otherwise the monodromy map will differ by a conjugation.

2.3.1 Monodromy under composition

Now we will discuss how monodromy map of a composition of finite sheeted coverings looks like in terms of the individual monodromy maps. Suppose we have two covering maps $q : (Y, y_1) \to (X, x_1)$ and $p : (Z, z_1) \to (Y, y_1)$, with associated monodromy maps $\phi : \pi_1(X, x_1) \to S_n$ and $\chi : \pi_1(Y, y_1) \to S_m$. Suppose the pre-images of the basepoint x_0 under p are $y_1, ..., y_n$ (i.e. we are fixing some ordering among them), and let us choose some paths $\alpha_1, \alpha_2, ...\alpha_n$ joining y_1 to $y_1, ..., y_n$ respectively (we may choose α_1 to be the constant path).

Consider the composite covering $r = q \circ p : (Z, z_1) \to (X, x_1)$. Suppose the pre-image points of y_i under q are $z_{i,1}, ..., z_{i,m}$, and thus we choose the lexicographic ordering for the pre-images of x_1 under r, i.e. we will enumerate these points as

$$z_{1,1}, ..., z_{1,m}, \quad ..., \quad z_{n,1}, ..., z_{n,m}.$$

For any based loop γ in (X, x_1), let us call the path lift of γ starting at y_i to be γ_i, for $1 \leq i \leq n$. We know that that γ_i ends at $y_{\phi(\gamma)(i)}$, by definition of the monodromy. Then the monodromy ψ for r is determined by:

$$\psi(\gamma)(i, j) = (\phi(\gamma)(i), \chi(\alpha_i * \gamma_i * \bar{\alpha}_{\phi(\gamma)(i)})(j)). \tag{2.1}$$

Let us make a few observations about the choices we made:

- If we had chosen some other collection of paths β_i joining x_1 to x_i, then the resulting monodromy using the β curves will be conjugate to the one coming from the α curves, the conjugating permutation is given by the permutation built out of blocks $\chi(\alpha_i * \overline{\beta}_i)$.
- If we chose some other ordering of the pre-image points of the basepoint x_1 under p, or their pre-images under q, then the monodromy of r the compo-

sition will also change by a conjugation, and the conjugating permutation is the one coming from the changing of the labeling.

2.4 Branched Coverings

By a branched covering in the piecewise linear category we will mean a map $p : M \to N$ so that there is a codimension two subcomplex B in M so that if we set $\tilde{B} = p^{-1}(B)$, then the restriction $p|_{M\setminus\tilde{B}} : M \setminus \tilde{B} \to N \setminus B$ is a honest covering map.

For a smooth branched cover we will put more restrictions, we want B to be a smooth codimension two submanifold with trivial normal bundle, and for any point $\tilde{b} \in \tilde{B}$, there product neighbourhoods around $\tilde{b}$ and b so that the map p looks like $(c, z) \to (c, z^n)$ for some $n \in \mathbb{N}$. This restriction forces the map $p : \tilde{B} \to B$ to be a covering map.

2.5 Monodromy of a branched covering

Given a branched covering space $p : M \to N$, then if we remove the branch locus B from N, and its pre-image $\tilde{B}$ from M, then the restriction $p|_{M\setminus\tilde{B}} : M \setminus \tilde{B} \to N \setminus B$ is a covering map, which completely determines the branched covering, by a result of Fox [25]. So by monodromy map of a branched covering map, we will mean the monodromy map of the associated covering map.

2.6 Cut and paste way to construct a branched covering from the monodromy data

Let us consider a disc branched over two points, with the monodromy map $\phi : F\langle a, b\rangle \cong \pi_1(D^2 \setminus \{p, q\}) \to S_2$ defined by $a \mapsto (12)$ and $b \mapsto (12)$, where a, b denote the simple closed curves surrounding the punctures p, q in the fundamental group. It is customary to encode the monodromy information by choosing a generating set of the fundamental group and labeling (or coloring) them by their corresponding monodromy permutations, and this completely specifies the monodromy map. For our example, we can simply label (or color) each of the two punctures with the transposition (12), see Figure 2.1.

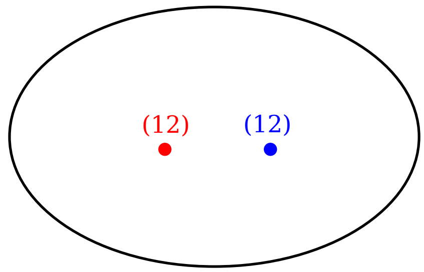

Figure 2.1: A disc branched over two points.

As discussed in the last section this describes a branched covering over the disc, but we will now describe an explicit cut and paste construction for surfaces, and visualize it with the example we are discussing.

1. First we will introduce some additional arcs so that if we cut along these arcs (called the branch cuts) we obtain a simply connected space. We will label the new arcs by $+$ and $-$ in and alternating way.

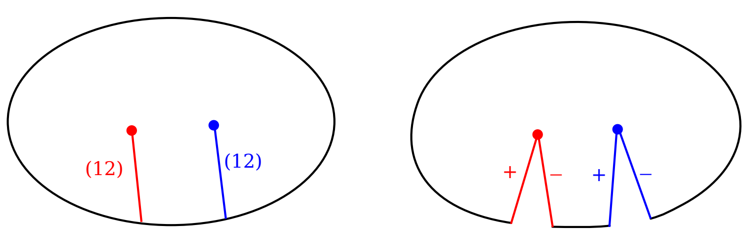

Figure 2.2: Disc branched over two points, before (left) and after (right) making branch cuts.

For our example, this is done simply by drawing two arcs from the punctures straight to the boundary, see Figure 2.2. We note that cutting along these arcs gives us a disc, which is simply connected.

2. We will take d (where the monodromy maps to S_d) disjoint copies of the space obtained at the end of the first step (after branch cuts).
   The point being that after the branch cuts were made, we get a simply connected space, and we know any covering space over this space will simply have to be a disjoint collection of the same space.

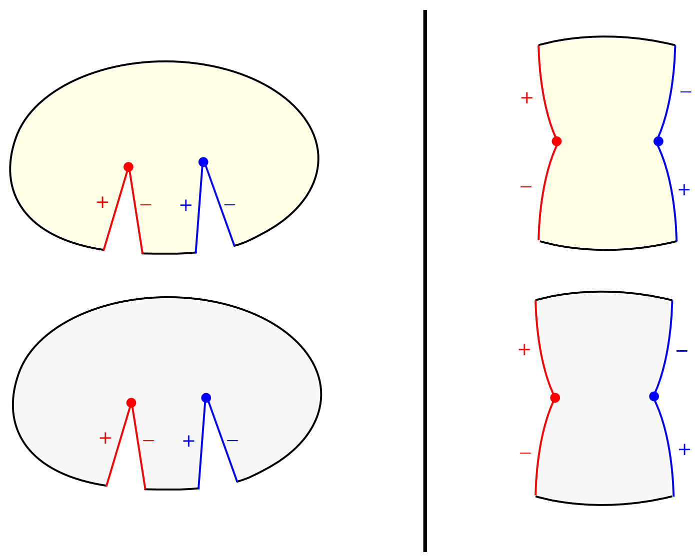

Figure 2.3: Left: Two disjoint copies (shaded in yellow and grey) of the disc obtained after making the branch cuts. The picture is on the right is homemorphic, in order to help visualize the next step.

   In our running example, we simply take two copies of the disc, except we use two different shades to indicate they correspond to different sheets of the covering, see Figure 2.3.

3. We glue the branch cuts using the monodromy data, i.e. we take the i-th branch cut in the j-th disjoint copy of the simply connected space decorated with $+$. and glue it to the i-th branch cut in the $\phi_i(j)$-th copy labelled with $-$.

In our running example, we only have two sheets, and in this case we glue the $+$ branch cuts with the corresponding $-$ branch cuts in the other sheet. We end up with a two fold covering of a twice punctured annulus over the twice punctured disc.

4. We have obtained the associated covering space coming from the monodromy; and we can complete the construction by filling in the branch points and its pre-image points.

   In our example, we end up getting a branched covering of an annulus over

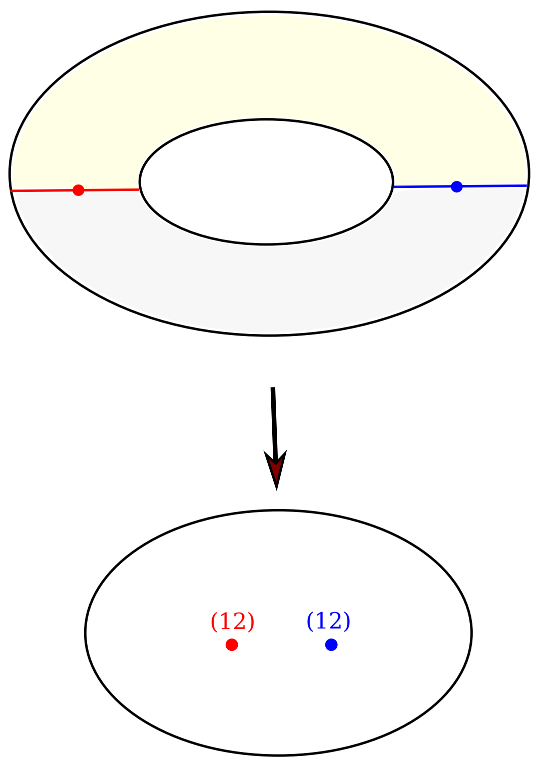

Figure 2.4: The resulting branched cover by making the necessary identification, and filling in the punctures.

the disc with two branch points, see Figure 2.4.

Even though we described this procedure for branched cover over surfaces, it is possible to do similar construction in higher dimensions, but they are harder to visualize, as the branch cuts are hypersurfaces. However colorings are a very convenient way of describing branched coverings, as popularized by Fox [26]. We will discuss colorings in more generality in Section 9.1.

2.7 Manifolds branched over spheres

One can hope to understand all closed oriented manifolds of a given dimension n coming from some sort of operation on a low-complexity n-manifold, like the sphere S^n. Another classical theorem of Alexander shows this is indeed the case:

Theorem 2.7.1 (Alexander [2]). *Every closed oriented piecewise linear n-manifold is a piecewise linear branched cover over the n-sphere.*

We remark here that in the above result there is no control over the number of sheets of the covering, and the branch locus can be an arbitrary codimension two subcomplex. Moreover, Bernstein and Edmonds [7] showed that in general the theorem cannot be improved. In particular, they showed that:

- Any branched covering of the n-torus over the n-sphere must have at least n-sheets (this result was shown first by Fox [27] in case $n = 4$).
- The quaternionic projective plane $\mathbb{HP}^2$ cannot be obtained as a branched cover of the 8-sphere where the branch locus is a submanifold.

However, one can hope that in low dimensions, we can realize all closed oriented n-manifolds as a branched over over the sphere, with the branch locus being a submanifold and the degree of the covering being n. It is easy to see this in the case $n = 1$, as S^1 is the only closed connected 1-manifold. By the classification of surfaces, we know that any closed oriented surface is determined by its genus g.

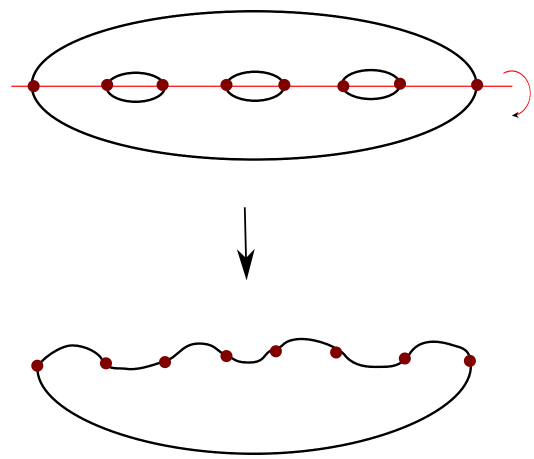

Figure 2.5: Consider the surface of genus g sitting in $\mathbb{R}^3$ with an axis of rotational symmetry. If we quotient out we get a sphere with as many branch points as the number of times the axis intersects the surface.

We know that quotienting the surface of genus g by the hyperelleptic involution gives us the 2-sphere with $2g + 2$ branch points, see Figure 2.5.

When $n = 3$, we have the following theorem in both smooth and piecewise linear categories:

Theorem 2.7.2 (Hilden [34]; Hirsch [38]; Montesinos [60]). *Every closed oriented three manifold is a three sheeted simple branched cover over S^3, with the branch locus being a knot.*

Here by simple branched covering, we mean above any branch point only two sheets can come together. There are similar results in dimension 4, but with some restrictions.

Theorem 2.7.3 (Piergallini [63]). *Every closed oriented piecewise linear four manifold is a four sheeted simple branched cover over S^4, with the branch locus being a transverse immersed piecewise linear surface.*

CHAPTER 3

THE BRAID GROUP

In this chapter, we will study braids from a more algebraic viewpoint. We will see several equivalent definitions of the braid group, and as we will see later on, certain viewpoints are more convenient to work with in some situations. In the later half of this chapter we will record several results about braid groups for future use.

3.1 Equivalent definitions of the braid group

The braid groups were first defined (implicitly) by Hurwitz in [39], but was first explicitly studied by Artin [4, 5]. The braid group on n strands has the following equivalent descriptions:

3.1.1 Braids as loops in configuration spaces

Consider the ordered configuration space of n distinct points in the plane $\mathbb{C}$ (or equivalently $\mathbb{R}^2$, or the open unit disc)

$$Conf_n(\mathbb{C}) = \{(z_1, ..., z_n) \in \mathbb{C}^n | z_i \neq z_j \text{ for all } i \neq j\}.$$

This space is also described as the complement of the braid arrangement (i.e. the hyperplane arrangement comprising of the various fat diagonals $\{z_i = z_j\}$). Since all the points in the configuration space are distinct, we may quotient out by the natural permutation action of the symmetric group S_n and obtain the unordered configuration space:

$$UConf_n(\mathbb{C}) = \{[z_1, ..., z_n] \in \mathbb{C}^n | z_i \neq z_j \text{ for all } i \neq j\},$$

where $[z_1, ..., z_n]$ denotes the unordered tuple with elements $z_1, ..., z_n$. We note that the quotient map is a regular covering map of degree $n!$.

Definition 3.1.1. The *braid group* B_n is the fundamental group of the ordered configuration space $Conf_n(\mathbb{C})$.

Definition 3.1.2. The *pure braid group* PB_n is the fundamental group of the unordered configuration space $UConf_n(\mathbb{C})$.

By covering space theory, we get an exact sequence:

$$1 \to PB_n \to B_n \to S_n \to 1.$$

3.1.2 Braids as collection of strands

A geometric braid collection of properly embedded n-strands in $\mathbb{C} \times I$ going from left to right (along the I direction) so that the projection of their endpoints onto the $\mathbb{C}$ factor are the same collection of points. A braid will be an isotopy class of such geometric braid (where the isotopy is through braids).

We can concatenate two braids on the same number strands by stacking them horizontally. Under this operation of concatenation, the collection of all n-braids, form a group. Here the identity braid is n-parallel strands with no crossings, and inverses are given by the reverse of the mirror of a braid.

3.1.3 Braids as mapping classes

The mapping class group of a surface S is defined to be the group of isotopy classes of orientation preserving diffeomorphisms of the surface which restrict to the identity on the boundary of S. The braid group on n-strands can be canonically identified with the mapping class group of the closed ball B^2 with n marked points.

3.1.4 Braids as automorphisms of free groups

Let us denote by F_n the free group on n letters $x_1, \cdots, x_n$, and its automorphism group by $Aut(F_n)$. The braid group on n-strands can be identified with the following subgroup of the automorphism group:

$$\{f \in Aut(F_n) |\ f(x_i) \text{ is conjugate to some } x_j, f(x_1 \cdots x_n) = x_1 \cdots x_n\}.$$

Remark 3.1.3. Our conventions (which are consistent with majority of the literature) for concatenating loops in the fundamental group (and concatenating geometric braids) is left to right; whereas our conventions for composing mapping classes (and more generally functions) is from right to left. Consequently, the identifications between one of our first two formulations of the braid group and and one of the last two formulations will not be a group isomorphism but a group anti-isomorphism, i.e. a bijective group anti-homomorphism. Of course this issue could be fixed by defining the opposite group for two of these formulations, but then one has to keep track of this whenever one tries to use a result from a source using the opposite conventions.

Remark 3.1.4. These groups were first defined by Hurwitz (who called them Monodromy Groups A and B, ”when translated”), however this viewpoint was forgotten until it was rediscovered by Fox and Neuwirth [24].

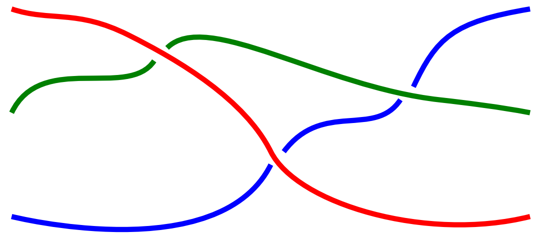

Figure 3.1: A three stranded braid

3.2 Outline of the equivalence of various definitions

3.2.1 From collections of strands to configuration spaces and back

Given any collection of strands in $\mathbb{C} \times I$, we can think of the intersection of the strands with $\mathbb{C} \times \{t\}$ for each $t \in I$. Since the geometric braid cannot go backwards we see that, for each t the intersection is a collection of n distinct points, or an element of the configuration space. As t varies in I, we get a path in the configuration space, which is in fact a loop by our requirement that the projection along the endpoint of I is the same collection of points.

Conversely, given an element of $\pi_1(UConf_n(\mathbb{C}))$, we may choose a loop in the configuration space which represents it. The trace of this loop in $\mathbb{C} \times I$ gives us a geometric braid.

Moreover, isotopy of a geometric braid (through braids) correspond precisely to homotopy of based loops in the configuration space, which leads to the identification between the first two viewpoints.

Figures 3.1 and 3.2 illustrate this equivalence in the case of a three stranded braid.

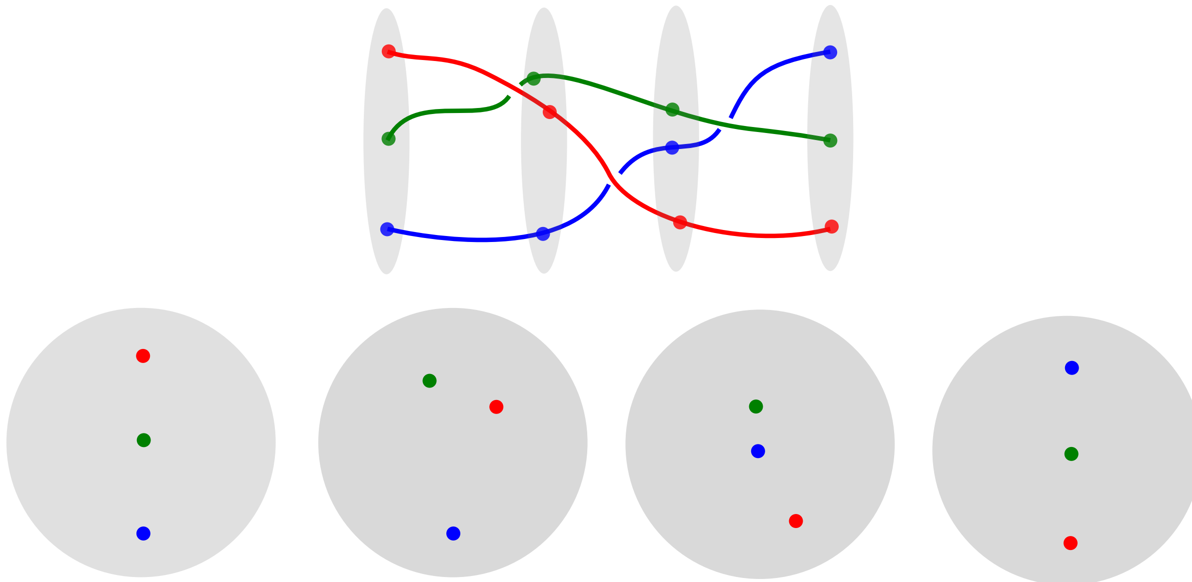

Figure 3.2: We can view three stranded braid in Figure 3.1 as a collection of three points in $\mathbb{C}$ by sliding the sic (copy of $\mathbb{C}$) from left to right and see where the strands intersect

3.2.2 From mapping classes to collections of strands and back

The Alexander trick (see [64]) tells us that any homeomorphism of the closed ball B_2 which is pointwise fixed on the boundary is isotopic to the identity. Thus given a mapping class of B_2 with n marked points, we can look at the trace of this isotopy, and the trace of the marked points in the interior of $B^2 \times I$ gives us a geometric closed braid.

Conversely, a geometric n-braid is an isotopy of n distinct points in B^2 (note that the interior of B^2 is homeomorphic to $\mathbb{C}$), and by the Isotopy extension theorem, can be extended to an isotopy of B^2. The time one map of this isotopy gives rise to the required mapping class.

3.2.3 From mapping classes to automorphisms

Given any mapping class of B^2 with n marked points, this induces a homeomorphism of the n-times punctured disc onto itself (where we remove the branch points). In turn, this homeomorphism induces an automorphism on the fundamental group of the n-times punctured ball, which is isomorphic to the free group F_n, freely generated by loops $\{x_i\}_{1\leq i\leq n}$ surrounding the punctures. Since any homeomorphism of the punctured disc must send neighbourhood of a puncture to neighbourhood of some other puncture, it follows that any automorphism of the fundamental group must send a loop x_i to some conjugate of x_j for some j. Moreover we see that this homeomorphsim has to preserve the homotopy class of the loop parallel to the boundary, i.e. the element $x_1 ... x_n$ in the fundamental group. This gives us an automorphism with desired properties starting with any mapping class. That all such automorphisms arise from mapping classes is harder to prove, and we refer any interested reader to the original papers of Artin [4, 5].

3.3 Presentation of the braid group

3.3.1 Artin's presentation

If we let σ_i denotes positive half twists between i-th and $(i+1)$-th strand, the braid group B_n on n-strands has a presentation (due to Artin [4, 5])

$$B_n = \{\sigma_1, ..., \sigma_{n-1} | \sigma_i\sigma_{i+1}\sigma_i = \sigma_{i+1}\sigma_i\sigma_{i+1} \text{ for all } 1 \leq i < n-1, \sigma_i\sigma_j = \sigma_j\sigma_i \text{ if } |i-j| > 1\}$$

The relation $\sigma_i\sigma_{i+1}\sigma_i = \sigma_{i+1}\sigma_i\sigma_{i+1}$ is called the braid relation. The braid relation can be reformulated as $\sigma_{i+1}^{-1}\sigma_i\sigma_{i+1} = \sigma_i\sigma_{i+1}\sigma_i^{-1}$, which is the second Reidemeister move. The relation $\sigma_i\sigma_j = \sigma_j\sigma_i$ if $|i-j| > 1$ is called the far commutation relation, which corresponds to moving crossings of non overlapping regions past one another.

Let us note some consequences that follow easily from Artin's presentation:

1. All the Artin generators σ_i are conjugate, as seen directly from the alternative formulation of the braid relation. Consequently, the braid group is normally generated by a single element σ_1; and thus the abelianization of the braid group is the integers.

2. There is a group homomorphism $\exp : B_n \to \mathbb{Z}$ sending each generator $\sigma_i \mapsto 1$ (since both the braid and far commutation relations hold after applying this map). This homomorphism keeps track of the sum of the exponents when a braid is written as a word in the standard generators, and thus this homomorphism is known as the exponent sum. Note that the exponent sum coincides with the abelianization map.

3.3.2 Forgetful map from the braid group to the symmetric group

Looking at braids from the second viewpoint, if we forget all the crossing information and just look at where the endpoints go, we get a permutation Forget: $B_n \to S_n$. Forgetting the crossing information corresponds to adding the relation $\sigma_i^2 = 1$ to Artin's presentation of the braid group, and this gives us the classical presentation of the symmetric group S_n.

$$S_n = \{\sigma_1, ..., \sigma_{n-1} | \sigma_i^2 = 1 \text{ for all } 1 \leq i \leq n-1, \sigma_i\sigma_{i+1}\sigma_i = \sigma_{i+1}\sigma_i\sigma_{i+1} \text{ for all } 1 \leq i < n,$$

$$\sigma_i\sigma_j = \sigma_j\sigma_i \text{ if } |i-j| > 1\}$$

3.4 Center and centralizers

3.4.1 Center of the braid group

Proposition 3.4.1. *The center of the braid group B_n is an infinite cyclic group generated by the full-twist $\Delta^2 = (\sigma_1 ... \sigma_{n-1})^n$.*

3.4.2 Centralizers of elements in the braid group

For future use, let us record the a few facts about the structure of centralizers of braids.

Proposition 3.4.2. *(Kerékjártó [46, 18], Eilenberg [20]) For any m coprime to n, the centralizer of the periodic braid $(\sigma_1 ... \sigma_{n-1})^m$ in B_n is the infinite cyclic group generated by $\sigma_1 ... \sigma_{n-1}$.*

We refer the reader to [31, Section 5] for definitions of interior and tubular braids of a reducible braid and details of the proof of the following result.

Theorem 3.4.3. *[31, Theorem 1.1] (see also [51, Section 3]) The centralizer $Z(\beta)$ of a non periodic reducible braid β in regular form fits in a split exact sequence:*

$$1 \to Z(\beta_{[1]}) \times ... \times Z(\beta_{[t]}) \to Z(\beta) \to Z_0(\widehat{\beta}) \to 1,$$

where $\beta_{[1]}, ..., \beta_{[t]}$ are the various interior braids and $\widehat{\beta}$ is the associated tubular braid; and $Z_0(\widehat{\beta})$ is the subgroup of the centralizer $Z(\widehat{\beta})$ of the tubular braid $\widehat{\beta}$ consisting of elements whose permutation is consistent with β.

CHAPTER 4
BRAIDED EMBEDDINGS

One can hope that higher dimensional braids will play a similar role in higher dimensional knot theory. Braids have been generalized in higher dimensions in several different ways, our point of view is a natural one in studying embeddings of manifolds. In fact what we are calling braided embeddings have been studied by various mathematicians, using slightly different names: polynomial coverings by Hansen [32], d-fat covers by Petersen [62], folded embeddings by Carter and Kamada [16], and sometimes without explicitly using a name such as in the work of Hilden-Lozano-Montesinos [35]. Rudolph [66], Viro and Kamada [43, 44] studied braided surfaces in $\mathbb{R}^4$, obtaining analogues for Alexander's braiding theorem for surfaces. Carter and Kamada studied braided embeddings and immersions in low dimensions, and talked about existence and lifting problems. Etnyre and Furukawa [21] studied braided embeddings in all dimensions, and focused on their interplay with contact embeddings.

We work in both the smooth and piecewise linear category linear categories. We will not mention the categories separately in case they behave similarly, however when necessary we will deal with them separately.

4.1 Braided Embeddings

We say that an embedding $f : M \to N \times D^l$ is a *co-dimension l braided embedding* over N if the embedding composed with the projection to N, $pr_1 \circ f : M \to N$ is a (oriented in case both base and covering spaces are oriented) branched covering map.

Remark 4.1.1. If we do not specify the co-dimension, a braided embedding would be a co-dimension two embedding of M to $N \times D^2$.

We will study two natural problems related to braided emdeddings, the lifting problem and the isotopy problem.

Question 4.1.2. (Lifting Problem) Can every branched cover be lifted to a co-dimension l braided embedding?

Since we are always working with compact manifolds, by Whitney embedding theorem [70], they always embed in a sufficiently high dimensional disc, and hence for sufficiently large l, any branched covering lifts to a codimension l braided embedding (because it embeds in the disc factor). Hence it makes sense to ask the following:

Question 4.1.3. What is the smallest l so that a given branched cover can be lifted to a co-dimension l braided embedding?

Let us start begin by discussing the this question for some well known families of honest covering maps.

Example 4.1.4. $p_n : S^1 \to S^1$ defined by $z \mapsto z^n$, for $n \in \mathbb{N}$ (similar result holds for negative integers). For $n = 1$, the map p_1 is the identity and hence an embedding, so $l = 0$ in this case. For $n > 1$, we claim that the smallest such l is 2. It is clear that there are codimension two lifts. That there is no codimension one lift, is illustrated in Figure 4.1 for the case when $n = 3$.

Alternately, this statement also follows as a consequence of the intermediate value theorem.

Example 4.1.5. $a_n : S^n \to \mathbb{RP}^n$ induced by quotienting out by the antipodal action. In this case the smallest such l turns out to be $n + 1$. To see this note that since S^n embeds in the disc D^{n+1} (being the boundary of the closed disc), we have a braided embedding defined by $a_n \times i : S^n \to \mathbb{RP}^n \times D^{n+1}$ (where i is some embedding of S^n in D^{n+1}). That l cannot be any less than n is precisely the content of the Borsuk Ulam theorem [13].

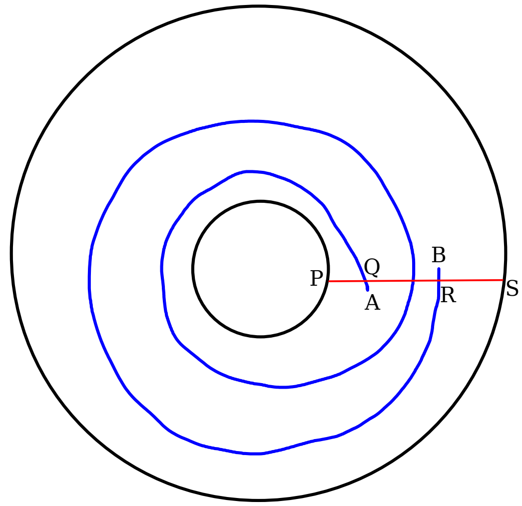

Figure 4.1: Suppose $n = 3$, and we have a codimension 1 braided embedding of S^1 over S^1. Suppose we have drawn a part of the image starting at A and ending at B, together with a transversal (constant slice of the annulus) meeting the image in three points. Since the leftmost (PQ) and rightmost (RS) segment of the transversal together with the segment along the curve from Q to R disconnects the annulus, there is no way to join B to A without causing an intersection.

So the lifting problem is a generalization of the Borsuk Ulam theorem, where instead of allowing two-fold covers, we allow arbitrary branched covers. The reason for allowing branched coverings instead of just coverings is that typically we will mostly be looking at (branched) coverings over the sphere, and since for $n > 1$, the n-sphere is simply connected, in order to get interesting manifolds, we need to allow branching. For this paper we are going to focus on co-dimension two liftings of branched covers over spheres, because knots in codimension two turn out to be most interesting.

Let us discuss some fundamental results about branched coverings and embeddings to motivate our discussion of lifting branched covers to braided embeddings.

4.2 Embeddings of manifolds

Let us now discuss results about embedding manifolds in Euclidean space (or equivalently the sphere).

Theorem 4.2.1 (Whitney [70] for smooth category, see [65] for piecewise linear category)**.** *Every closed n-manifold embeds in $\mathbb{R}^{2n}$.*

There are characteristic class obstructions for embedding an arbitrary n-manifold in lower dimensional Euclidean space, for instance $\mathbb{RP}^n$ does not embed in $\mathbb{R}^{2n-1}$ when n is a power of 2. However, just like the case of branched covers we have better bounds for low dimensional manifold. Every closed oriented surface embeds in $\mathbb{R}^3$, but as mentioned above, the real projective plane (or any of the non-orientable surfaces) do not embed in $\mathbb{R}^3$. It is a theorem of Hirsch [37] that every closed oriented three manifold embeds in $\mathbb{R}^5$, and this was extended to the non-orientable case by Wall. Hilden-Lozano-Montesinos [35] gave an alternate proof of Hirsch's result, which in fact constructs a braided embedding[1].

Theorem 4.2.2 (Hilden-Lozano-Montesinos)**.** *Every closed oriented three manifold has a three fold simple branched cover over S^3, which lifts to a braided embedding in $S^3 \times D^2$.*

It is important to remark that their proof did not start with an arbitrary three fold simple branched cover and lift it to an embedding, they had to alter the branch locus (without changing the manifold upstairs) and bring it to a special form where the branched covering did lift. As we shall see, there are branched coverings over the three sphere which do not lift to a braided embedding.

Let us now go down in dimension and discuss if we can braided embed closed oriented one and two dimensional manifolds in trivial disc bundle of the sphere (and hence in Euclidean space). Every one-manifold (disjoint union of circles) admits a codimension one[2] braided embedding in $S^1 \times D^1$. In Example 8.2.1, we see that the two fold branched cover of the genus g surface over the sphere obtained by quotienting by the hyperelleptic involution (see Figure 2.5) lifts to a co-dimension

[1] They used a slightly different terminology, but this is exactly what they proved.
[2] It admits a codimension zero embedding if and only if the manifold is connected

two braided embedding, and consequently every surface of genus g braided embeds in $S^2 \times D^2$.

Let us now turn to the some of main results of this thesis, where we discuss the lifting problem in codimension two:

Question 4.2.3. Which branched covers over the sphere S^n lift to co-dimension two braided embedding in $S^n \times D^2$?

The question is easy to answer for $n = 1$, as any branched cover over S^1 must in fact be a covering map, and if we restrict to each component it must be equivalent to (in the notation of Example 4.1.4) p_n for some $n \in \mathbb{Z} \setminus \{0\}$, and thus any such covering lifts (these are the classical closed braids). The situation becomes interesting for branched coverings of surfaces over the two-sphere, where we get different answers for the piecewise linear and smooth categories. We will study the lifting problem in more detail in Chapters 8, 9 and 10. The other main problem is the istotopy problem:

Question 4.2.4. (Istotopy Problem) Can we isotope any embedding in sphere S^n (or equivalently Euclidean space $\mathbb{R}^n$) to be a braided embedding?

Here we are taking about braiding about the standard S^{n-2} (equatorial sphere inside equatorial sphere in S^n), and we all such braided embeddings as closed braid. We will study this problem in the next chapter in the piecewise linear category.

4.3 Monodromy of a braided embedding

Just like a covering space is equivalently given by a monodromy representation of the base to the symmetric group, a braided embedding projecting to a honest covering map is given by a monodromy representation of the base to the braid group. Suppose $f : M \to N \times D^2$ is a braided embedding, with the composition to the first factor $pr_1 \circ f : M \to N$ an n-sheeted covering map. Let us choose a base-point $x \in N$. For any simple closed curve[3] γ based at x, if we restrict the bundle $N \times D^2 \to N$ to γ, we get a bundle $\gamma \times D^2 \to \gamma$. For any point $c \in \gamma$ the braided embedding f maps the n pre-image points of c under $pr_1 \circ f$ to n distinct points in the disc $\{c\} \times D^2$. Thus as we vary c along γ, we get a closed braid in the solid torus $\gamma \times D^2$ (or equivalently a loop in the configuration space $UConf_n(D^2)$), which gives rise to a well defined braid by cutting the solid torus $\gamma \times D^2$ at $x \times D^2$ (or equivalently looking at the element of the fundamental group $UConf_n(D^2)$ given by that loop). This map gives rise to a group homomorphism $\psi : \pi_1(N) \to B_n$, which we will refer to as braid monodromy.

To construct a braided embedding from such a braid monodromy, we recall that Fadell, Fox and Neuwirth [23, 24] showed that the configuration space $UConf_n(D^2)$ is aspherical, or in other words it is a $K(B_n, 1)$. Thus a map of spaces $N \to UConf_n(D^2)$ is equivalent to a group homomorphism at the level of fundamental groups $\pi_1(N) \to B_n$. We note that a braided embedding $f : M \to N \times D^2$ (so that the associated covering map is n-sheeted) is equivalent to a choice of n-distinct points in D^2 for each point in N, i.e. a map $N \to UConf_n(D^2)$.

In case $f : M \to N \times D^2$ is a braided embedding, with the projection to the first factor $pr_1 \circ f : M \to N$ a branched covering map, it is similarly determined by the associated braided embedding $f|_{M \setminus \tilde{B}} : M \setminus \tilde{B} \to (N \setminus B) \times D^2$ (or equivalently its braid monodromy $\pi_1(N \setminus B) \to B_n$) where we delete the branch locus and its pre-image. However, given a group homomorphism $\pi_1(N \setminus B) \to B_n$, one gets a braided embedding of the complement of the branch locus, but we need to be careful about extending over the branch locus (with appropriate restrictions, locally flat piecewise linear or smooth). We will discuss this issue in Chapter 7.

[3] For self intersecting closed curves $\alpha : S^1 \to N$, we can pullback the bundle $N \times D^2$ by α and get a solid torus over S^1, and the same statement holds.

4.4 Braid Monodromy under composition

Similar to Section 2.3.1, we can determine the braid monodromy for composition of two braided embeddings. Let us suppose the braid monodromies of the braided embeddings are given by $\Phi : \pi_1(X, x_1) \to B_n$ and $X : \pi_1(Y, y_1) \to S_m$ lifting $\phi : \pi_1(X, x_1) \to S_n$ and $\chi : \pi_1(Y, y_1) \to S_m$, respectively.

We have $\Psi(\gamma)$ is a reducible braid determined by the tubular braid $\Phi(\gamma)$, and the interior braid corresponding to the i-th tubular braid is given by $X(\alpha_i * \gamma_i * \bar{\alpha})$.

CHAPTER 5
BRAIDING IN THE PIECEWISE LINEAR CATEGORY IN AMBIENT DIMENSION AT MOST 5

5.1 Introduction

In this chapter we study generalizations of Alexander's theorem we saw in Chapter 1 in higher ambient dimension. Braided surfaces were first introduced by Rudolph [66] for surfaces with boundary, but the notion we will be using is due to Viro. Viro defined the notion of a closed braid for a closed oriented surface in $\mathbb{R}^4$, which can be thought of as the closure of a certain type (one with trivial boundary) of braided surface in the sense of Rudolph. The notion of braided embedding was defined in general by Etnyre and Furukawa [21], and they have been studied previously by Carter and Kamada [16].

The first analogue of Alexander's theorem for surfaces is due to Rudolph [66], who showed that every oriented ribbon surface is smoothly isotopic to a closed braid. Alexander's theorem was generalized to closed, oriented surfaces in $\mathbb{R}^4$ by Viro and independently by Kamada. Viro announced his results in a lecture in 1990, but his proof was never published. Kamada gave an alternative proof [43, 44] using the motion picture method to describe surfaces in $\mathbb{R}^4$.

The main result of this chapter is to show that, in the piecewise linear category, Alexander's theorem can be generalized to ambient dimension 5.

Theorem 5.1.1 (**PL Generalized Alexander's Theorem**). *Any closed, oriented, piecewise linear $(n-2)$-link in $\mathbb{R}^n$ can be piecewise linearly isotoped to be a closed braid for $3 \leq n \leq 5$.*

Our approach is similar to Alexander's original proof in [3] (see also [10, Theorem 2.1], or [44, Theorem 4.2]) in the classical case. We give an alternate proof of Kamada's generalization of Alexander's Theorem in dimension 4. For completeness, we also include the proof of the classical case of dimension 3. We also recover another classical result of Alexander [2], that says that any closed oriented piecewise linear k-manifold is a piecewise linear branched cover over the sphere S^k, see Remark 5.3.5.

One may wonder if there are analogues of Alexander's theorem for higher co-dimension links.

Question 5.1.2. Given a natural number k, is there a natural number $n \geq k+2$ so that any closed, oriented k-manifold embeds in $\mathbb{R}^n$, and any such embedding is isotopic to a closed braid?

It is well known that the embedding problem (i.e. the first part of Question 9.5.3) holds as long as $n \geq 2k$, see [65, Theorem 5.5] for piecewise linear category and [70] for smooth category. By Theorem 5.1.3 below, in the piecewise linear category, when $k \geq 2$ and $n \geq 2k$, we have that any embedding is isotopic to a closed braid, so the answer to Question 9.5.3 is affirmative. Moreover, we can ask whether a given k-link in $\mathbb{R}^n$ is always isotopic to a closed braid? The following result gives a partial answer to that question.

Theorem 5.1.3. *Any closed, oriented, piecewise linear k-link in $\mathbb{R}^n$ can be piecewise linearly isotoped to be a closed braid for $2n \geq 3k+2$.*

In the Section 2, we define closed braids and positive links, and we show that thse notions are equivalent, thereby reducing the braiding problem to the problem of isotoping a link to be positive. In the Section 3, we describe cellular moves, which will be used to replace a negative simplex with some positive simplices. In Sections 4 and 5, we study co-dimension two and higher co-dimension embeddings repectively. We will show that under the hypotheses of Theorems 5.1.1 and

5.1.3, any closed link can be isotoped to be positive, completing the respective proofs.

5.2 Closed Braids and Positive Links

We assume that, unless otherwise stated, all spaces are piecewise linear, all embeddings are piecewise linear and locally flat, all isotopies are piecewise linear and ambient, and all other maps (radial projections, coverings, and branched coverings) are topological[1]. By linear we will mean linear in the affine sense. By a branched covering, we will mean a covering map in the complement of a co-dimension two subcomplex (not necessarily a submanifold).

Let k and l be natural numbers with $l \geq 2$. Let $f : M^k \to \mathbb{R}^{k+l}$ be an embedding of a closed oriented k-manifold (possibly disconnected); we call the image a (co-dimension l) k-link. We will be mostly concerned with co-dimension two embeddings, i.e. $l = 2$.

We say that f is a *co-dimension l braided embedding* if $f(M)$ is contained in a regular neighborhood $N(S^k) = S^k \times D^l$ of the standard sphere (unit sphere in $\mathbb{R}^{k+1} \subset \mathbb{R}^{k+l}$) such that the embedding composed with the projection to the sphere, $pr_1 \circ f : M \to S^k$ is an oriented branched covering map. Note that in case $k = 1$, we have $pr_1 \circ f$ is just an oriented covering map since the branch locus is empty, also if further $l = 2$, then $f(M)$ is a closed braid (in the classical sense). We generalize this notion and call the image $f(M)$ of a co-dimension l braided embedding f a *co-dimension l closed braid*. We will just say f is a braided embedding, and $f(M)$ is a closed braid if co-dimension is clear from the context. By *braiding* we will mean isotoping a link to be a closed braid. We will identify M with $f(M)$, and think of f as an inclusion. A simplex of M is understood to be in $\mathbb{R}^{k+l}$.

Figure 5.1 shows a schematic of a closed braid in higher dimension.

[1] Radial projections need not be piecewise linear, see Chapter 1 in [65].

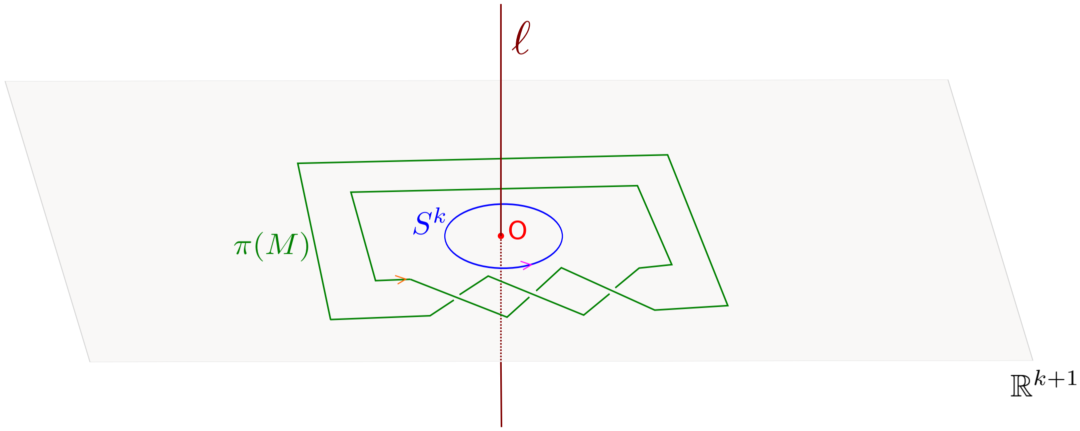

Figure 5.1: Schematic figure of closed braid $\mathbb{R}^{k+2}$

Let us choose (and fix) a $l-1$ dimensional subspace ℓ of $\mathbb{R}^{k+l}$, which will play the role of the braiding axis. Let $\pi : \mathbb{R}^{k+l} \to \mathbb{R}^{k+1}$ denote orthogonal projection to $\ell^{\perp}$, and let O denote the origin of $\mathbb{R}^{k+1}$.

We say that a k-simplex $\sigma = [p_0, ..., p_k]$ in $\mathbb{R}^{k+l}$ is in *general position* with respect to ℓ if any of the following equivalent conditions hold:

1. There is no hyperplane in $\mathbb{R}^{k+l}$ that contains both σ and ℓ.

2. There is no hyperplane in $\mathbb{R}^{k+1}$ that contains both $\pi(\sigma)$ and O.

3. The vectors $\pi(p_0), ..., \pi(p_k)$ are linearly independent.

4. The determinant of $[\pi(p_0)|\pi(p_1)|...|\pi(p_k)]$ is nonzero.

We can always assume each simplex is in general position (with respect to ℓ), because if not, then by slightly perturbing the vertices, we can put it in general position.

General Position. We will be needing several general position arguments, and we will prove one of them. They all follow the same pattern: the degenerate case happens if and only if a continuous function vanishes. So, if the system was nondegenerate, then any slight perturbation does not change that fact, and if the system was degenerate, it would be possible to make it non-degenerate with a slight perturbation.

We say that a simplex $[p_0, ..., p_k]$ in $\mathbb{R}^{k+l}$ in general position (with respect to ℓ) is *positive* if the simplex $[O, \pi(p_0), ..., \pi(p_k)]$ has the standard orientation of $\mathbb{R}^{k+1}$ (i.e. $[\pi(p_0)|\pi(p_1)|...|\pi(p_k)]$ has positive determinant), otherwise we say it is *negative*. We say that an embedded link $f : M^k \to \mathbb{R}^{k+l}$ is a *positive* (with respect to ℓ) if the image of each simplex is in general position with respect to ℓ and positive. Hereafter, the axis ℓ will be in the background; it will be understood that a simplex is positive/negative/in general position means it is positive/negative/in general position with respect to ℓ.

Let $p : \mathbb{R}^{k+1} \backslash O \to S^k$ be the radial projection. For any piecewise linear manifold M^k with a given cellular decomposition, let δM denote the union of all $(k-2)$-faces of cells of M.

The following theorem shows that, to prove Theorem 5.1.1, it suffices to show we can isotope any link to be positive.

Theorem 5.2.1. *Let $f : M^k \to \mathbb{R}^{k+l} \setminus \ell$ be an embedding, then the composition h defined by*

$$M^k \xrightarrow{f} \mathbb{R}^{k+l} \setminus \ell \xrightarrow{\pi} \mathbb{R}^{k+1} \setminus O \xrightarrow{p} S^k$$

is an oriented branched covering map if and only if all simplices of M are positive. In other words, the notions of closed braid and positive link are equivalent.

Proof. If M is a closed braid, then the restriction of h to any particular simplex σ must be orientation preserving, and it follows that all simplices of M must be positive.

Let us now assume that M is a positive link. Let $\Sigma := h(\delta M)$. We will show that h restricts to a covering map on $M \setminus h^{-1}(\Sigma)$. Now any point x of $M \setminus h^{-1}(\Sigma)$ could either be an interior point of a k-simplex, or on the interior of a $(k-1)$-face shared by two k-simplices. We will show that in both these cases, we can find a compact, regular neighbourhood N of x such that $h|_N$ is injective.

Let x be in the interior of the k-simplex $\sigma = [p_0, ..., p_k]$. Then for any y in σ we see that the ray passing through O and $\pi(y)$ meets $\pi(\sigma)$ exactly once, since $\pi(p_0), ..., \pi(p_k)$ form a basis for $\mathbb{R}^{k+1}$. Thus in this case $h|_\sigma$ is injective.

Let us now suppose that x is in the interior of the intersection of the adjacent simplices $\sigma = [p_0, ..., p_k]$ and $\tau = [p_1, q_0, p_2, ..., p_k]$. For σ and τ to be compatible, the induced orientation on the $(k-1)$-face $\nu = [p_1, ..., p_k]$ they share must be opposite, i.e. the determinant of the matrix $[\pi(p_0)|\pi(p_1)|...|\pi(p_k)]$ is positive, and the determinant of the matrix $[\pi(q_0)|\pi(p_1)|...|\pi(p_k)]$ is negative. Suppose y is in σ and the ray passing through O and $\pi(y)$ meets $\pi(\tau \setminus \nu)$, then we see that for some non-negative scalars $c_0, ..., c_k, d_1, ..., d_k$ and positive scalars d_0, λ we have

$$c_0\pi(p_0) + c_1\pi(p_1) + ... + c_k\pi(p_k) = \lambda(d_0\pi(q_0) + d_1\pi(p_1) + ... + d_k\pi(p_k)).$$

So we have $c_0\pi(p_0) - \lambda d_0\pi(q_0) \in \text{ Span}\{\pi(p_1), ..., \pi(p_k)\}$, and hence

$$c_0 \det[\pi(p_0)|\pi(p_1)|...|\pi(p_k)] = \lambda d_0 \det[\pi(q_0)|\pi(p_1)|...|\pi(p_k)]$$

which is a contradiction to our assumption that both σ and τ are positive. Thus in this case $h|_{\sigma\cup\tau}$ is injective.

Thus in either case, for a compact neighborhood N of x, $h|_N$ is a continuous bijection between compact Hausdorff spaces and hence a homeomorphism onto its image. Thus $h|_{M\setminus h^{-1}(\Sigma)} : M \setminus h^{-1}(\Sigma) \to S^k \setminus \Sigma$ is a local homeomorphism, and in fact a covering map since for any $y \in S^k \setminus \Sigma$, the fiber $h^{-1}(y)$ is compact and discrete. Also we can check that h is orientation preserving. Thus h is an oriented branched covering, as required. $\square$

Remark 5.2.2. The map h above is only continuous since the radial projection p is so.

However, we can compose $\pi \circ f$ with the pseudo-radial projection[2] instead of the radial projection p, and then the resulting composition will be a piecewise linear branched cover.

Let us choose (and fix) a unit vector $v \in \ell \subset \mathbb{R}^{k+l}$, let ℓ_v denote the line $\mathbb{R}v$, and let $\pi_v : \mathbb{R}^{k+l} \to \mathbb{R}^{k+l-1}$ denote orthogonal projection to $\ell_v^{\perp}$. By the *v-coordinate* of a point $p \in \mathbb{R}^{k+l}$ we will mean the scalar projection of p onto v. We say that a point p on a k-simplex σ of M^k in $\mathbb{R}^{k+l}$ is an *overcrossing* (respectively *undercrossing*) if there is another point $q \in M$ with $\pi(p) = \pi(q)$ and difference of v-coordinate of p and the v-coordinate of q is positive (respectively negative).

5.3 Cellular moves

In this section we describe cellular moves, which we will use repeatedly in the next section to isotope any link to be positive.

Suppose we have a embedded oriented $(k+1)$-disk D in $\mathbb{R}^{k+l}$ such that D meets M^k in a k-disk σ in ∂D which is a union of simplices of both M and ∂D and the induced orientations coming from M and ∂D are opposite. Let M' be the manifold obtained from M by replacing σ with $\overline{\partial D \setminus \sigma}$ (with the orientation on the new simplices coming from ∂D), Proposition 4.15 of [65] shows that M and M' are ambient isotopic. We call such replacement a *cellular move* along D. Hereafter, we will keep calling the manifold M even after applying cellular move.

Remark 5.3.1. We want the new manifold to be oriented, so we need the orientations (induced by σ) on the co-dimension one faces of σ, to agree with the induced orientation coming from the new simplices. This forces the orientation on the new simplices, which is why we require the orientations of the simplices common to M and ∂D to be as above.

[2]Pseudo-radial projection is the linear extension of the restriction of the radial projection to the vertices of the domain, see Chapter 2 in [65].

We will use cellular moves for constructing all our isotopies; they will be of two types:

1. Moving the vertices of M slightly for general position arguments.

2. Replacing a negative simplex with a union of positive simplices.

For the first type of isotopy, we note that for any vertex x of M^k, the union of all k-simplices of M which contain x is a k-cell, and slightly moving x is a cellular move. We note that after moving x slightly, a simplex will remain positive (respectively negative) if it was initially positive (respectively negative). We will say more about the second type of isotopy in Remark 5.3.3, after we make a general observation.

The *join* of two subsets A and B of $\mathbb{R}^n$ is defined to be

$$A * B := \{\lambda a + (1-\lambda)b : a \in A, b \in B, \lambda \in [0,1]\}.$$

We will only use a special case where $A = \{a\}$ is a single point, and $a * B$ is called a *cone*.

Lemma 5.3.2. *Let $\sigma = [p_0, ..., p_k]$ be a k-simplex of M^k in general position in $\mathbb{R}^{k+l}$, and suppose we can find a point $q \in \mathbb{R}^{k+l}$ such that $D = -(q * \sigma)$ (the minus sign indicates that D is oppositely orientated as compared to $q * \sigma$) meets M only in σ, and $\pi(\mathring{D})$ contains O. Then the result of cellular move along D is that σ is replaced by the other simplices of ∂D, and all the new simplices are oppositely oriented compared to σ.*

Proof. We see that the orientations of all the k-faces of $[q, p_0, p_1, ..., p_k]$ agree with the orientations of σ, since when expressed in the basis $\pi(p_0), ..., \pi(p_k)$, all coefficients of $\pi(q)$ are negative since $O \in \pi(\mathring{D})$. Thus all the new simplices are oppositely oriented compared to σ since the induced orientations on new faces come from $-[q, p_0, p_1, ..., p_k]$. □

Remark 5.3.3. In particular, if σ was a negative face to begin with, we can isotope σ to a union of positive simplices, provided we can find a q as in Lemma 5.3.2.

Remark 5.3.4. If we choose q to be any point such that $q * \sigma$ meets M only in σ, and all the coefficients of $\pi(q)$ in the basis $\pi(p_0), ..., \pi(p_k)$ are nonzero, then the result of the cellular move along $-(q * \sigma)$ will be a k-link with each simplex in general position (assuming each k-simplex of M was already in general position), and the orientations of the new simplices can be read off from the sign of the corresponding coefficient. In particular, if one chooses q such that all the coefficients are positive, then the orientations of the new simplices after applying the cellular move would be the same as that of σ.

Remark 5.3.5. We have obtained an alternate way to look at another classical theorem of Alexander (see [2]), which states that every closed oriented piecewise linear k-manifold is a branched cover over S^k. Any such manifold M embeds in $\mathbb{R}^N$ for some $N > k$, and as we saw above, for a generic orthogonal projection to $\mathbb{R}^{k+1}$, all the simplices will be non-degenerate. For any negative simplex σ of M in $\mathbb{R}^{k+1}$, we can choose a point $q \in \mathbb{R}^{k+1}$ such that $q * \sigma$ contains O in its interior. Replacing[3] σ with the other simplices of $-q * \sigma$ gives us a new piecewise linear map from M to $\mathbb{R}^{k+1}$, with one fewer negative simplex. Thus by induction on the number of negative simplices, we can always construct a map from M to $\mathbb{R}^{k+1}$ with all simplices being positive, and by Remark 5.2.2, we get a piecewise linear branched cover of M over S^k by composing with the pseudo-radial projection. It seems likely that this approach will produce a branched cover with fewer number of sheets than Alexander's original construction.

The following lemma shows that it is always possible to find embedded disks to do cellular moves if the crossings are only of one type.

[3]Right now, we are just constructing a new piecewise linear map, and not saying that this operation is an isotopy. However if N is sufficiently large, by Theorem 5.1.3 we can carry out the entire construction by an isotopy.

Lemma 5.3.6. *Suppose $f : M \to \mathbb{R}^{k+l}$ is a embedded closed oriented k-link, and let σ be a k-simplex of M in general position in $\mathbb{R}^{k+l}$ that does not have both overcrossings and undercrossings. Then there is a point $q \in \mathbb{R}^{k+l}$ such that $O \in \pi(\mathring{D})$ and $D \cap M = \sigma$, where $D = -(q * \sigma)$.*

Proof. Let us assume that all crossings are overcrossings (respectively undercrossings). Choose a point $q \in \mathbb{R}^{k+l}$ such that $O \in \pi(\mathring{D})$ and $\pi(q) \notin \pi(M)$. Note that changing only the v-coordinate of q does not change the projection $\pi_v(D)$ (and hence $\pi(D)$), and we will change the v-coordinate of q if necessary. Let $x \in M \setminus \sigma$ be such that there is a point $y_x \in D$ whose image under π_v is the same (since $\pi_v|_D$ is injective, for any given x, there can be at most one y_x) . If we can ensure that the difference of the v-coordinate of x and the v-coordinate of y_x is negative (respectively positive), then we would have $D \cap M = \sigma$. We can in fact reduce to checking this condition for finitely many such points x, as follows: let τ be a simplex of M, then $\pi_v(\tau) \cap \pi_v(D)$ will be a bounded polytope, hence by Proposition 2.7 of [65], the convex hull of finitely many points. So as long as we ensure that the v-coordinates of all points which map to these extreme points of $\pi_v(\tau) \cap \pi_v(D)$ satisfy the required inequality, we have that $D \cap \tau = \sigma \cap \tau$. Now, if this holds for all simplices τ of M then we would have $D \cap M = \sigma$ as required. Since M is compact, there are finitely many simplices τ, and thus we only have to check the inequality for finitely many points.

Now given a point $x \in M \setminus \sigma$ with $\pi_v(x) \in \pi_v(D) \setminus \pi_v(\sigma)$[4], let z be the unique point in σ whose projection under π_v is the point of intersection of $\pi_v(\sigma)$ and the line passing through $\pi_v(x)$ and $\pi_v(q)$. Then we will have that x is below (respectively above) D as long as q is above (respectively below) the point where the line $\pi_v(q) + \ell_v$ (i.e. the translate of ℓ_v which projects to $\pi_v(q)$) meets the line joining x

[4]Note that if $\pi_v(x) \in \pi_v(\sigma)$, then we already know if the crossing at $\pi_v(x)$ is an overcrossing or undercrossing, and this is independent of the v-coordinate of q. This is why we require the condition that σ does not have both overcrossings and undercrossings in the statement of the lemma.

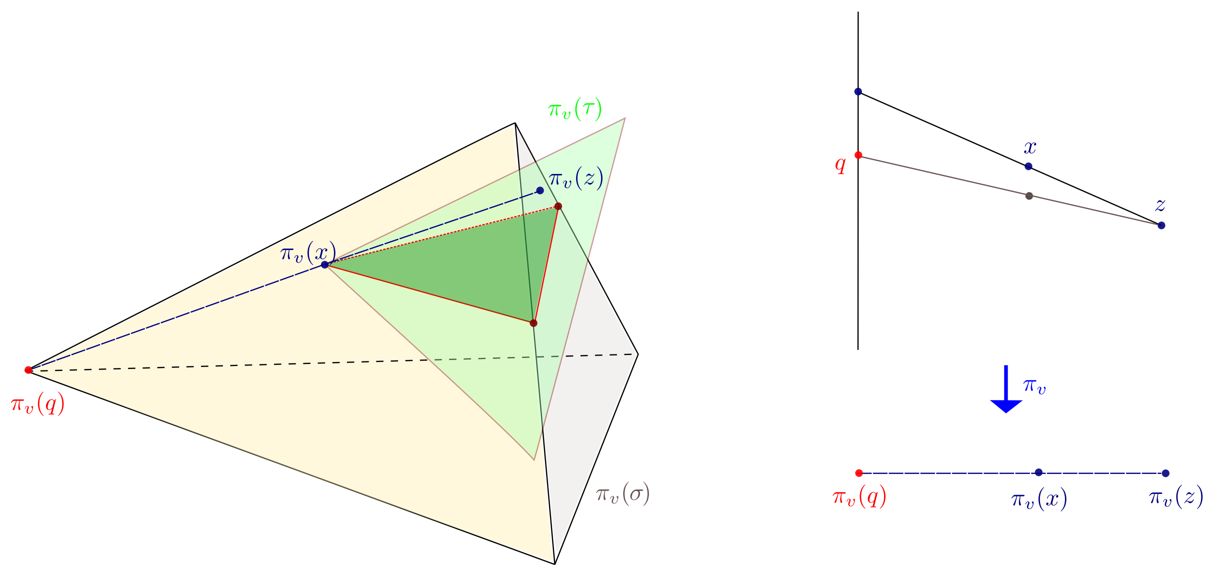

Figure 5.2: The figure in the left shows how τ intersects $q * \sigma$ under the projection π_v. the dashed line segment in dark blue is the line passing through $\pi_v(x)$ and $\pi_v(q)$. The figure on the right shows the plane spanned by this line segment and v projecting onto the line segment.

and z. Thus we see that each such point x gives rise to a lower (respectively upper) bound of v-coordinate of q, and we can simultaneously satisfy finitely many such bounds. The result follows. □

Remark 5.3.7. Sometimes we will not be able to find a q as in Lemma 5.3.6, but we may be able to subdivide σ into cells so that the crossings in each subcell is only of one type and then we have similar results as Lemmas 5.3.6 and 5.3.2. Suppose $f : M \to \mathbb{R}^{k+2}$ is a embedded closed oriented link, and let τ be a k-dimensional cell contained in a negative k-simplex σ of M in $\mathbb{R}^{k+2}$. If τ does not have both overcrossings and undercrossings, then there is a point $q \in \mathbb{R}^{k+2}$ such that $D = -(q * \tau)$ meets M only in τ, and $\pi(\mathring{D})$ contains O. Moreover, the result of cellular move along D is that τ is replaced by a union of positive simplices.

5.4 Co-dimension two braiding

In the first subsection, we will use the tools developed so far to complete the proof of Theorem 5.1.1. We ask some questions about co-dimension two braidings in other cases in the second subsection. We observe that since we have co-dimension $l = 2$, then $\ell = \ell_v$ and $\pi = \pi_v$.

5.4.1 Isotoping a co-dimension two link to be positive

To prove our main result it remains to show the following.

Theorem 5.4.1. *For $1 \leq k \leq 3$, each embedded closed oriented link $f : M^k \to \mathbb{R}^{k+2}$ is isotopic to a positive link.*

Strategy of proof. We will use induction on the number of "negative k-simplices". If all crossings are of one type then we can use cellular moves to replace (isotope) a negative k-simplex with a number of positive k-simplices. Sometimes we will have to break up a negative k-simplex into smaller k-simplices (temporarily increasing the number of negative k-simplices) and show that we can use cellular moves to replace each of the subsimplices, thereby reducing the number of negative k-simplices.

Notation. Let S be a subset of M. We say that a point $x \in S$ is a *double point* of S if $|\pi|_S^{-1}(\pi(x))| \geq 2$, a *triple point* of S if $|\pi|_S^{-1}(\pi(x))| \geq 3$, a *quadruple point* if $|\pi|_S^{-1}(\pi(x))| \geq 4$, and a *quintuple point* of S if $|\pi|_S^{-1}(\pi(x))| \geq 5$. We call the collection of all double (respectively triple) points of a subset S of M the *double* (respectively *triple) point set* of S and denote it by $\mathcal{D}_S$ (respectively $\mathcal{T}_S$), and we call their closure in S the *double* (respectively *triple) point complex* of S and denote it by $\overline{\mathcal{D}_S}$ (respectively $\overline{\mathcal{T}_S}$). If S is not mentioned explicitly, it is understood that S is M. For any k-simplex σ of M, let $\mathscr{T}_\sigma$ denote the closure in σ of $\sigma \cap \mathcal{T}_M$.

Figures. A note on the figures; in the cases $k = 1, 2$, when we are illustrating special cases of crossings on negative k-simplices we will frequently show both an immersed picture, where we will show all the simplices crossing, and a preimage picture, where we indicate all the crossing points in the negative k-simplex. In the case $k = 3$, we can only draw preimage pictures.

Proof of Theorem 5.4.1. We argue the 3 cases for k separately.

Case: $k = 1$ (Alexander, [3]). The proof is by induction on the number of negative 1-simplices of the triangulation of M.

General Position. We can ensure that all the crossings are isolated double points, and there are no triple points.

Special Case. If a negative 1-simplex does not have both overcrossings and undercrossings, then we can use Lemma 5.3.6 to replace the 1-simplex with positive 1-simplices.

General Case. We can break up a negative 1-simplex into smaller 1-simplices such that no part has both overcrossings and undercrossings, and we can apply

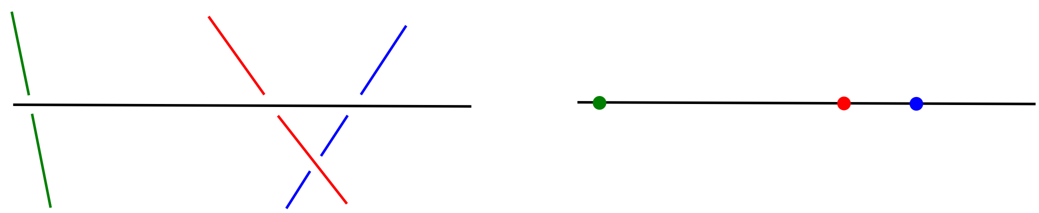

Figure 5.3: Immersed Pictures of 1-simplices intersecting. Preimage picture of the black 1-simplex, where the crossing points are shown.

Lemma 5.3.6 to each of the subsimplices. We note that applying such a cellular move to one such subsimplex does not introduce any new crossings on the other subsimplices of our original negative 1-simplex. Thus we can reduce the number of negative 1-simplices, and we are done by induction for the case $k = 1$.

Digression. For $k = 2, 3$ we have to deal with the fact that if we break up a k-simplex and apply cellular move to the various parts, the result will not be triangulated any more. Of course we could subdivide the adjacent k-simplices so that the result is in fact triangulated, but this may increase the number of negative k-simplices, which we do not want to happen. We will need to modify the induction hypothesis in cases $k = 2, 3$. For this reason, following Kamada (see Chapter 26 in [44]), we will introduce the notion of a division of a piecewise linear manifold.

A *division* for a link $M^k \subseteq \mathbb{R}^{k+2}$ is a collection of k-simplices $\{\sigma_1, ..., \sigma_l\}$ whose union is M, and such that for distinct i and j, if $\sigma_i \cap \sigma_j$ is nonempty, it is contained in faces of both σ_i and σ_j, and is a face of σ_i or σ_j. We say that the σ_i's are k-simplices of the division for M, and the notion of a positive/negative k-simplex is defined as before. We say that a k-simplex σ is *inner* (respectively *outer*) if its intersection with any other k-simplex τ is a face of σ (respectively τ). If σ is inner, then we can break σ up into smaller cells and apply cellular moves on each subcell, and the result would be a division. We can only move a vertex x of a k-simplex σ of M slightly without changing the number of k-simplices of the division if x is a vertex of every k-simplex τ that contains x. In particular if σ is outer, we can slightly move any

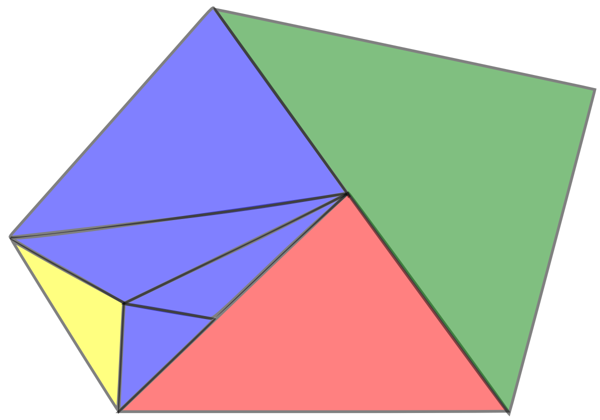

Figure 5.4: A part of a division, where the yellow simplex is both inner and outer, the blue simplices are inner and not outer, the green simplex is outer and not inner, and the red simplex is neither inner nor outer.

of its vertices slightly without changing the number of k-simplices of the division. A division is a triangulation if and only if all k-simplices are both inner and outer. We say a division is *good* if all the negative k-simplices are outer. Lemmas 5.3.2 and 5.3.6 still hold if we have a division of M.

Notation. For any k-simplex σ of M^k, let $X(\sigma)$ denote the union of all the k-simplices which are not adjacent to or equal to σ, let $Y(\sigma)$ denote the complement of σ in M, let $\overline{Y(\sigma)}$ denote the closure of $Y(\sigma)$ in M, and let $Z(\sigma)$ denote the union of all the k-simplices of M whose intersection with σ has dimension at most $k-2$.

We return to the proof of Theorem 5.4.1.

Case: $k = 2$. The proof is by induction on the number of negative 2-simplices of the division of M.

General Position for the initial triangulation. We may assume that all the crossings are double point lines and isolated triple points in the interior of respective 2-simplices, and there are no quadruple points.

Proof. We will make modifications to M in three steps, at each step assuming results from the previous steps hold. In the first step we can make sure that all

2-simplices intersect "nicely" pairwise, and in the last step we will make sure that all triples of 2-simplices intersect "nicely", after which we get the required general position statement. Step 2 is a special case of Step 3, where we make sure all non-adjacent triples of 2-simplices intersect "nicely". By slightly moving each vertex of (the triangulation of) M, we may assume that:

1. The projection of a vertex x of (the initial triangulation of) M is not contained in a hyperplane generated (=affinely spanned) by the projection a 2-simplex τ of M , if $x \notin \tau$.

   If y_1, y_2, y_3 are vertices of a 2-simplex τ of M with $x \notin \tau$. If $\pi(x)$ is contained in the hyperplane H defined by $\pi(y_1), \pi(y_2), \pi(y_2)$ then that means $\alpha(\pi(x)) = 0$ where α is the dual (with respect to the standard inner product) linear functional defined by choosing a unit normal to H in $\pi(\mathbb{R}^4) = \mathbb{R}^3$. By a slight perturbation of x one can ensure that $\alpha(\pi(x)) \neq 0$, and moreover this is generic, i.e. a small perturbation of x would not change the non-vanishing of $\alpha(\pi(x))$. We can keep on perturbing the vertices slightly until the above condition holds.

   This ensures that the projection of two 2-simplices can only intersect in a line segment, that the projection of two 2-simplices that only share a vertex cannot intersect along any edge of either 2-simplex, that the projection of two 2-simplices that share an edge do not intersect elsewhere. Consequently, $\overline{\mathcal{D}_M}$ and $\pi(\overline{\mathcal{D}_M})$ are graphs.

2. For any 2-simplex σ of M, we have that $\pi(\overline{\mathcal{D}_{X(\sigma)}})$ meets $\pi(\sigma)$ and $\pi(\partial\sigma)$ transversely.

   We will only perturb the vertices of σ, and so $\pi(\overline{\mathcal{D}_{X(\sigma)}})$ will stay fixed. Let $[p_1, p_2]$ be an edge of $\pi(\overline{\mathcal{D}_{X(\sigma)}})$. If we make sure that the points p_1, p_2 are not in the hyperplane generated by $\pi(\sigma)$, and the projections of vertices q_1, q_2 and

q_3 of σ are maximally affinely independent with p_1, p_2 (i.e. there is no hyperplane in $\mathbb{R}^3$ containing σ and $[p_1, p_2]$, or equivalently $p_2 - p_1$, $\pi(q_2) - \pi(q_1)$ and $\pi(q_3) - \pi(q_1)$ are linearly independent, or equivalently the determinant of $[p_2 - p_1 | \pi(q_2) - \pi(q_1) | \pi(q_3) - \pi(q_1)]$ is nonzero), then $[p, q]$ and σ have the required property. If we move the vertices of σ slightly, this property still remains true, hence we can make sure that the required property holds for each edge of $\pi(\overline{\mathcal{D}_{X(\sigma)}})$. Slightly perturbing the vertices of M would not change this, and hence we can make sure the property holds for all 2-simplices of M.

3. For any 2-simplex σ of M, we have that $\pi(\overline{\mathcal{D}_{Y(\sigma)}})$ meets $\pi(\sigma)$ and $\pi(\partial\sigma)$ transversely, except at projection of points of $\partial\sigma$ which are not triple points.

   Given any vertex x of M, we can make sure that the set of normal vectors (based at $\pi(x)$) in $\mathbb{R}^3$ to the hyperplane generated by projections of all the 2-simplices that have x has a vertex are maximally affinely independent (i.e. if we think of $\pi(x)$ as the origin, any three of these normal vectors are linearly independent) by perturbing other (i.e. except x) vertices of such 2-simplices. This condition ensures that for any three 2-simplices that share the vertex x, their projection can intersect in at most one point. We can make sure the above condition holds for all vertices x of M. For any 2-simplex σ of M, we can make sure that there is no triple point in any edge of σ by perturbing the vertices of σ slightly, while fixing the hyperplane generated by the projection of σ.

Thus, the projection of any triple of 2-simplices intersect at most one point, and triple points occur in the interior of their respective simplices. □

General Position for a division. For a negative simplex ν, when applying a cellular move along $D = -(q * \nu)$, we may assume that the q and ν are chosen so that $\pi(\overline{\mathcal{D}_{M\setminus\hat{\nu}}})$ meets $\pi(\partial D)$ and $\pi(\delta D)$ transversely. Consequently, there are no quadruple points, and moreover all triple points are isolated and lie in the interior of their respective 2-simplices.

Special Cases. Let us look at some special cases (which will contain previous special cases) of crossings in a negative 2-simplex:

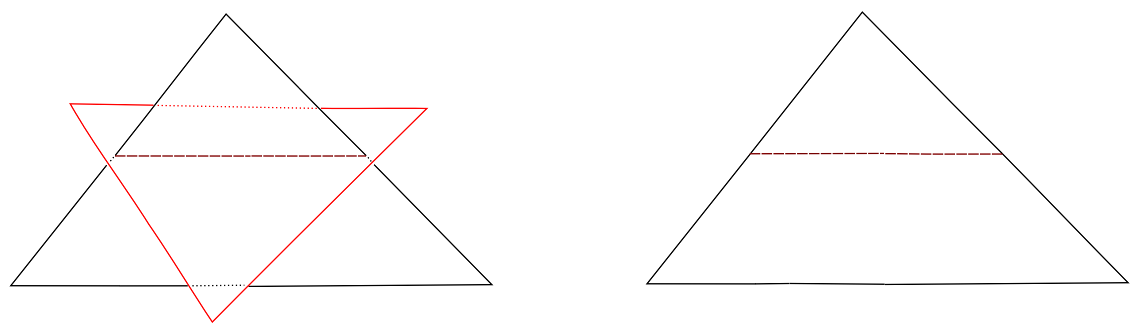

Figure 5.5: Immersed and Preimage Pictures: two non adjacent 2-simplices intersecting in a double point line, illustrating special case 1.

1. Suppose σ is a negative 2-simplex that does not have both overcrossings and undercrossings, see Figures 5.5 and 5.6.

   We can replace σ with a union of positive 2-simplices by Lemma 5.3.6.

2. Suppose σ is a negative 2-simplex such that there are no triple points, see Figure 5.7.

   In this case we can break σ up into smaller 2-simplices which are inner, and moreover each of the subsimplices does not have both overcrossings and undercrossings, and we can use Lemma 5.3.6 to replace each of them with positive 2-simplices. So we can reduce the number of negative 2-simplices by one.

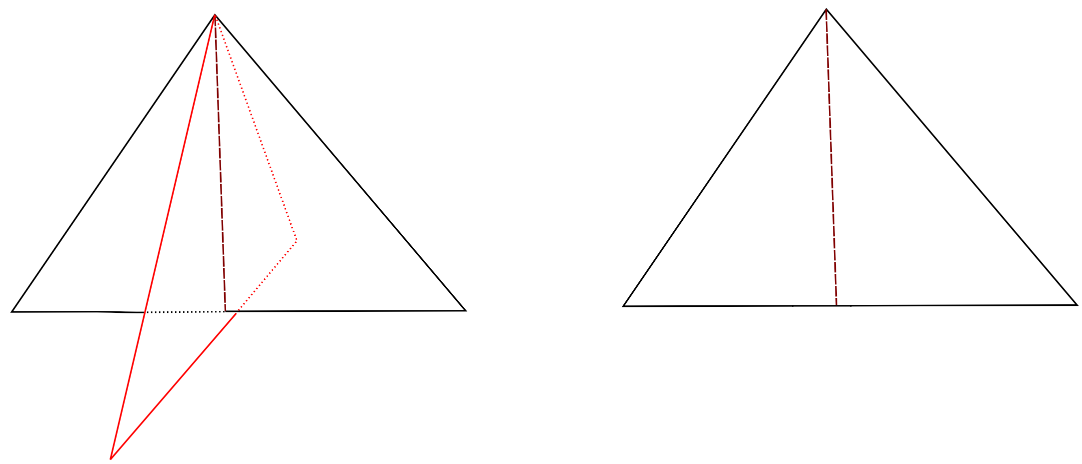

Figure 5.6: Immersed and Preimage Pictures: two 2-simplices sharing a vertex intersecting in a double point line, illustrating special case 1.

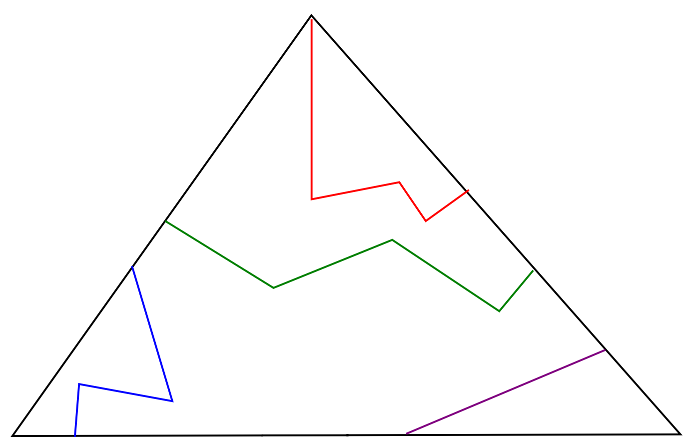

Figure 5.7: Preimage Picture: crossings without triple points, illustrating special case 2.

3. Suppose σ is a negative 2-simplex with exactly one triple point $p \in \sigma$, see Figure 5.8.

   We know that the line segment $[O, \pi(p)]$ can meet the projection of each of the three 2-simplices giving rise to the triple point only in $\pi(p)$ (since all the 2-simplices are in general position), and we choose a point $q \in \mathbb{R}^4$ (the v-coordinate will be changed later if necessary) such that O is in the line

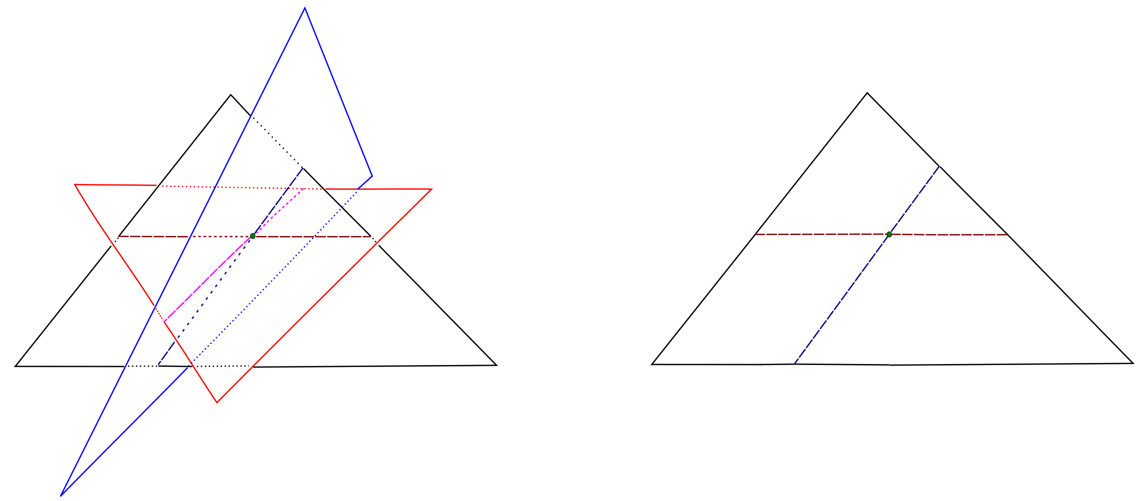

Figure 5.8: Immersed and Preimage Pictures: three non adjacent simplices intersecting in an isolated triple point, illustrating special case 3.

segment $(\pi(q), \pi(p))$. As in the proof of Lemma 5.3.6, by choosing the v-coordinate of q to be sufficiently positive (or negative), we have $[q, p] \cap M = \{p\}$.

Figure 5.9: Replacing a small neighborhood of an isolated triple point by cellular move.

By compactness we have $d([q, p], \overline{Y(\sigma)}) > 0$, and hence we can choose a small 2-simplex $[p_0, p_1, p_2]$ in σ containing p such that $[q, p_0, p_1, p_2]$ meets M only at $[p_0, p_1, p_2]$, and we can use cellular move to replace $[p_0, p_1, p_2]$ by positive 2-simplices, see Figure 5.9. The rest of σ can be broken up into smaller inner

2-simplices each of which does not have both overcrossings and undercrossings, and by Lemma 5.3.6, we can replace them with positive 2-simplices and hence we are done.

General Case. Suppose σ is any negative 2-simplex, see Figure 5.10.

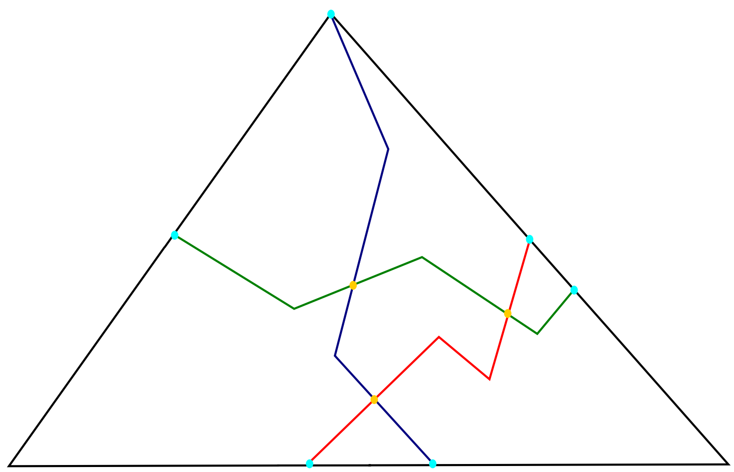

Figure 5.10: Preimage Picture: crossings with triple points, illustrating the general case.

We break σ up into smaller inner 2-simplices each of which has at most one interior triple point and then use the above special cases. Thus we can reduce the number of negative simplices, and we are done by induction for the case $k = 2$.

Case: $k = 3$. It suffices to prove the following claim, since the initial triangulation is a good division.

Claim 5.4.2. *Every embedded closed oriented link M^3 in $\mathbb{R}^5$ with a good division is isotopic to a positive link.*

The proof of the claim is by induction on the number of negative 3-simplices on the good division.

Remark 5.4.3. After we prove the claim, it follows that the result holds for any division, because we can subdivide any division further so that it becomes a good division.

General Position. We may assume that the double point complex is a 2-dimensional CW-complex, the triple point complex is a graph, all quadruple points are isolated and in the interior of respective 3-simplices, and there are no quintiple points. Moreover we can also assume that all triple points are disjoint from 1-faces of 3-simplices, and for any vertex x of $\overline{\mathcal{T}_M}$, the set $\pi|_M^{-1}(\pi(x))$ contains exactly one point on the 2-faces of 3-simplices of M.

Remark 5.4.4. This can be proved in a similar way we proved the general position statement in the case $k = 2$, and we outline an argument below. By slightly moving each vertex of (the triangulation of) M, we may assume that for the initial triangulation we have:

1. The projection of a vertex x of M is not contained in a hyperplane generated by the projection a 3-simplex τ of M, if $x \notin \tau$. Consequently, $\overline{\mathcal{D}_M}$ and $\pi(\overline{\mathcal{D}_M})$ are 2-dimensional CW-complexes.

2. For any 3-simplex σ of M, $\pi(\overline{\mathcal{D}_{Y(\sigma)}})$ and the edges of $\pi(\overline{\mathcal{D}_{Y(\sigma)}})$ meets $\pi(\sigma)$ and $\pi(\partial\sigma)$ transversely, except at projection of points of $\partial\sigma$ which are not triple points. Hence, $\overline{\mathcal{T}_M}$ and $\pi(\overline{\mathcal{T}_M})$ are graphs, and for any vertex x of $\overline{\mathcal{T}_M}$, the set $\pi|_M^{-1}(\pi(x))$ contains exactly one point on the 2-faces of 3-simplices of M.

3. For any 3-simplex σ of M, $\pi(\overline{\mathcal{T}_{Y(\sigma)}})$ meets $\pi(\sigma)$ and $\pi(\partial\sigma)$ transversely, except at projection of points of $\partial\sigma$ which are not quadruple points.

Now we have the required general position statement for the initial triangulation. At each step of applying cellular move along $D = -(q * \nu)$, we may assume that ν is chosen so that there are no vertices of $\overline{\mathcal{T}_M}$ in the 2 faces of ν except the case that such a point is in $\overline{\mathcal{T}_M} \setminus \mathcal{T}_M$, q is chosen so that $\pi(\overline{\mathcal{D}_{M\setminus\mathring{\nu}}})$ and $\pi(\overline{\mathcal{T}_{M\setminus\mathring{\nu}}})$ meets $\pi(\partial D)$ and $\pi(\delta D)$ transversely. We will then have the required general position statement.

Special Cases. We will look at some special cases (which typically will contain previous special cases) of crossings in a negative 3-simplex:

1. Suppose σ is a negative 3-simplex such that all crossings are overcrossing (respectively undercrossing).

   We can replace σ with a union of positive 3-simplices by Lemma 5.3.6.

2. Suppose σ is a negative 3-simplex such that there are no triple points.

   In this case we can break σ up into smaller inner 3-simplices such that the crossings are only overcrossing or undercrossing (but not both), and we can use Lemma 5.3.6 to replace each of them with positive 3-simplices. So we can reduce the number of negative 3-simplices by one.

3. Suppose σ is a negative 3-simplex with exactly one triple point line segment $[p_0, p_1]$ (with p_0 and p_1 not in a vertex or edge of σ) coming from 3-simplices τ (above σ) and η (below σ) [5] which are not adjacent to σ, and such that $\pi(\tau) \cap \pi(\eta)$ contains the projection of $[p_0, p_1]$ in its interior, and there are no quadruple points in σ, see Figure 5.11.

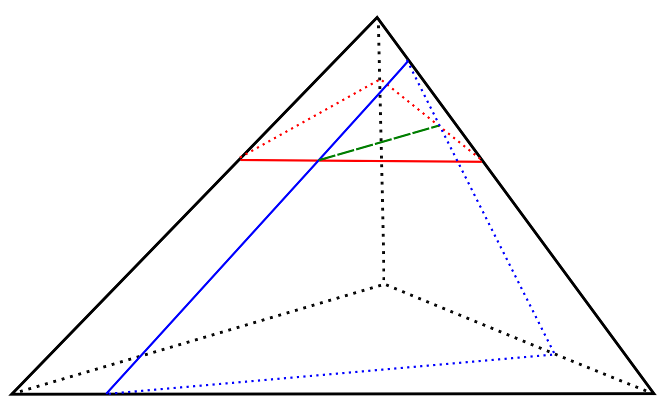

Figure 5.11: Preimage Picture: a 3-simplex intersecting with two non adjacent 3-simplices in a triple point line segment, illustrating special case 3.

[5]Note that if both τ and η are above (respectively below) σ, then the crossings in σ corresponding to τ and η are both undercrossings (respectively overcrossings), and we are in special case 2.

Since the 3-simplices τ and η are in general position the 2-simplex $[O, \pi(p_0), \pi(p_1)]$ meets $\pi(\tau)$ and $\pi(\eta)$ only in $[\pi(p_0), \pi(p_1)]$. We choose a point $q \in \mathbb{R}^5$ (the v-coordinate will be changed later if necessary) such that O is in the interior of $[\pi(q), \pi(p_0), \pi(p_1)]$, and consequently the 2-simplex $[\pi(q), \pi(p_0), \pi(p_1)]$ meets $\pi(\tau)$ and $\pi(\eta)$ only in $[\pi(p_0), \pi(p_1)]$. The hypotheses ensures that in $[\pi(q), \pi(p_0), \pi(p_1)]$ we do not see other (i.e. except $[\pi(p_0), \pi(p_1)]$) lines of over or under crossings starting from the vertices $\pi(p_0), \pi(p_1)$. Just like in the proof of Lemma 5.3.6, we may choose the v-coordinate of q to be sufficiently positive (or negative) such that:

(a) If ρ is a 3-simplex whose intersection with σ is 2 dimensional, then the cone D meets ρ only in $\sigma \cap \rho$.

(b) $[q, p_0, p_1]$ does not intersect $Z(\sigma)$.

By compactness, the distance between $[q, p_0, p_1]$ and $Z(\sigma)$ is positive, and hence we can choose a cell ν in σ containing $[p_0, p_1]$ such that $q * \nu$ meets M only in ν. Using Remark 5.3.7, we can use a cellular move to replace ν with a finite union of positive 3-simplices, and can break the rest of σ into smaller inner 3-simplices and use Lemma 5.3.6 to replace them with positive 3-simplices. So we can reduce the number of negative 3-simplices by one.

4. Suppose σ is a negative 3-simplex such that $\mathscr{T}_\sigma$ is non empty but does not meet σ in a vertex or an edge, see Figure 5.12.

   There will be finitely many points $p_1, ..., p_m$ in the interior of σ which are either a quadruple point or a vertex of the triple point complex $\overline{\mathcal{T}_M}$. We can choose points $q_1, ..., q_m$ such that $O \in (\pi(q_i), \pi(p_i))$ and each of these line segments $[q_i, p_i]$ are mutually disjoint. Like before, we can find 3-simplices P_i containing p_i in σ such that $q_i * P_i$ are mutually disjoint, and then we can use cellular moves to replace each P_i with union of positive 3-simplices. The rest

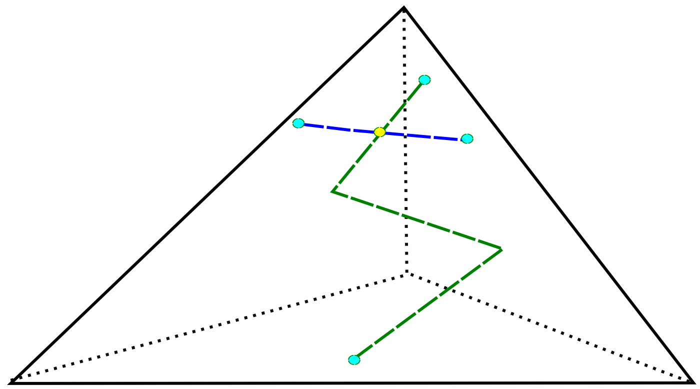

Figure 5.12: Preimage Picture: a 3-simplex with triple point lines meeting at a quadruple point, illustrating special case 4 (double points not indicated).

of σ can be broken up into smaller inner 3-simplices such that we are in the previous special cases. The hypothesis and our general position statement ensures that for all subsimplices which contain triple point line segments, we are in the previous special case. As we have seen, we can replace each of these 3-simplices by positive 3-simplices, and hence we can reduce the number of negative 3-simplices by one.

The special cases of crossings in negative 3-simplices we considered so far are analougus to the ones we saw in the case $k = 2$. In next two special cases we will consider the "new" type of crossings, when $\mathscr{T}_\sigma$ meets a vertex or an edge of σ, and we will need a new idea.

5. Suppose σ is a negative 3-simplex, with the only crossings coming from 3-simplices τ (above) and η (below) who share a vertex p_0 with σ. Moreover, there is triple point semiopen line segment $(p_0, p_1]$ in σ, and $\pi(\tau) \cap \pi(\eta)$ contains $\pi(p_0, p_1]$ in its interior, see Figure 5.13.

   Let σ_1, σ_2 be the subcells of σ such that the hyperplane generated by $\pi(\tau)$ breaks $\pi(\sigma)$ into the two parts $\pi(\sigma_1)$ and $\pi(\sigma_2)$, and let us assume that $\pi(\sigma_1)$ is in the same half-space as O. As in the proof of Lemma 5.3.6, we can choose a

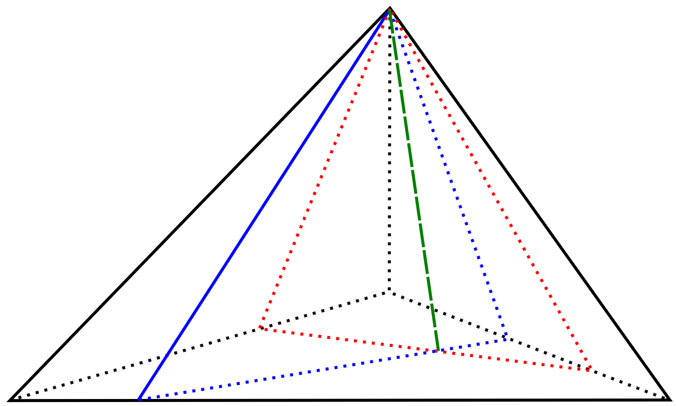

Figure 5.13: Preimage Picture: three adjacent 3-simplices sharing a vertex intersecting in a triple point semiopen line segment, illustrating special case 5.

point (by making the v-coordinate sufficiently positive) q such that the cone $q * \sigma_1$ meets M only in σ_1, and O is in the interior of $\pi(q * \sigma_1)$. We use a cellular move to replace σ_1 by the other faces of this cone. If τ is negative, it must be a outer 3-simplex (since we assumed that the division is good), and hence we can move some of the other (except p_0) vertices of τ a little (so that the projection of the vertices lie in the half-space generated by the old $\pi(\tau)$, containing O) so that σ_2 does not have any triple point. If τ is positive, we can apply a cellular move on a smaller subsimplex (so that all the new 3-simplices are positive) of τ containing the triple points, so that σ_2 does not have any triple point. By using the above special cases, we see that we can replace σ_2 with a union of positive 3-simplices, and we have reduced the number of negative 3-simplices by one.

A similar argument works in the next special case:

6. Suppose σ is a negative 3-simplex, with the only crossings coming from 3-simplices τ (above) and η (below), where only one of τ or η shares an edge with σ. Moreover, there is triple point semiopen line segment $(p_0, p_1]$ in σ, where p_0 lies in the common edge, and $\pi(\tau) \cap \pi(\eta)$ contains $\pi(p_0, p_1]$ in its

interior, see Figure 5.14.

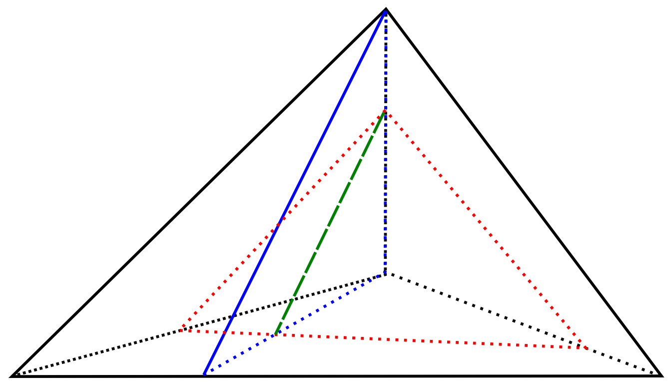

Figure 5.14: Preimage Picture: a 3-simplex intersecting with a non-adjacent 3-simplex and one sharing an edge in a triple point semiopen line segment, illustrating special case 6.

General Case. Suppose σ is any negative 3-simplex.

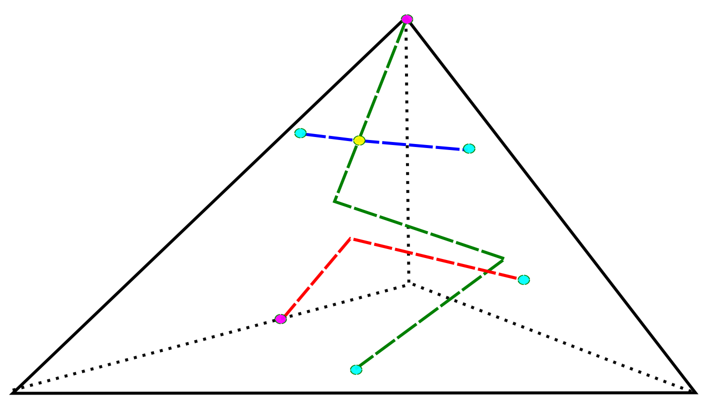

Figure 5.15: Preimage Picture: a 3-simplex with triple points (some of whom converge to a vertex or an edge) and quadruple points, illustrating the general case (double points not indicated).

Let us first consider all the points where $\mathscr{T}_\sigma$ meets a vertex or an edge of σ, and by special cases 5 and 6, we can find small inner 3-simplices containing these points where we can apply cellular moves and replace them with positive 3-simplices. We can break the rest σ up into small inner 3-simplices so that we are special case 4, and as we have seen, we can replace each of the subsimplices with positive 3-simplices, thereby reducing the number of negative 3-simplices by one. This completes the proof of Theorem 5.4.1 for the case $k = 3$. $\square$

5.5 Higher co-dimension braiding

In the first subsection, we will use the tools developed so far to complete the proof of Theorem 5.1.3. We end with some questions about higher co-dimension braidings in the second subsection.

5.5.1 Isotoping higher co-dimension link to be positive

To prove Theorem 5.1.3 it remains to show the following.

Theorem 5.5.1. *Any closed oriented piecewise linear k-link $f : M \to \mathbb{R}^{k+l}$ can be piecewise linearly isotoped to be a closed braid for $2l \geq k + 2$.*

Remark 5.5.2. In case $k = 1$ or 2, then $l = 2$ satisfies the hypothesis of the above theorem, and we know in this case the result follows from Theorem 5.4.1. In the rest of the section, we will assume that $l \geq 3$. We will also assume that $l \leq k + 1$, since otherwise[6] it is easy to see that the Theorem holds, as there will be no crossings in the projection under π_v. In fact one can show if $l > k+1$, then any two embeddings of M^k in $\mathbb{R}^{k+l}$ are isotopic (see [65, Corollary 5.9]) .

The proof will be similar to the proof of case $k = 2$ of Theorem 5.4.1, and we will not discuss special cases of negative simplices this time.

Proof. The proof will be by induction on the number of negative simplices in the division of M. Let us consider the projection under $\pi_v : \mathbb{R}^{k+l} \to \mathbb{R}^{k+l-1}$, and see what we can say about the crossings under the given hypothesis $2l \geq k + 2$.

For any two simplices σ and τ, we may assume that $\pi_v(\sigma)$ and $\pi_v(\tau)$ intersect transversely in $\pi_v(\mathbb{R}^{k+l}) = \mathbb{R}^{k+l-1}$, and in that case the intersection of the affine

[6] The proof given still holds if $l > k + 1$, one just has to interpret statements (like negative dimensional space) correctly.

subspaces generated by them have dimension $2k-(k+l-1)=k-l+1$. We may assume that for any triple of simplices τ, σ and ν, that $\pi_v(\sigma\cap\tau)$ intersects $\pi_v(\sigma\cap\nu)$ transversely in $\pi_v(\sigma)$, and in that case the intersection has dimension $k-2(k-l+1)=k-2l+2\leq 0$. Consequently, all triple points are isolated and can be assumed to be in the interior of their respective simplices.

General Position for the initial triangulation. We may assume that all the crossings are double point complex is $(k-l+1)$-dimensional CW-complex, all triple points are isolated and in the interior of respective k-simplices, and there are no quadruple points.

General Position for a division. When applying a cellular move along $D=-(q*\nu)$, we may assume that the q and ν are chosen so that $\pi_v(\overline{\mathcal{D}_{M\setminus\mathring{\nu}}})$ meets $\pi_v(\partial D)$ and $\pi_v(\delta D)$ transversely. Consequently, there are no quadruple points, and moreover all triple points are isolated and lie in the interior of their respective k-simplices.

Now given any negative simplex σ, it will contain finitely many triple points $p_1,...,p_m$ in its interior. We can choose points $q_1,....,q_m$ such that $O\in(\pi_v(q_i),\pi_v(p_i))$ and each of these line segments $[q_i,p_i]$ are mutually disjoint, and do not intersect the rest of M. Using Remark 5.3.7 we can find k-simplices P_i containing p_i in σ such that q_i*P_i are mutually disjoint, and then we can use cellular moves to replace each P_i by a union of positive k-simplices. The rest of σ can be broken up into smaller inner k-simplices such that there are only crossings of one type, and then by Lemmas 5.3.2 and 5.3.6, we can replace σ with a union of positive simplices. We have reduced the number of negative simplices by one, and hence we are done by induction. $\square$

CHAPTER 6

LIFTING HONEST COVERINGS TO BRAIDED EMBEDDINGS

In this and subsequent chapters, we will study the lifting problem in various different scenarios. In this chapter we will discuss the lifting problem in the context of honest covers. We will go over general results of Hansen and Peterson, and discuss the lifting problem of coverings of surfaces in detail. Along the way, we found an error in a thirty year old result, see Remark 6.3.6. We also give a affirmative answer to the question of lifting all honest coverings over orientable surfaces, although it will rely on results from later chapters.

6.1 Hansen's criterion for lifting of covers

Given a honest covering map, we have the following criterion for lifting it to a codimension two braided embedding.

Proposition 6.1.1. *[32] A finite sheeted covering map $p : M \to N$ lifts to a braided embedding $f : M \to N \times D^2$ if and only if the associated permutation monodromy map $\phi : \pi_1(N) \to S_n$ lifts to a braid monodromy $\psi : \pi_1(N) \to B_n$, so that $Forget \circ \psi = \phi$.*

The key ingredient for the proof of the above proposition is Fadell, Fox, and Neuwirth's result that the configuration space is aspherical, and we already outlined the proof of the hard direction in Section 3.3. Again, given a branched covering map, we can delete the branch locus and see if the resulting covering lifts using this criterion, and if it does we can try to extend it over the branch locus.

It follows from the above criterion that any covering over a space with free fundamental group lifts to a braided embedding. Moreover, one has a complete characterization when the fundamental group is finitely generated and abelian.

Proposition 6.1.2. *[62, Theorem 5.5] If $\pi_1(X)$ is finitely generated and abelian, then a covering $p : Y \to X$ lifts to a braided embedding iff $p_*(\pi_1(Y))$ contains all the torsion of $\pi_1(X)$.*

In particular, this implies:

Claim 6.1.3. *All finite sheeted coverings over an n-torus lifts to a braided embedding.*

This claim is also follows by combining Proposition 2.2.5 and Proposition 6.2.1.

Hansen's criterion also gives us examples of non-liftable covers. Since the braid groups B_n are known to be torsion free, we get the following immediate obstruction to lifting:

Claim 6.1.4. *If $\alpha \in \pi_1(N)$ is torsion, and the permutation monodromy of α is non-trivial, then the permutation monodromy does not lift to a braid monodromy.*

In particular, if we apply this claim for the monodromy of the cover $a_2 : S^2 \to \mathbb{RP}^2$, then we recover Borsuk Ulam theorem in this dimension.

6.2 Liftings of composition of branched coverings

Suppose we have two branched covering maps $q : Y \to X$ and $p : Z \to Y$, so that their composition $r = q \circ p$ is also a branched covering.

Proposition 6.2.1. *If $p : Y \to X$ lifts to a codimension-l braided embedding with trivial normal bundle, and $q : Z \to Y$ lifts to a codimension-l braided embedding; then so does the composition $r = q \circ p$.*

Proof. We identify the normal bundle of the image braided embedding of Y in $X \times D^l$ with $Y \times D^l$, and then use the braided embedding of Z in $Y \times D^l$ to obtain a braided embedding lifting r. □

Remark 6.2.2. We note that the trivial normal bundle condition is always satisfied in case of honest coverings, and in that case this result is proved in [62, Theorem 4.1].

We will see how the monodromy map of such a composite braided embedding looks like in the next subsection. Let us now discuss a partial converse to the above proposition.

Proposition 6.2.3. *If $r : Z \to X$ lifts to a codimension-l braided embedding, then so does $q : Z \to Y$ (possibly to a non-locally flat braided embedding).*

Proof. Consider a braided embedding $R : Z \to X \times D^l$ lifting r. By composing with projection to the second factor, we obtain a separating map (i.e. which sends different pre-images of a point in the base space to distinct points) $s = pr_2 \circ R : Z \to D^l$. We claim that s is also a separating map for p (i.e. $p \times s : Z \to Y \times D^l$ is a braided embedding lifting p). To see this, consider an arbitrary point $y \in Y$ and consider two pre-image points z_1 and z_2 under p. If it happens that $s(z_1) = s(z_2)$, then s cannot be a separating map for r since $r(z_1) = q(y) = r(z_2)$. The result follows. $\square$

Remark 6.2.4. In the setting of the above proposition, p need not lift to a braided embedding, for instance see Remark 6.3.6.

Remark 6.2.5. The above proposition also generalizes to maps other than branched coverings, like the ones considered by Melikhov [58].

6.3 Liftings of two fold coverings over the Klein bottle

Let us consider two 2-fold coverings over the Klein bottle K, which has fundamental group $\pi_1(K) = \langle a, b | a^2 b^2 \rangle$.

Example 6.3.1. The first cover we will consider is the orientation double cover, that unwraps both the one-handles so the resulting cover is a torus. In other words this corresponds to the monodromy map:

$$a \mapsto (12), b \mapsto (12).$$

Example 6.3.2. The second cover we will consider is the also two sheeted cover, but one which unwraps only the first one-handle. In other words this corresponds to the monodromy map:

$$a \mapsto (12), b \mapsto I.$$

The resulting cover is a connected non-orientable surface which has zero Euler characteristic, i.e. it is the Klein bottle.

6.3.1 Liftability the above examples to braided embeddings

Let us now consider the problem about lifting of the two coverings over the Klein bottle to braided embeddings, or equivalently if we can lift the permutation monodromy maps to a braid monodromy.

Claim 6.3.3. *The orientation double cover $f : \mathbb{T} \to K$ of the torus over the Klein bottle lifts to a braided embedding.*

Proof. We have the braid monodromy $\pi_1(K) \to B_2$ sending

$$a \mapsto \sigma_1, b \mapsto \sigma_1^{-1},$$

which lifts the permutation monodromy in Example 6.3.1. □

Claim 6.3.4. *The two sheeted cover $g : K \to K$ of the Klein bottle over itself described in Example 6.3.2 does not lift to any braided embedding.*

Proof. Suppose not, say there is a braid monodromy $\pi_1(K) \to B_2$ lifting it which sends

$$a \mapsto \sigma_1^m, b \mapsto \sigma_1^n \quad \text{for some integers } m \text{ and } n.$$

It must be the case that m is odd and n is even, as we obtain the symmetric group S_2 from the braid group B_2 by adding the relation $\sigma_1^2 = 1$. Then the image of a^2b^2

is $\sigma_1^{2(m+n)}$, which cannot be the identity as $2(m+n)$ is not divisible by 4.

□

Remark 6.3.5. Up to equivalence, there are only two connected two sheeted covering of the Klein bottle, the ones we discussed above. There is also a disconnected covering, with permutation monodromy

$$a \mapsto I, b \mapsto I,$$

which lifts to the braid monodromy

$$a \mapsto 1, b \mapsto 1.$$

Remark 6.3.6. We obtain the following commuting diagram of covering maps by using the two coverings and pull-backs.

$$\begin{tikzcd} \mathbb{T} \arrow[r, "g^*f"] \arrow[d, "f^*g"'] & K \arrow[d, "g"] \\ \mathbb{T} \arrow[r, "f"] & K \end{tikzcd}$$

We see that by Claims 6.3.3 and 6.1.3 both the coverings f and f^*g lift to braided embeddings, and hence by Proposition 6.2.1, so does their composition $f^*g \circ f = g^*f \circ g$. However, by Claim 6.3.4, g does not lift to any braided embedding. This gives a counterexample to one half of one direction of [62, Theorem 4.2][1]. The gap in the proof of [62, Theorem 4.2] arises from subtleties in continuous variation of roots with respect to coefficients of polynomials.

[1]The other parts of this Theorem are essentially the same as the results mentioned in Section 6.2. However the hypothesis and the proofs of statements vary slightly, as here we restrict to finite sheeted coverings; and allow branched coverings.

6.3.2 Liftability of covers over the Klein bottle

In this subsection we will explore some covers over Klein bottle which do (not) lift to braided embeddings. For notational convenience, in this section we will change our presentation of the fundamental group of the Klein bottle K by replacing the generator with its inverse. Thus $\pi_1(K) = \langle x, y | x^2 = y^2 \rangle$. So the question about liftability of covers can be rephrased as:

Question 6.3.7. Given two permutations a and b with $a^2 = b^2$, can we find braids α and β lifting a and b respectively, and $\alpha^2 = \beta^2$?

The answer, as we have seen is not always yes, and let us try to find what some of the the obstructions are. The first one comes from the sign of the permutations (and exponent sum of braids).

Claim 6.3.8. *If the answer to Question 6.3.7 is affirmative, then permutations a and b have to have the same sign, i.e. both are even or both are odd.*

Proof. Suppose not, say a is even and b is odd. Then $\exp(\alpha)$ is even and $\exp(\beta)$ is odd, so $\exp(\alpha^2)$ is divisible by four while $\exp(\beta^2)$ is not, contradicting $\alpha^2 = \beta^2$. □

The next question we may ask is if a and b satisfying $a^2 = b^2$ have the same sign, then can we find lifts α and β with the required properties? The answer is 'No' as the following claim and example shows.

Claim 6.3.9. *If the answer to Question 6.3.7 is affirmative, then permutations a and b have to be conjugate.*

Proof. By [30], roots in the braid group are unique up to conjugation, and thus if $\alpha^2 = \beta^2$ in the braid group, the braids α and β are conjugate, whence the associated permutations a and b have to be conjugate in the symmetric group. □

Example 6.3.10. Consider $a = (123456)$ and $b = (153)(164)$, then $a^2 = (135)(264) = b^2$, and a and b are not conjugate since they have different cycle types. Thus by the claim above, the corresponding cover does not lift.

Proposition 6.3.11. *Any covering of a torus over the Klein bottle lifts to a braided embedding.*

Proof. If we have any covering of torus over the Klein bottle, then it must factors through the orientation double cover by Proposition 2.2.9. We know that by claims 6.1.3 and 6.3.3, both these coverings lift to braided embedding, and hence so does the composition by Proposition 6.2.1 (or by [62, Theorem 4.1]).

□

6.3.3 Lifting of coverings over general surfaces

Now that we have seen several non-liftable covers over a non-orientable surface (and it is easy to generalize this to higher geneus non-orientable surfaces), we can restrict our attention to orientable surfaces and ask if every covering lifts. The answer turns out to be 'Yes', but the only proof we have will use results about lifting branched coverings, discussed in later chapters.

Theorem 6.3.12. *Every covering of over an orientable surface lifts to a braided embedding.*

Proof. Given any covering $p : \Sigma_g \to \Sigma_h$, we can compose with the two sheeted branched covering q of Σ_h over S^2 obtained by quotienting by the hyperelleptic involution. The resulting composition $r = q \circ p : \Sigma_g \to S^2$ is a branched covering. By Theorem 8.3.1, we know that any branched covering over the sphere lifts to a braided embedding. The result now follows from Proposition 6.2.3.

□

CHAPTER 7

EXTENDING BRAIDED EMBEDDINGS OVER THE BRANCH LOCUS

In the previous chapter we saw a criterion to lift honest covers to codimension two braided edmbeddings. In this chapter, consider the scenario where the associated covering of a branched cover lifts to a braided embedding, and we discuss when we can extend it to obtain a braided embedding lifting the branch cover. It turns out that the results vary between the smooth and piecewise linear categories. We will begin by introducing some terminology in the first section; finding local models in dimension two in the second section, and extend it in higher dimensions in the third section.

7.1 Completely split links

We will say that a link L in the solid torus $S_1 \times D^2$ is a completely split link in regular form there are disjoint sub-discs $D_1, ..., D_k$ so that each component of L lies in a different solid tori $S^1 \times D_i^2$. We will say that a link in the solid torus $S_1 \times D^2$ is a completely split link if it is isotopic in the solid torus to a completely split link in regular form.

We will say a link in the solid torus $S_1 \times D^2$ is a completely split unlink if it is a completely split link and each component is an unknot (i.e. bounds a ball in S^3).

We define a closed braid $\hat{\beta}$ to be a standard unknot in the solid torus if $\beta \in B_n$ is conjugate to $\sigma_1 ... \sigma_{n-1}$ (all positive crossings) or $\sigma_1^{-1} ... \sigma_{n-1}^{-1}$ (all negative crossings).

We define a closed braid to be a standard unlink in the solid torus if it a completely split link so that each component is a standard unknot.

Let us consider the following subsets of the braid group, as introduced by Kamada (see [44, Section 16.5] for details)

$$A_n := \{b \in B_n | \text{ the closure } \hat{b} \text{ of } b \text{ is completely split unlink}\}$$

$$SA_n := \{b \in B_n | b \text{ is conjugate to } \sigma_1^{\pm 1}\}$$

We observe that A_n consists of precisely all the elements of B_n such that coning over $\hat{b} \in D_1^2 \times S^1$, produces a locally flat disk in $D_1^2 \times D_2^2$, and $SA_n \subset A_n$.

7.2 Local models near branch points in dimension two

In this section we will find necessary and sufficient conditions for extend a braided embedding of a punctured two dimensional disc (the puncture being one branch point removed) over the puncture. In the next section we will extend it to a more general setup.

Suppose we have a braided embedding (in either piecewise linear or smooth categories) over a disc D_b^2 with a single branch point O, $f : \sqcup_{i=1}^{j} D_i^2 \hookrightarrow D_b^2 \times D^2$, with $p_i := pr_1 \circ f|_{D_i} : D_i^2 \to D_b^2$ a branched covering map with at most one branch point at O. Note that j equals the number of cycles (including the fixed elements) in the permutation corresponding to a loop surrounding O in the monodromy representation. Let us suppose the points above O_i is the unique point in D_i^2 mapping to O under p_i. We note that $pr_2 \circ f$ maps the O_i to distinct points in D^2, as all of them project to the same point O under $pr_2 \circ f$ and f is an embedding. Hence we can choose a small closed disc C_ϵ around O so that when we set $C_i = p_i^{-1}(C_\epsilon)$, the images $pr_2 \circ f(C_i)$ are disjoint for different i.

Let us look at the braid monodromy of braided embedding induced from f, once we remove O and O_i's. Since the fundamental group of $D_b^2 \setminus \{O\}$ is infinite cyclic freely generated by any circle γ_r of radius r, where $0 < r < 1$. Thus the braid monodromy is completely determined by $\psi(\gamma_r)$, and we will call this the *braid sur-*

rounding the branch point O. Note that if we pick C_ϵ to be the disc of radius ϵ centered at the origin, then $\psi(\gamma_\epsilon) = f(\sqcup_{i=1}^{j} \partial C_i)$ is the closure of the braid surrounding the branch point in the solid torus $\gamma_\epsilon \times D^2$. Let us now see what constraints we get on the braids surrounding the branch point O.

7.2.1 Piecewise linear category

In case we are working in the piecewise linear category, we may assume that we chose the disc C_ϵ small enough so that f is defined on $\sqcup_{i=1}^{j} C_i$ by coning $\sqcup_{i=1}^{j} f(\partial C_i)$ over the points $f(O_i)$, independently for each i. Since the images $f(C_i)$ are disjoint, we see that the braid surrounding the branch point must be reducible if $j > 1$.

Moreover since the embedding must be locally flat it must be locally flat near the points O_i which means the image $f(\partial C_i)$ must be an unknot in the solid torus $\gamma_\epsilon \times D^2$. Thus we see that $\psi(\gamma_\epsilon)$, the braid surrounding the branch point must be a completely split unlink.

Conversely given any closed braid which completely split unlink (without loss of generality, let us assume it is in regular form) and satisfies the appropriate permutation restrictions (i.e. agrees with the permutation monodromy at O), we can extend it to a (locally flat) piecewise linear braided embedding over the entire disc. To see this let us assume the various components $L_1, .., L_j$ of the closed braid lie in disjoint solid tori $S_1 \times N_1, ..., S_1 \times N_j$. For each $i \in \{1, ..., j\}$, let us pick a point $n_i \in N_i$, and we can then set $f(O_i) = (O, n_i)$, and we can cone L_i (in $\partial C_\epsilon \times D^2$) at $f(O_i)$, and get a well defined braided embedding over C_ϵ. Note that since the projections under p_2 of various coning operations are concentrated within the disjoint discs N_i, we see that the above map is indeed injective. Therefore we obtain,

Lemma 7.2.1. *A braided embedding of a disjoint union of circles (i.e. a closed braid), it extends piecewise linearly to a braided embedding of a disjoint union of discs with one branch point if and only if the closed braid is a completely split unlink.*

7.2.2 Smooth Category

Similarly to the piecewise linear category, we see that the braid surrounding the branch point must be completely split, however there are more conditions to smoothly extend it over a branch point. Let us restrict f (and call this restriction f_i) to one of the nontrivial (i.e. we have actual branching) components D_i^2 and see what braid we get. The Jacobian matrix at the O_i will look like $Df_i = [0|A]$, as $pr_1 \circ f$ has a local model $z \mapsto z^n$ with $n > 1$. Since f_i is an embedding Df_i must have rank 2, and hence A is an invertible 2×2 matrix. By inverse function theorem $pr_2 \circ f$ is a local diffeomorphism. So the circle $\{|z| = a\}$ in D^2 embeds in D_2^2 via $pr_2 \circ f_i$ for small a. By the Schoenflies theorem in the plane and isotopy extension theorems we see that $p_2 \circ f_i$ is isotopic to either the identity or complex conjugation near O_i[1]. Thus, f_i is locally equivalent (= isotopic in a sufficiently small neighborhood of O_i) to f_+ or f_-, where the maps $f_\pm : D_a^2 \to D_b^2 \times D^2$ defined by $z \mapsto (z^n, z)$ and $z \mapsto (z^n, \bar{z})$. It therefore suffices to understand what the braids surrounding the branch points in the local models $f_\pm$ are. By choosing the n-th roots of unity as collection of n distinct points, it is clear geometrically that we get a positive (respectively negative) partial twist for f_+ (respectively f_-); i.e. the braid surrounding the branch point is (upto conjugation) $\sigma_1 ... \sigma_{n-1}$ (respectively $\sigma_1^{-1} ... \sigma_{n-1}^{-1}$). We can also argue this more analytically as follows.

Let us say our convention is that for the disc D^2 we project out the second factor to get a knot diagram. To be precise, for any $0 < a < 1$ the circle $\gamma_a = \{|z| = a\}$ in D_a^2 maps to the circle γ_b in D_b^2, where $b = a^n$, and $f_\pm(\gamma_a)$ gives rise to a closed braid in the solid torus $\gamma_b \times D^2$, and ignoring the second coordinate of D^2, we get the knot diagram, where crossings happen at the point where the first three coordinates of $f_\pm$ agree. If $z_1^n = z_2^n$, it necessarily must be the case that the complex arguments

[1] An alternate way to think about this is the contractibility of the space of embeddings of disc to a disc, see https://mathoverflow.net/questions/181424/contractibility-of-space-of-embeddings-of-a-disc .

of z_1 and z_2 differ by $\frac{2k\pi}{n}$, where $0 < k < n$ is an integer. For the third coordinates of $f_\pm$ to agree, we need to have the cosines of these arguments to agree. Now we observe that for each integer k satisfying $0 < k < n$, the equation

$$\cos(\theta) = \cos(\theta + \frac{2k\pi}{n}) \text{ or equivalently } -2\sin(\theta + \frac{k\pi}{n})\sin(\frac{k\pi}{n}) = 0$$

has exactly one solution in $[0, \pi)$, namely $\theta = \frac{(n-k)\pi}{n}$. Thus we see there are exactly $n-1$ crossing points, and by looking at the sines at these points we see that they are positive crossings for f_+ and negative crossings for f_-, i.e. the braids surrounding these branch points are standard unknots. The actual braids we get can be chosen to be $\sigma_1 ... \sigma_{n-1}$ and $\sigma_1^{-1} ... \sigma_{n-1}^{-1}$ by choosing the base-point with complex argument 0.

Remark 7.2.2. We remark here that if τ is any permutation of $\{1, ..., n\}$ then $\sigma_1^{\eta_1} ... \sigma_{n-1}^{\eta_{n-1}}$ is conjugate to $\sigma_{\tau(1)}^{\eta_{\tau(1)}} ... \sigma_{\tau(n-1)}^{\eta_{\tau(n-1)}}$. To see this note that we can go between the two words by applying a sequence of far commutation relations and conjugations. In particular, there is nothing special about the braid $\sigma_1 ... \sigma_{n-1}$ we got for f_+, we can apply any permutation τ and we would get the same braid closures.

In other words, we have:

Lemma 7.2.3. *A braided embedding of a disjoint union of circles (i.e. a closed braid), it extends smoothly to a braided embedding of a disjoint union of discs with one branch point if and only if the closed braid is a completely split standard unlink.*

7.3 Extending in higher dimensions

In this section we address the question:

Question 7.3.1. Given a co-dimension 2 braided embedding on the complement of the branch locus, when can we extend the braided embedding over the branch locus (smoothly or in a locally flat p.l.)?

We will answer this question completely when the branch locus is a submanifold with trivial normal bundle. We will mostly use this result for branched covers over the sphere, and whenever the branch locus is embedded as a codimension two submanifold, it has a Seifert hypersurface [52], which trivializes the normal bundle.

As we saw in the last section, when we are looking at branched cover of surfaces (i.e. the branch locus is just a discrete set of points), we had conditions on the braid surrounding the branch points for the braided embedding to extend over the branch point. Of course, the same constraint is there for each braid corresponding to meridian around the branch point, and as we see below, these are enough.

In case the branch locus is a manifold, the various meridians are conjugate as long as the branch points belong to the same connected components. Consequently, in the above case, one needs to verify that for each connected component, the braid surrounding the branch points satisfy the appropriate conditions for us to extend the braided embedding over the branch locus.

We will analyze the situation in the smooth and the piecewise linear categories seriously below. We will use the local models discussed in the last section, to first deal with the special case when the branch locus B and its pre-image $\tilde{B}$ are both connected, and then show the general case reduces to the above special case by using the structure of centralizers of reducible braids, see [31].

7.3.1 Smooth Category

Here we will answer Question 7.3.1 in the smooth category.

Proposition 7.3.2. *Suppose we have a smooth branched cover $p : M \to N$ with branch locus $B \subseteq N$ being a submanifold with trivial normal bundle $\nu B \cong B \times D^2$. Suppose we choose points $b_1, ..., b_k$, one for each connected component of B. If we are given a smooth braided proper embedding $g_1 : M \setminus \nu_0\tilde{B} \hookrightarrow (N \setminus \nu_0 B) \times D^2$ lifting the honest covering*

$p_1 : M \setminus \nu_0\tilde{B} \hookrightarrow N \setminus \nu_0 B$ induced from p, then g_1 extends to a smooth braided embedding $g : M \hookrightarrow N \times D_2$ lifting p if and only if each of the braids surrounding the branch points b_i are completely split standard unlinks.

We observe that if $\hat{b}_i$ is another point is the same connected component as b_i, then the meridians surrounding b_i and $\hat{b}_i$ are conjugate in the fundamental group of $N \setminus \nu_0 B$, and consequently so are the braids surrounding b_i and $\hat{b}_i$. Thus we see that the condition stated in the the above proposition is independent of which particular points from each connected components of B is chosen.

Proof. Suppose g_1 does extend to a smooth braided embedding g. Then for any i, if we restrict g to the slice $\{b_i\} \times D^2$ in νB, then we see that we get a smooth braided embedding over a disc D^2 with exactly one branch point. By the local model we studied in the previous section we see that the braid surrounding the branch point b_i has to be a completely split standard unlink.

It remains to show the converse, so let us now suppose we have a braided embedding g_1 so that the braid surrounding the branch points are completely split standard unlinks. It suffices to construct a braided embedding of $h : \nu\tilde{B} \hookrightarrow \nu B \times D^2$, so that the braided embedding on the boundary $h_1 : \tilde{B} \times S^1 \hookrightarrow (B \times S^1) \times D^2$ coming from h agrees with that coming from g_1. Observe that in the above case we can isotope both the braided embeddings g_1 and h in the above case, so the braided embedding is invariant in a collar neighbourhoods of the boundary, and then identify the collar neighbourhoods, and thereby obtaining a smooth braided embedding g lifting p.

Recall that since we are considering a smooth branched covering $p : M \to N$, then the restriction of $p|_{\tilde{B}} : \tilde{B} \to B$ is a covering map. To define this map, we can define the braided embedding on each connected component of B individually. Without loss of generality, let us now assume B is connected. Suppose the fundamental group of B has the presentation $\langle x_1, ..., x_s | r_1, ..., r_t\rangle$ (recall we are assuming our manifolds are compact, and thus the branch locus being a closed submanifold also has the same property. Consequently, its fundamental group is finitely generated. However, the reader can observe that the same argument given here also works if $\pi_1 B$ is not finitely presented).

Since B has trivial normal bundle, the boundary of νB is diffeomorphic to $B \times S^1$, and so has fundamental group

$$\pi_1(\partial\nu B) \cong \pi_1(B) \times \mathbb{Z} \cong \langle x_1, ..., x_p, \mu | r_1, ..., r_q, [x_i, \mu] \text{ for all } 1 \leq i \leq s\rangle.$$

Here μ denotes the loop (meridian) corresponding to the S^1 factor, and $[x_i, \mu]$ denotes the commutator of x_i and t. The braided embedding g_1 induces a braided embedding $g_2 : \tilde{B} \times S^1 \hookrightarrow (B \times S^1) \times D^2$, which in turn gives rise to the braid monodromy map $\psi_2 : \pi_1(B \times S^1) \cong \pi_1(B) \times \mathbb{Z} \to B_n$, where the covering p_2 (i.e. restriction of p to $\tilde{B} \times S^1$) is n-sheeted. To define the braided embedding h of $\nu\tilde{B}$, we will first construct a braided embedding lifting $p|_{\tilde{B}} : \tilde{B} \to B$ induced from the braided embedding g_2.

Recall from Subsection 3.4, we have a map $\Theta : Z(\psi_2(\mu)) \to Z_0(\overline{\psi_2(\mu)})$ sending a braid commuting with $\psi_2(\mu)$ to a braid commuting with the associated tubular braid $\overline{\psi_2(\mu)}$. To this end, note that for each $1 \leq i \leq t$ of the braids $\psi_2(x_i)$ commute with $\psi_2(\mu)$, and consequently the image $\psi_2(\pi_1(B) \times \{0\})$ is contained in $Z(\psi_2(\mu))$. Thus we get a well defined group homomorphism $\psi_3 : \pi_1(B) \to B_m$ defined on the generators by sending $x_i \mapsto \Theta \circ \psi_2(x_i)$. This braid monodromy induces a braided embedding: $g_3 : \tilde{B} \to B \times D^2 \cong \nu B$. Taking products with a disc, we obtain a proper braided embedding $g_4 : \nu\tilde{B} \to \nu B \times D^2$ lifting $p|_{\nu\tilde{B}} : \nu\tilde{B} \to \nu B$, and restricting g_4 to the boundary of the normal bundles we obtain the braided embedding $g_5 : \tilde{B} \times S^1 \to (B \times S^1) \times D^2$, with braid monodromy defined by $\psi_5 : \pi_1(\partial\nu B) \to B_n$, so that for any $\gamma \in \pi_1(\partial\nu B)$ with the tubular braids under

ψ_2 and ψ_5 agreeing, i.e. $\overline{\psi_2(\gamma)} = \overline{\psi_4(\gamma)}$; although the interior braids (and hence $\psi_2(\gamma)$ and $\psi_5(\gamma)$) may differ in the following way. The interior braids of ψ_5 are all identity, since we uniformly took products with a disc. By hypothesis, we know that the interior braids $\{\alpha_k\}$ of $\alpha := \psi_2(\mu)$ is a standard positive or negative braid, i.e. conjugate to $(\sigma_1 ... \sigma_k)^{\pm 1}$ for some k. We know that centralizer of the above braid is the cyclic subgroup generated by itself. Thus for any i, the k-th interior braids of $\psi_2(x_i)$ has to be powers of α_k.

The idea now is to twist the braided embedding g_4 so that the induced braided embedding g_5 agrees with that of g_2. Let us first consider the special case B is a circle S^1, with fundamental group $\langle x \rangle \cong \mathbb{Z}$. $\tilde{B}$ will be a disjoint union of circles, and each component of the normal bundle $\nu\tilde{B}$ will be a solid torus. In order to construct a braided embedding $h : \nu\tilde{B} \hookrightarrow \nu B \times D^2$ so that the braid monodromy of which agrees with that of ψ_2, we will modify g_4 by applying Dehn twists on those components of $\nu\tilde{B}$ so that the interior braids match with that of $\psi_2(x)$.

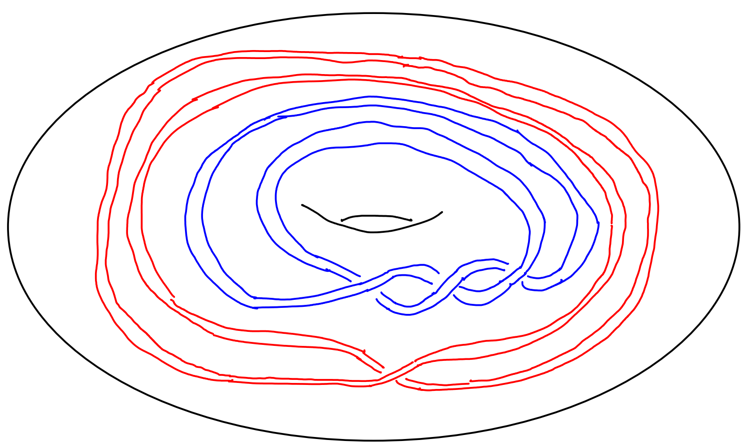

Figure 7.1: When B is S^1, the figure illustrates a braided embedding of $\nu\tilde{B}$ in $B \times D^2$

More formally, we will pre-compose the braided embedding g_4 with a diffeomorphism of $\nu\tilde{B}$ which preserves each solid tori setwise, and induces a number (this number is equal to the exponent of the corresponding interior braid of $\psi_2(x)$)

of Dehn twist[2] on the boundary of the solid torus. The braided embedding h so constructed has the property that the induced braided embeddings on the boundary h_1 is isotopic to that of g_5 (since the braid monodromies agree), and thus we can patch up h and g_1 to extend the braided embedding over the branch locus.

To make the above idea work in general we need to come up with an analogue of Dehn twists in higher dimension, and ensure we can carry out a similar construction as above even when the fundamental group of B is complicated. To elaborate on the latter point, suppose we did some twisting of g_4 so the interior braid corresponding to x_1 agrees with that of $\psi_2(x_1)$, but now if we do some twisting so that the interior braids of x_2 agree, we need to make sure this does not alter the interior braids of x_1.

Let us begin with the analogues of Dehn twists, which we will call D-twists.

Definition 7.3.3. Suppose X is any smooth manifold, and Y is any hypersurface of X with a tubular neighbourhood $Y \times [0, 2\pi]$. Then we can define a diffeomorphism of $X \times S^1$ as follows: we cut $X \times S^1$ along $Y \times S^1$, and define

$$Y \times [0, 2\pi] \times S^1 \to Y \times [0, 2\pi] \times S^1,$$

by sending:

$$(y, \theta, z) \mapsto (y, \theta, e^{i\theta} z).$$

we see that this map agrees with the identity at the boundary $Y \times \{0, 2\pi\} \times S^1$, and as such we can extend this to the rest of $X \times S^1$ by identity. We will call this *D-twist* of $X \times S^1$ along $Y \times S^1$ and denote it by T_Y.

Also, we observe that this map T_Y extends to a diffeomorphism S_Y of $X \times \overline{D^2}$

[2]Recall for any diffeomorphism of the boundary of a solid torus which preserves the meridian can be extended to a diffeomorphism of the entire solid torus.

by essentially the same formula: let us define

$$Y \times [0, 2\pi] \times \overline{D^2} \to Y \times [0, 2\pi] \times \overline{D^2}$$

by

$$(y, \theta, z) \mapsto (y, \theta, e^{i\theta} z),$$

and the identity map elsewhere.

Notice that when X is the unit circle and Y is a single point in X, the D-twist T_Y is exactly the Dehn twist $T_Y \times S^1$ along a meridian, and S_Y is the extension of this diffeomorphism to the entire solid torus.

Returning to the case X being a manifold, if γ is a simple closed curve in X which intersects Y in some finite set of points $y_1, ..., y_l$, then we claim that the effect of T_Y on the torus $\gamma \times S^1$ is the Dehn twist along the meridian $\{y_1\} \times S^1$ to the power $\langle \gamma, Y \rangle$ times, where $\langle \gamma, Y \rangle$ denotes the algebraic intersection number of γ with Y. For, if there is one intersection it is easy to see that the only change happens near that point and it is a positive or negative Dehn twist about the meridian, depending on the sign of the intersection. If there are multiple such intersections, we will get several meridional Dehn twists, with signs corresponding to that of the intersection.

Special Case: Let us assume the map $p : \tilde{B} \to B$ is a diffeomorphism. We would like to realize the braided embedding $g_2 : B \times S^1 \to (B \times S^1) \times D^2$ as the boundary of braided embedding $h : \nu B \to \nu B \times D^2$. In this context, the closure of $\beta = \psi_2(\mu)$ is a standard unknot, and we know that the centralizer of $\psi_2(\mu)$ is an infinite cyclic group generated by itself. Thus if we restrict the braid monodromy map $\psi_2 : \pi_1(\partial \nu B)$ to the subgroup $\pi_1(B)$ (obtained by fixing a particular point in S^1), we see that the restriction maps from $\pi_1(B)$ to $Z(\beta) \cong \mathbb{Z}$. Thus it must factor through the first homology $H_1(B)$, or in other words is an element of $Hom(H_1(B), \mathbb{Z})$. By the universal coefficient theorem for cohomology, this element is the image of some cohomology class in $H^1(B)$ (there may be multiple preimages depending on if the corresponding Ext term is non-trivial). By Poincare duality there is a homology class in $H_{\dim B-1}(B)$ dual to it, which is represented by an embedded [52] hypersurface Y. It follows that if we pre-compose the braided embedding $g_4 : \nu\tilde{B} \hookrightarrow \nu B \times D^2$ with the diffeomorphism $S_Y : \nu\tilde{B} \to \nu\tilde{B}$ (recall B and $\tilde{B}$ are diffeomorphic), we obtain a braided embedding h with the required properties.

General Case: Given the braided embedding $g_2 : \tilde{B} \times S^1 \hookrightarrow (B \times S^1) \times D^2$, we had its braid monodromy map $\psi_2 : \pi_1(B \times S^1) \to B_n$. Let C be one component of $\tilde{B}$, by restricting g_2 to the component $C \times S^1$, we get a braided embedding $g_2|_{C\times S^1} : C \times S^1 \hookrightarrow (B \times S^1) \times D^2$, and we claim that this braided embedding is the composition of two braided embeddings:
$s : C \times S^1 \hookrightarrow (C \times S^1) \times D^2$ (the associated cover $id \times p$ unwraps only the S^1-direction), and the braided embedding $C \times S^1 \hookrightarrow (B \times S^1) \times D^2$ (the associated cover preserves the S^1 direction, and we get a covering $p|_C : C \to B$ in the orthogonal direction). To see this note that if we restrict the braid monodromy $\psi_2 : \pi_1(B \times S^1) \to B_n$ to the subgroup $\pi_1(C \times S^1)$ obtained from (corresponding to the covering map $p|_C \times id : C \times S^1 \to B \times S^1$), if we ignore the tubular braids not corresponding to C, we see that the tubular braids are all identity (and the number of such strands of the tubular braid is the number of sheets of the cover $p|_C : C \to B$), and the various interior braids are conjugate (the number of strands in an interior braid equals the number of times the S^1 factor is unwrapped, say l). If we choose a particular base point in C over the base point in B, the interior braids coming from that factor gives us a braid monodromy $\psi_6 : \pi_1(C \times S^1) \to B_l$. It suffices to show that we can realize this braid monodromy by twisting, i.e. we will precompose each νC with an appropriate D-twist realizing appropriate interior braids, and doing this

for each component C of $\tilde{B}$ will give us a braided embedding h with the required properties. Thus, we reduce to the special case considered above when $p : \tilde{B} \to B$ is a diffeomorphism, and the result follows. □

7.3.2 Piecewise Linear Category

We have a similar result in the piecewise linear category, when the branch locus is a submanifold. The reader will note that this results requires braids surrounding branch points to be completely split unlinks (as opposed to standard unlinks), which is to be expected given our local model near a branch point in the last section.

Proposition 7.3.4. *Suppose we have a piecewise linear branched cover $p : M \to N$ with branch locus $B \subseteq N$ being a submanifold with trivial regular neighbourhood $\nu B \cong B \times D^2$, and $p|_{\tilde{B}} : \tilde{B} \to B$ is a covering map. Suppose we choose points $b_1, ..., b_k$, one for each connected component of B. If we are given a locally flat piecewise linear braided proper embedding $g_1 : M \setminus \nu_0 \tilde{B} \hookrightarrow (N \setminus \nu_0 B) \times D^2$ lifting the honest covering $p_1 : M \setminus \nu_0 \tilde{B} \hookrightarrow N \setminus \nu_0 B$ induced from p, then g_1 extends to a locally flat smooth braided embedding $g : M \hookrightarrow N \times D_2$ lifting p if and only if each of the braids surrounding the branch points b_i are completely split unlinks.*

The proof will be similar to that of the smooth category, once again there will be a special case, and a reduction from the general case to the special case. The latter step is essentially the same as the proof in the smooth category, however we will need to approach the special case differently, as the author does not know any sort of classification which braids closures are unknots, let alone a precise understanding of their centralizers.

Proof. By our study of local models in the last section, it is clear that the hypothesis (of braids surrounding branch points be completely split unlinks) is a necessary condition. It suffices to show it is a sufficient condition as well.

Special Case: let us assume the map $p : \tilde{B} \to B$ is the identity map. We would like to realize the braided embedding $g_2 : B \times S^1 \to (B \times S^1) \times D^2$ as the boundary of braided embedding. We will obtain h simply by coning g_2. Thinking of a slice D^2_ν of the normal bundle as the cone $p * S^1$, we see that $B \times D^2_\nu \times D^2$ is nothing but the parametric join $B \times S^1 \times D^2$ along $B \times p$.

Let us choose the origin O in the disc D^2, we see that for each $b \in B$,the image of g_2 in $\{b\} \times S^1 \times D^2$ is an unknot (because we are in the special case), we can cone this at the point $\{b\} \times \{p\} \times \{O\}$, and obtain a locally flat braided disc in $\{b\} \times D^2_\nu \times D^2$. By doing this coning operation for each $b \in B$, we obtain a locally flat piecewise linear proper braided embedding h which induces the braided embedding g_2 in the boundary, and can be used to extend g_1.

General Case: Without loss of generality we may assume B is connected (we can run the same argument for each component of B), however $\tilde{B}$ may have multiple components. In this case we need to choose an appropriate number of points O_i, and cone over them. However, we need to make sure that this procedure gives us an embedding, we would like to vary the points O_i in D^2 (continuous) parametrically in B so the result of the coning is injective. To do this formally, we will make use of the tubular braids. Given braided embedding $g_2 : \tilde{B} \times S^1 \hookrightarrow (B \times S^1) \times D^2$, just like in the smooth category, we obtain a braided embedding $g_3 : \tilde{B} \hookrightarrow B \times D^2$ by looking at the tubular braids of the braid monodromy ψ_2 of g_2 (we have less control over the interior braids in this case, but the tubular braids behave similarly). By looking at a small neighbourhood of this braided embedding, we again obtain a braided embedding $g_4 : \nu\tilde{B} \to \nu B \times D^2$ lifting $p|_{\nu\tilde{B}} : \nu\tilde{B} \to \nu B$. We can replace the braided embeddings on the boundary of this untwisted braided embedding g_4 with the one coming from g_2, and use the small neighbourhoods in the disc D^2 (i.e, the points O_i is determined by the braided embedding g_3) to do the coning operation. The result follows. □

CHAPTER 8

LIFTING BRANCHED COVERINGS OVER THE TWO-SPHERE

In this chapter we will study the lifting problem for branched covers over the two-sphere. We will see that the answers differ in the smooth and piecewise linear categories.

8.1 Braid Systems and Permutation Systems

Since the fundamental group of a sphere with m punctures has the presentation $\langle x_1, ..., x_m | x_1 .... x_m \rangle$ where the x_i is the loop surrounding the i-th puncture, we can store permutation and braid monodromies of the punctures sphere as tuples. Let G be any group with any subset H, let us define

$$P_g^m(G, H) := \{(h_1, ..., h_m) | h_i \in H, h_1 ... h_m = g\}$$

We omit H from the notation if $H = G$, and we omit g from the notation if $g = e$.
An element of $P^m(S_n)$ will be called a permutation system.
An element of $P^m(B_n, A_n)$ will be called a braid system.
An element of $P^m(B_n, SA_n)$ will be called a simple braid system.

8.2 Lifting simple branched covers

Let us begin by discussing liftings of two fold branched covers over the two sphere.

Example 8.2.1. The monodromy of the branched covering described in Figure 2.5 can be described by the permutation system $((12), (12), (12), (12), (12), (12), (12), (12))$. One possible lift is given by the braid system $(\sigma_1, \sigma_1, \sigma_1, \sigma_1, \sigma_1^{-1}, \sigma_1^{-1}, \sigma_1^{-1}, \sigma_1^{-1})$. We observe that this example generalizes to arbitrary genus, and any two fold branched cover over the sphere lifts to a braided embedding.

For simple branched covers over the sphere, Carter and Kamada [16, Theorem 3.8] answered Question 4.2.4 affirmatively, using the classification of simple branched covers due to Lüroth [55] and Clebsch [17] (see [8, Section 4] for a proof in English),

Proposition 8.2.2. *Any transposition (=simple permutation) system can be brought to the form*

$$((12), ..., (12), (13), (13), (14), (14), ..., (1n), (1n))$$

(with an even number of (12)*'s) using some sliding moves and conjugation.*

Once a permutation system is brought to this standard form, it is easy to find a braid system lifting it. If we recursively define $\alpha_1 := \sigma_1$, and $\alpha_k := \sigma_k \alpha_{k-1} \sigma_k^{-1}$, we see that α_{k-1} is a braid lifting $(1k)$ which is conjugate to the standard generator σ_1. Then we see that the braid system $(\alpha_1, \alpha_1^{-1}, ..., \alpha_1, \alpha_1^{-1}, \alpha_2, \alpha_2^{-1}, \alpha_3, \alpha_3^{-1}, ..., \alpha_{n-1}, \alpha_{n-1}^{-1})$ lifts the permutation system
$((12), (12), ..., (12), (12), (13), (13), (14), (14), ..., (1n), (1n))$. After this one can apply the sliding and conjugation moves in reverse to the braid system and finally get a braid system lifting the original permutation system.

We will build on Lüroth and Clebsch's method of proof to show that the answer Question 4.2.4 is yes for any branched cover over the 2-sphere. Before doing that, let us illustrate the idea of proof of Proposition 8.2.2 with an example, and then show that we can then get a braid system lifting the permutation system by applying the reverse process to the braid system.

Example 8.2.3. Let us consider a 4-fold simple branched cover with Hurwitz permutation system $((12), (34), (13), (24), (14), (23))$. We will perform sliding moves to get the permutation system to standard form

$$((12),(34),(13),(24),(14),(23)) \xrightarrow{s_5} ((12),(34),(13),(24),(23),(14))$$

$$\xrightarrow{s_4^{-1}} ((12),(34),(13),(23),(34),(14)) \xrightarrow{s_2^{-1}} ((12),(13),(14),(23),(34),(14))$$

$$\xrightarrow{s_3} ((12),(13),(23),(14),(34),(14)) \xrightarrow{s_4} ((12),(13),(23),(13),(14),(14))$$

$$\xrightarrow{s_2} ((12),(12),(13),(13),(14),(14))$$

Now it is easy to find a braid system that lifts the given permutation system once it is in standard form.

The braids $\alpha_1 = \sigma_1$, $\alpha_2 = \sigma_2\sigma_1\sigma_2^{-1}$ and $\alpha_3 = \sigma_3\sigma_2\sigma_1\sigma_2^{-1}\sigma_3^{-1}$ lift $(12), (13)$ and (14), respectively. Clearly each $\alpha_i \in SA_4$ being a conjugate of σ_1. Now we see that the braid system $(\alpha_1, \alpha_1^{-1}, \alpha_2, \alpha_2^{-1}, \alpha_3, \alpha_3^{-1})$ lifts $((12),(12),(13),(13),(14),(14))$. We can apply the inverses of the sliding moves we applied earlier to $(\alpha_1, \alpha_1^{-1}, \alpha_2, \alpha_2^{-1}, \alpha_3, \alpha_3^{-1})$ and get

$$(\alpha_1, \alpha_1^{-1}, \alpha_2, \alpha_2^{-1}, \alpha_3, \alpha_3^{-1}) \xrightarrow{s_2^{-1}} (\alpha_1, \alpha_2, \alpha_2^{-1}\alpha_1^{-1}\alpha_2, \alpha_2^{-1}, \alpha_3, \alpha_3^{-1}) = (\alpha_1, \alpha_2, \sigma_2^{-1}, \alpha_2^{-1}, \alpha_3, \alpha_3^{-1})$$

$$\xrightarrow{s_4^{-1}} (\alpha_1, \alpha_2, \sigma_2^{-1}, \alpha_3, \alpha_3^{-1}\alpha_2^{-1}\alpha_3, \alpha_3^{-1}) = (\alpha_1, \alpha_2, \sigma_2^{-1}, \alpha_3, \sigma_3^{-1}, \alpha_3^{-1})$$

$$\xrightarrow{s_3} (\alpha_1, \alpha_2, \sigma_2^{-1}\alpha_3\sigma_2, \sigma_2^{-1}, \sigma_3^{-1}, \alpha_3^{-1}) = (\alpha_1, \alpha_2, \alpha_3, \sigma_2^{-1}, \sigma_3^{-1}, \alpha_3^{-1})$$

$$\xrightarrow{s_2} (\alpha_1, \alpha_2\alpha_3\alpha_2^{-1}, \alpha_2, \sigma_2^{-1}, \sigma_3^{-1}, \alpha_3^{-1}) = (\alpha_1, \sigma_3, \alpha_2, \sigma_2^{-1}, \sigma_3^{-1}, \alpha_3^{-1})$$

$$\xrightarrow{s_4} (\alpha_1, \sigma_3, \alpha_2, \sigma_2^{-1}\sigma_3^{-1}\sigma_2, \sigma_2^{-1}, \alpha_3^{-1})$$

$$\xrightarrow{s_5^{-1}} (\alpha_1, \sigma_3, \alpha_2, \sigma_2^{-1}\sigma_3^{-1}\sigma_2, \alpha_3^{-1}, \alpha_3\sigma_2^{-1}\alpha_3^{-1}) = (\alpha_1, \sigma_3, \alpha_2, \sigma_2^{-1}\sigma_3^{-1}\sigma_2, \alpha_3^{-1}, \sigma_2^{-1})$$

Thus we see that $(\alpha_1, \sigma_3, \alpha_2, \sigma_2^{-1}\sigma_3^{-1}\sigma_2, \alpha_3^{-1}, \sigma_2^{-1})$ lifts the given permutation system

$((12), (34), (13), (24), (14), (23))$.

For closed two braids, being a completely split unlink is equivalent to being a completely split standard unlink, whence the lifting question for simple branched covers are equivalent for the piecewise linear and smooth categories. However, this does not hold more generally, so let us consider the two categories separately.

8.3 Lifting in the piecewise linear category

Theorem 8.3.1. *Every branched cover of a surface over S^2 can be lifted to a piecewise linear braided embedding.*

The proof will follow from the following slightly stronger Proposition 8.3.2 below, which in particular shows that one can lift to a braided embedding which can be perturbed to be simple.

Notation: For $n < m$, there are canonical inclusions $\iota_{n,m} : S_n \hookrightarrow S_m$ and $i_{n,m} : B_n \hookrightarrow B_m$, and for notational convenience, we will be implicitly using these maps to make identifications. For example if $\rho \in \iota_{n,m}(S_n)$ then we can think of $\rho \in S_n$, and conversely any element of S_n can be thought to be an element of S_m (and similarly for the braid groups).

Proposition 8.3.2. *Every permutation system $(\rho_1, ..., \rho_m)$ in S_n lifts to a braid system $(\alpha_1, ..., \alpha_m)$ in B_n so that*

1. *If $\rho_j \in S_k$ with smallest such k, α_j has a braid word of the form $\beta_j \sigma_{k-1}^{\pm 1} \gamma_j$, where β_j and γ_j are in B_{k-1}.*
2. *Moreover if $\rho_j \in S_k$ with smallest such k is a transposition, then α_j has a braid word of the form $\beta_j \sigma_{k-1}^{\pm 1} \beta_j^{-1}$, where β_j is in B_{k-1}.*

Proof. The proof will be by induction on n.

Base case: $n = 2$. Every permutation system in S_2 looks like $((12), ..., (12))$ with a even number of (12)'s. The braid system $(\sigma_1, \sigma_1^{-1}, ..., \sigma_1, \sigma_1^{-1})$ lifts $((12), (12), ..., (12), (12))$ satisfying the above conditions.

Inductive step: Let us assume the statement holds for $q = n-1$. Suppose we have the permutation system $(\rho_1, ..., \rho_m)$ in S_n. For each ρ_i, let us factorize $\rho_i = \varrho_i\tau_i$ so that $\varrho_i \in S_{n-1}$, and τ_i is a transposition of the form (a, n), where $a \in \{1, 2, ..., n-1\}$ (such a factorization is not unique, and certain ϱ_i or τ_i can be the identity, in which case we can drop it from the permutation system). We will do fission to the original permutation system to obtain $(\varrho_1, \tau_1 ..., \varrho_m, \tau_m)$. We will use inverse sliding moves to bring all the ϱ_i's to the left of all the τ_i, as follows:

$$(\varrho_1, \tau_1, ..., \varrho_{m-1}, \tau_{m-1}, \varrho_m, \tau_m) \xrightarrow{s_{2m-2}^{-1}} (\varrho_1, \tau_1 ..., \varrho_{m-1}, \varrho_m, \tilde{\tau}_{m-1}, \tau_m) \xrightarrow{s_{2m-4}^{-1} s_{2m-3}^{-1}} ...$$

$$\xrightarrow{s_2^{-1} ... s_m^{-1}} (\varrho_1, ..., \varrho_{m-1}, \varrho_m, \tilde{\tau}_1, ..., \tilde{\tau}_{m-1}, \tilde{\tau}_m)$$

where each $\tilde{\tau}_i$ is a conjugate of τ_i and is of the form (a, n). Now we will break this permutation system into permutation tuples $\Theta = (\varrho_1, ..., \varrho_{m-1}, \varrho_m)$, $\Phi = (\tilde{\tau}_1, ..., \tilde{\tau}_{m-1}, \tilde{\tau}_m)$, and apply sliding moves and its inverses to modify Φ, as described below.

† Let r be the largest number smaller than n so that there is a transposition in Φ so that $(r, n) = \tilde{\tau}_i$ for some i. Let $i_1 < i_2 < ... < i_j$ be the indices so that $\tilde{\tau}_i = (r, n)$. We use sliding moves to bring $\tilde{\tau}_{i_{2k-1}}$ to the $i_{2k} - 1'$ th spot, i.e. bring it to the very left of $\tilde{\tau}_{i_{2k}}$. If j is even, we bring $\tilde{\tau}_{i_j}$ to the extreme right of the permutation tuple. After applying this sequence of sliding moves to $(\tilde{\tau}_1, ..., \tilde{\tau}_{m-1}, \tilde{\tau}_m)$, the permutation system will now look like (we illustrate the case when j is odd, where there will be a single (r, n) at the very right):

$$(\mu_1, \nu_1, (r, n), (r, n), \mu_2, \nu_2, (r, n), (r, n), \mu_3, \nu_3, ..., \mu_k, \nu_k, (r, n))$$

where μ_i's are permutation tuples with each element of the form (a, n) for some

$a < n$, and ν_i's are permutation tuples not containing any n, so each element is of the form (b, r) for some $b < r$. Now we consider the new permutation tuple which is formed by deleting the sub-permutation systems $((r, n), (r, n))$

$$\downarrow (\mu_1, \nu_1, \mu_2, \nu_2, \mu_3, \nu_3, ..., \mu_k, \nu_k, (r, n))$$

We can then use inverse sliding moves on this permutation tuple to bring the ν_j's to the left

$$\rightarrow (\nu_1, \nu_2, \nu_3, ..., \nu_k, \tilde{\mu}_1, \tilde{\mu}_2, \tilde{\mu}_3, ..., \tilde{\mu}_k, (r, n))$$

Let us now append $(\nu_1, \nu_2, \nu_3, ..., \nu_k)$ to the right of Θ and set $\Phi = (\tilde{\mu}_1, \tilde{\mu}_2, \tilde{\mu}_3, ..., \tilde{\mu}_k, (r, n))$, and apply the same procedure (beginning in †) to it. At each step the length of this permutation tuple reduces by at least 2, and in a finite number of steps Φ will be empty. At that stage Θ will be a permutation system in S_{n-1}, and by the induction hypothesis we can find a braid system lifting it with the stated properties.

Now we can apply to this braid system the reverse of the entire process we applied to the permutation system, i.e.

- we will introduce the braid system (η_r, η_r^{-1}) corresponding to the places we deleted the permutation system $((r, n), (r, n))$, where

$$\eta_r := (\sigma_r ... \sigma_{n-2})\sigma_{n-1}(\sigma_r ... \sigma_{n-2})^{-1} = \sigma_r ... \sigma_{n-2}\sigma_{n-1}\sigma_{n-2}^{-1} ... \sigma_r^{-1}$$

- we will apply $s_k^{\mp 1}$ to the braid system if we applied $s_k^{\pm 1}$ to the permutation system.

After we apply all these moves we will be left with a braid system

$$(\alpha_1, \delta_1, ..., \alpha_{m-1}, \delta_{m-1}, \alpha_m, \delta_m)$$

lifting the permutation system

$$(\varrho_1, \tau_1, ..., \varrho_{m-1}, \tau_{m-1}, \varrho_m, \tau_m),$$

Claim 8.3.3. *This braid system has properties 1 and 2 as in the statement.*

Properties 1 and 2 for the α_i's will follow from the induction hypothesis. The following observations will show that the δ_i's have the properties 1 and 2 as in the statement.

- The first time we introduce the braid η_r, it is of the form $\beta\sigma_{n-1}^{\pm 1}\beta^{-1}$ where $\beta \in B_{n-1}$, and when we apply sliding moves or their inverses to it, we conjugate it by an element of B_{n-1}, and so it remains of that form.

- Note that the only times we applied the sliding moves of the form $((r,n),(s,n)) \to ((s,r),(r,n))$, it was the case that $s < r$. Moreover, since (s,r) is a permutation in S_{n-1}, we ensured that we applied inverse sliding moves to it to bring it to Θ, and then used the induction hypothesis to find a braid $\beta\sigma_{r-1}^{\pm 1}\beta^{-1}$ lifting it, where $\beta \in B_{r-1}$. While applying the reverse procedure this braid does not change until it becomes adjacent to the braid $\eta_r^{\pm 1}$ lifting (r,n), and then we apply the inverse sliding move

$$(\beta\sigma_{r-1}^{\pm 1}\beta^{-1}, \eta_r^{\pm 1}) \to (\eta_r^{\pm 1}, \eta_r^{\mp 1}\beta\sigma_{r-1}^{\pm 1}\beta^{-1}\eta_r^{\pm 1})$$

Now we will show that $\eta_r^{\mp 1}\beta\sigma_{r-1}^{\pm 1}\beta^{-1}\eta_r^{\pm 1}$ is of the form $\gamma\sigma_{n-1}^{\pm 1}\gamma^{-1}$, where $\gamma \in$

B_{n-1}, by repeatedly applying (equivalent form of) the braid relation

$$\sigma_{i+1}^{-1}\sigma_i^{\pm 1}\sigma_{i+1} = \sigma_i\sigma_{i+1}^{\pm 1}\sigma_i^{-1}.$$

We will consider the case that the exponent of η_r above is 1, the other case is similar.

$$\eta_r^{-1}\beta\sigma_{r-1}^{\pm 1}\beta^{-1}\eta_r = \beta\eta_r^{-1}\sigma_{r-1}^{\pm 1}\eta_r\beta^{-1}$$

$$= \beta(\sigma_r\sigma_{r+1}...\sigma_{n-2}\sigma_{n-1}^{-1}\sigma_{n-2}^{-1}...\sigma_{r+1}^{-1}\sigma_r^{-1})\sigma_{r-1}^{\pm 1}(\sigma_r\sigma_{r+1}...\sigma_{n-2}\sigma_{n-1}\sigma_{n-2}^{-1}...\sigma_{r+1}^{-1}\sigma_r^{-1})\beta^{-1}$$

$$= \beta\sigma_r\sigma_{r+1}...\sigma_{n-2}\sigma_{n-1}^{-1}\sigma_{n-2}^{-1}...\sigma_{r+1}^{-1}(\sigma_r^{-1}\sigma_{r-1}^{\pm 1}\sigma_r)\sigma_{r+1}...\sigma_{n-2}\sigma_{n-1}\sigma_{n-2}^{-1}...\sigma_r^{-1}\beta^{-1}$$

$$= \beta(\sigma_r\sigma_{r+1}...\sigma_{n-2})\sigma_{n-1}^{-1}\sigma_{n-2}^{-1}...\sigma_{r+1}^{-1}\sigma_{r-1}\sigma_r^{\pm 1}\sigma_{r-1}^{-1}\sigma_{r+1}...\sigma_{n-2}\sigma_{n-1}(\sigma_{n-2}^{-1}...\sigma_{r+1}^{-1}\sigma_r^{-1})\beta^{-1}$$

$$= \beta(\sigma_r\sigma_{r+1}...\sigma_{n-2})\sigma_{r-1}\sigma_{n-1}^{-1}\sigma_{n-2}^{-1}...(\sigma_{r+1}^{-1}\sigma_r^{\pm 1}\sigma_{r+1})...\sigma_{n-2}\sigma_{n-1}\sigma_{r-1}^{-1}(\sigma_{n-2}^{-1}...\sigma_{r+1}^{-1}\sigma_r^{-1})\beta^{-1}$$

$$= ... = \beta(\sigma_r\sigma_{r+1}...\sigma_{n-2})(\sigma_{r-1}\sigma_r...\sigma_{n-2})\sigma_{n-1}^{\pm 1}(\sigma_{n-2}^{-1}...\sigma_r^{-1}\sigma_{r-1}^{-1})(\sigma_{n-2}^{-1}...\sigma_{r+1}^{-1}\sigma_r^{-1})\beta^{-1}$$

Assuming the claim, we see that the braids $\alpha_i \in B_{n-1}$ and $\alpha_i\delta_i \in B_n$ have the same closure since they are related by conjugation and stabilization,

$$\alpha_i \doteqdot \gamma_i^{-1}\alpha_i\gamma_i \nearrow \gamma_i^{-1}\alpha_i\gamma_i\sigma_{n-1}^{\pm 1} \doteqdot \alpha_i\gamma_i\sigma_{n-1}^{\pm 1}\gamma_i^{-1} = \alpha_i\delta_i$$

Here, following Morton, we are denoting conjugation by $\doteqdot$ and stabilization by $\nearrow$. Thus the braid system

$$(\alpha_1\delta_1, ..., \alpha_{m-1}\delta_{m-1}, \alpha_m\delta_m)$$

lifts the permutation system $(\rho_1, ..., \rho_{m-1}, \rho_m)$ with all the required properties.

$\square$

The above proof is notationally inconvenient, so let us work out some examples explicitly.

Example 8.3.4. Let us consider the permutation system $\rho = ((123), (24), (14)(23), (34))$. We use fusion on each permutation to construct the new permutation system $\rho = ((123), (24), (23), (14), (34))$ Now we will use sliding moves to move each transposition containing 4 to the right.

$$((123), (24), (23), (14), (34)) \xrightarrow{s_2^{-1}} ((123), (23), (34), (14), (34))$$

Now we will just focus on the transpositions on the right containing 4 and use sliding moves there.

$$((123), (23), (34), (14), (34)) \xrightarrow{s_3} ((123), (23), (13), (34), (34))$$

We now observe that

$$(\sigma_2\sigma_1, \sigma_2^{-1}, \sigma_1^{-1}\sigma_2^{-1}\sigma_1, \sigma_3, \sigma_3^{-1})$$

ia a braid system lifting

$$((123), (23), (13), (34), (34))$$

with the required properties as in statement. Now we apply s_3^{-1} to this braid system.

$$(\sigma_2\sigma_1, \sigma_2^{-1}, \sigma_1^{-1}\sigma_2^{-1}\sigma_1, \sigma_3, \sigma_3^{-1}) \xrightarrow{s_3^{-1}} (\sigma_2\sigma_1, \sigma_2^{-1}, \sigma_3, \sigma_3^{-1}\sigma_1^{-1}\sigma_2^{-1}\sigma_1\sigma_3, \sigma_3^{-1})$$

Now observe that $\sigma_3^{-1}\sigma_1^{-1}\sigma_2^{-1}\sigma_1\sigma_3 = \sigma_1^{-1}\sigma_3^{-1}\sigma_2^{-1}\sigma_3\sigma_1 = \sigma_1^{-1}\sigma_2\sigma_3^{-1}\sigma_2^{-1}\sigma_1$. Now we apply s_2 to this braid system.

$$(\sigma_2\sigma_1, \sigma_2^{-1}, \sigma_3, \sigma_1^{-1}\sigma_2\sigma_3^{-1}\sigma_2^{-1}\sigma_1, \sigma_3^{-1}) \xrightarrow{s_2} (\sigma_2\sigma_1, \sigma_2^{-1}\sigma_3\sigma_2, \sigma_2^{-1}, \sigma_1^{-1}\sigma_2\sigma_3^{-1}\sigma_2^{-1}\sigma_1, \sigma_3^{-1})$$

We obtain a braid system $(\sigma_2\sigma_1, \sigma_2^{-1}\sigma_3\sigma_2, \sigma_2^{-1}, \sigma_1^{-1}\sigma_2\sigma_3^{-1}\sigma_2^{-1}\sigma_1, \sigma_3^{-1})$ lifting the permutation system $((123), (24), (14)(23), (34))$ with the required properties.

Example 8.3.5. Let us consider the permutation system

$$\rho = ((143), (24), (34), (23), (13)).$$

We use fission on each permutation to construct the new permutation system $\varrho = ((13), (34), (24), (34), (23), (13))$ We will now be using sliding moves and its inverse to this system, (almost) as described before.

$$((13), (34), (24), (34), (23), (13))$$

$$\xrightarrow{s_2} ((13), (23), (34), (34), (23), (13))$$

$$\downarrow ((13), (23), (23), (13))$$

$$\downarrow ((13), (13))$$

We see that the braid system $(\sigma_1\sigma_2\sigma_1^{-1}, \sigma_1\sigma_2^{-1}\sigma_1^{-1})$ Using the sliding moves in reverse to this braid system and introducing appropriate braid subsystems at places we deleted permutation subsystems, we get a braid system lifting ϱ.

$$(\sigma_1\sigma_2\sigma_1^{-1}, \sigma_1\sigma_2^{-1}\sigma_1^{-1})$$

$$\uparrow (\sigma_1\sigma_2\sigma_1^{-1}, \sigma_2, \sigma_2^{-1}, \sigma_1\sigma_2^{-1}\sigma_1^{-1})$$

$$\uparrow (\sigma_1\sigma_2\sigma_1^{-1}, \sigma_2, \sigma_3, \sigma_3^{-1}, \sigma_2^{-1}, \sigma_1\sigma_2^{-1}\sigma_1^{-1})$$

$$= (\sigma_1\sigma_2\sigma_1^{-1}, \sigma_2, \sigma_3, \sigma_3^{-1}, \sigma_2^{-1}, \sigma_1\sigma_2^{-1}\sigma_1^{-1})$$

$$\xrightarrow{s_2^{-1}} (\sigma_1\sigma_2\sigma_1^{-1}, \sigma_3, \sigma_3^{-1}\sigma_2\sigma_3, \sigma_3^{-1}, \sigma_2^{-1}, \sigma_1\sigma_2^{-1}\sigma_1^{-1})$$

$$= (\sigma_1\sigma_2\sigma_1^{-1}, \sigma_3, \sigma_2\sigma_3\sigma_2^{-1}, \sigma_3^{-1}, \sigma_2^{-1}, \sigma_1\sigma_2^{-1}\sigma_1^{-1})$$

By fusion we see that

$$(\sigma_1\sigma_2\sigma_1^{-1}\sigma_3, \sigma_2\sigma_3\sigma_2^{-1}, \sigma_3^{-1}, \sigma_2^{-1}, \sigma_1\sigma_2^{-1}\sigma_1^{-1})$$

is a braid system lifting ρ.

Example 8.3.6. Let us consider the permutation system

$$\rho = ((143), (15), (25), (45), (25), (35), (45), (25), (15)).$$

We will use sliding moves and destabilizations as earlier.

$$((143), (15), (25), (45), (25), (35), (45), (25), (15))$$

$$\xrightarrow{s_4} ((143), (15), (25), (24), (45), (35), (45), (25), (15))$$

$$\xrightarrow{s_5} ((143), (15), (25), (24), (34), (45), (45), (25), (15))$$

$$\searrow ((143), (15), (25), (24), (34), (25), (15))$$

$$\xrightarrow{s_4^{-1}s_3^{-1}} ((143), (15), (24), (34), (35), (25), (15))$$

$$\xrightarrow{s_4^{-1}s_3^{-1}} ((143), (15), (24), (34), (35), (25), (15))$$

$$\xrightarrow{s_3^{-1}s_2^{-1}} ((143), (24), (34), (15), (35), (25), (15))$$

$$\xrightarrow{s_6 s_5} ((143), (24), (34), (15), (23), (13), (35))$$

$$\xrightarrow{s_5^{-1}s_4^{-1}} ((143), (24), (34), (23), (13), (35), (35))$$

$$\searrow ((143), (24), (34), (23), (13))$$

From the previous example we know that $(\sigma_1\sigma_2\sigma_1^{-1}\sigma_3, \sigma_2\sigma_3\sigma_2^{-1}, \sigma_3^{-1}, \sigma_2^{-1}, \sigma_1\sigma_2^{-1}\sigma_1^{-1})$ is a braid system lifting $((143), (24), (34), (23), (13))$

We will get required braid system by following the above mentioned process. Using the sliding moves in reverse to this braid system and introducing appropriate braid subsystems at places we deleted permutation subsystems, we will get a braid system lifting ρ.

8.4 Lifting branched covers in the smooth category

For any natural number $n \geq 2$, consider the branched cover over the sphere with permutation system $(\rho, ..., \rho)$, where $\rho = (12...n)$ is an n-cycle, which is repeated n times.

Claim 8.4.1. *For even n, the permutation system $(\rho, ..., \rho)$ lifts to a smooth braided embedding.*

Proof. Note that if we take $\alpha = \sigma_{n-1}...\sigma_1$ and $\beta = \sigma_{n-1}^{-1}...\sigma_1^{-1}$, then both α and β lift ρ, and both these braids give rise to valid smooth local models near branch points (see Section 7.2). Note that $\alpha^{\frac{n}{2}}$ is the Garside element Δ, see [29]. Recall, the Garside element has the property that $\Delta\sigma_i^{\pm} = \sigma_{n-i}^{\pm}\Delta$ for all i. Thus it follows that

$$\Delta\beta = \Delta\sigma_{n-1}^{-1}...\sigma_1^{-1} = \sigma_1^{-1}...\sigma_{n-1}^{-1}\Delta = \alpha^{-1}\Delta;$$

and hence $\Delta\beta^{\frac{n}{2}} = \alpha^{-\frac{n}{2}}\Delta = \Delta^{-1}\Delta = 1$. Hence The braid system $(\alpha, ..., \alpha, \beta, ..., \beta)$ smoothly lifts the given permutation system, where both α and β appears $\frac{n}{2}$ times in the braid system. $\square$

Claim 8.4.2. *For odd n, the permutation system $(\rho, ..., \rho)$ does not lift to a smooth braided embedding.*

Proof. Recall from Section 7.2, that for any braid surrounding a branch point, it has to be conjugate to either $\sigma_{n-1}...\sigma_1$ or $\sigma_{n-1}^{-1}...\sigma_1^{-1}$, in particular the exponent sum has to be $\pm(n-1)$. However, there is no way of adding up an odd number of $\pm(n-1)$ and getting 0. Consequently, there cannot be any lift, as required.

□

Remark 8.4.3. The above claim shows that there are some differences between braided embeddings in the piecewise linear and smooth categories. While all branched covers over S^2 lift in the former, there are infinitely many cyclic branched covers in the smooth category which do not lift.

Remark 8.4.4. We see that we obtain the following algebraic obstruction to lifting a branched cover over S^2 smoothly, given the permutation system, we need to be able to assign positive or negative signs to the various disjoint cycles appearing in the permutation system, so that the total sum is zero. We also can refine this by looking at connected components, for instance the permutation system

$$((123)(456), (123)(456), (123)(456))$$

cannot be lifted to a braid system smoothly, although if we assign positive signs to (123) and negative signs to (456) the total sum is 0.

CHAPTER 9

LIFTING BRANCHED COVERINGS OVER THE THREE-SPHERE

In this chapter, we will consider the case of branched covers over the three sphere S^3. We will see that there are algebraic obstructions (torsion) to lifting branched covers over S^n, when $n \geq 4$. There is no such easy obstructions in three dimension, because knot groups are torsion free.

We would mostly restrict to the case of simple branched covers (actually only simple three and four colorings) in this section, and contrast with the case one dimension lower, where we saw every simple branch cover lifted to a braided embedding, in both piecewise linear and smooth categories. In fact by our analysis of local models earlier, we saw that in any dimension and over any manifold, a simple branched cover lifts in the piecewise linear category if and only if it lifts in the smooth category.

9.1 Colorings

Definition 9.1.1. For any group G, we define a G-coloring to be a homomorphism (or anti-homomorphism) from the fundamental group of the link complement to G. By the Wirtinger presentation of the link group, it is equivalent to color (or label) each strand of any link diagram by elements of G such that at the crossings the Wirtinger relations are satisfied.

For instance, a Fox-n coloring of a link is a homomorphism from link group[1] to the dihedral group D_n (which canonically is a subgroup of the symmetric group S_n), so that meridians go to reflections. In particular, a tricoloring of a link is a

[1] By this we will mean the fundamental group of link complement.

homomorphism from link group to $D_3 \cong S_3$. We will use the following colors to indicate a simple S_3 or B_3 colorings, see Figure 9.1.

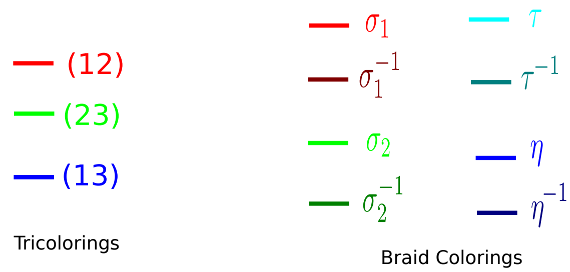

Figure 9.1: We will use these colors to indicate the colorings on the strands. In the right, σ_1 and σ_2 are the standard generators of B_3, and $\tau = \sigma_2^{-1}\sigma_1\sigma_2 = \sigma_1\sigma_2\sigma_1^{-1}$, and $\eta = \sigma_2\sigma_1\sigma_2^{-1} = \sigma_1^{-1}\sigma_2\sigma_1$.

Remark 9.1.2. Our convention is that we read group elements from left to right in fundamental groups (which includes braid groups) and symmetric group (the elements of which we think about as a product of cycles), and from right to left in mapping class groups (this is the standard convention for composing functions). Consequently, the some of the colorings we will consider will be group anti-homomorphisms (depending on the conventions of multiplication in the target group), which is why we included it in the definition of G-colorings. For any given coloring, it will be clear from the context if we are talking about a homomorphism or anti-homomorphism. An alternate notational convention would be to take the opposite group when necessary, so that a coloring is always a homomorphism.

It turns out that a branched covering is completely determined by its monodromy data of the associated covering space, and following Fox, we will call such homomorphisms colorings.

9.2 Torus Knots

It is known that [14] a torus knot $T_{p,q}$ (by symmetry, let us assume that p is odd) tricolorable if and only if p is a multiple of 3, and q is even, and moreover in those cases the tricoloring is conjugate to ”main tricoloring”, as illustrated by Figure 9.2 (the color pattern repeats both horizontally and vertically as p and q vary):

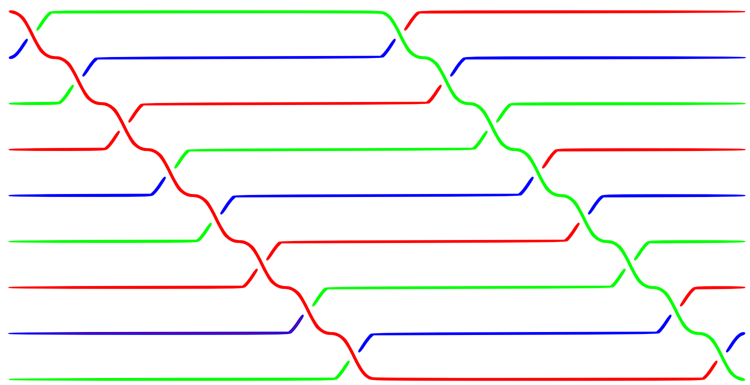

Figure 9.2: Main Tricoloring on the (9,2) torus knot

It follows that if we can show that this tricoloring lifts to a simple B_3-coloring, then all tricolorings on torus knots lift to simple braid coloring. Indeed, the following braid coloring pattern shows that there indeed is a lift (observe that for the lift of (1,3), we need to use both τ and η to obtain a valid coloring), see Figure 9.3.

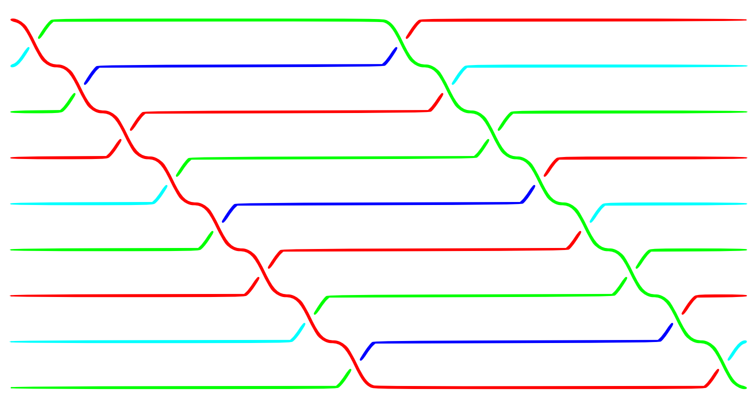

Figure 9.3: Simple B_3-coloring on the (9,2) torus knot

Let us summarize the above discussion:

Proposition 9.2.1. *A torus knot $T_{p,q}$ is tricolorable if and only if one of p and q is an odd multiple of 3, and the other is even. In this case, we moreover have that there is only one tricoloring (up to conjugation), and the tricoloring lifts to a simple B_3-coloring.*

It turns out other sorts of colorings are possible for torus links, and there is no known classification (to the best of the author's knowledge) of tricolorings of torus links. For example, consider the following tricoloring on $T_{4,4}$ in Figure 9.4:

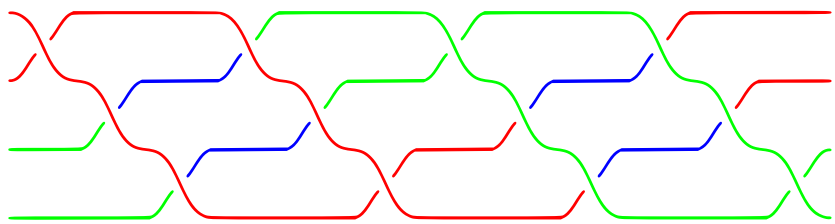

Figure 9.4: A tricoloring on the (4,4) torus link

While this tricoloring lifts to a simple braid coloring, as illustrated by Figure 9.5;

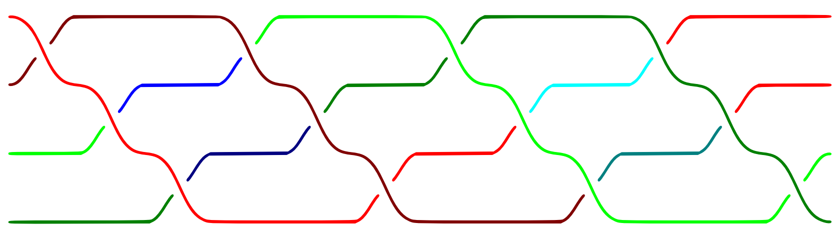

Figure 9.5: Simple B_3-coloring on the (4,4) torus link

Etnyre and Furukawa [21] show that it is possible to modify the branch locus by Montesinos 3- moves to obtain a branched cover over a knot, see Figure 9.6: which

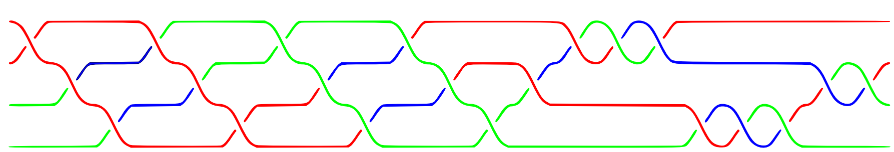

Figure 9.6: A non-liftable tricoloring.

does not lift to a braided embedding. In fact the above example is one of an infinite family of Etnyre and Furukawa, which starts of with a liftable simple S_n coloring on a torus link, but after some Montesinos 3- moves one obtains a S_n colored knot which do not lift. These examples suggest something subtle is going on with changing the branch locus with 3-moves, while it does not change the branched manifold upstairs, one frequently can go from a liftable branched covering to a non-liftable one (and vice versa).

We now discuss lifts of non-simple branched covers of the Hopf link (the simplest torus link after the unlink).

Example 9.2.2. The link group of the Hopf link is $\langle x, y | xy = yx \rangle$, where x and y are meridians. It follows that we need two commuting elements to define a coloring. However, the lifting problem for branched coverings of the three sphere, branched over the Hopf link is not the same as the problem of lifting a covering over the torus, since we now have constraints on which braids the meridians can go to, as we want the braided embedding to be smooth (or piecewise linear locally flat). Recall, that the only braids lifting the n-cycle $(12...n)$ to a smooth braided embedding, must be conjugate (by a pure braid) to either $\alpha_n = \sigma_{n-1}...\sigma_2\sigma_1$, or to $\beta_n = \sigma_{n-1}^{-1}...\sigma_2^{-1}\sigma_1^{-1}$. The center of α_n (respectively β_n) is known to be generated by α_n (respectively β_n). However, the only power of α_n (respectively β_n) which have exponent sum $\pm n$ is $\alpha_n^{\pm 1}$ (respectively $\beta_n^{\pm 1}$). Hence it follows that if we take a to be the n-cycle $(12...n)$, and $b = a^p$ for some p coprime to n so that b is different from a and a^{-1}, then the permutation coloring on the Hopf link determined by a, b does not lift to a smooth braided embedding.

9.3 Two-bridge knots and links

Recall that two bridge links (see [28] for details) in S^3 are parameterized by a rational number $\frac{p}{q}$, and such a link always has a Wirtinger presentation of the form

$\langle a, b | aw = wb \rangle$ if it is a knot, and $\langle a, b | aw = wa \rangle$ if it is a link. Here a, b are meridians and w is a word in a, b. If there is a homomorphism from the link group to braid group B_3 sending the meridians to half twists, then those half twists have to satisfy the relation $\star$ of the link group (where $\star$ denotes either $aw = wb$ or $aw = wa$). We can take double branched cover of the disc with three points (recall B_3 is the mapping class group of the thrice punctured disc), and those half twists lift to Dehn twist in the mapping class group of S_1^1, the once punctured torus. In general, the study of mapping class group of a surface and some cover is called Birman-Hilden theory [12], but in this particular cases it is fairly straightforward since the mapping class groups are isomorphic. Thus the original problem translates to: can we find two Dehn twists which satisfies the relation $\star$. This problem of relations between two Dehn twists in an orientable has been studied by Thurston [68], who showed that two Dehn twists either satisfy the braid relation (if and only if the geometric intersection number of the corresponding curves is 1), or they commute (if and only if the geometric intersection number of the corresponding curves is 0, however note that this cannot happen for two distinct simple closed curves in once punctured torus), or they do not have any relation. For a non-trivial 2-bridge link, the above relation $\star$ is always non trivial, and thus the two Dehn twists have to satisfy the braid relation. Consequently, we have:

Theorem 9.3.1. *Given any two-bridge link, and any Wirtinger presentation of link group $\langle a, b | r \rangle$. Suppose the link has a non-trivial tricoloring (i.e. the relation r holds when we set $a = (12)$ and $b = (23)$), then the tricoloring lifts to a group homomorphism to B_3 if and only if the relation r holds when we set $a = \sigma_1$ and $b = \sigma_2$.*

Remark 9.3.2. (Closures of two strand braids): The closure of the 2-braid σ_1^n is tricolorable if and only if n is a multiple of 3. If n is a multiple of 3, any non-constant tricoloring on closure $\widehat{\sigma_1^n}$, lifts to a unique braid coloring (up to conjugation in the braid group B_3), by repeating the following braid coloring, see Figure 9.7. When

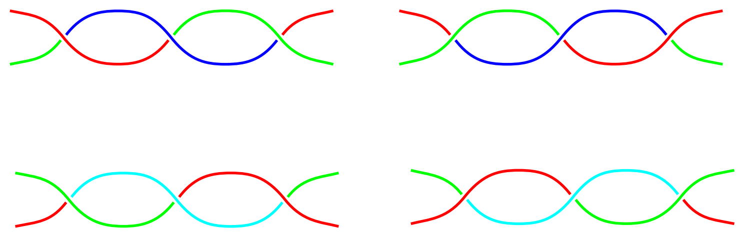

Figure 9.7: We indicate the various possibilities of colorings with three half twists, if the initial colorings are σ_1 and σ_2.

n is even, the closure $\widehat{\sigma_1^n}$ is a link, and the above theorem implies that the tricoloring does not lift to a braid coloring if we want the induced orientation on each component going the opposite way.

Since the word problem in braid groups is solvable [4], the above results give a complete characterization of which tricolorings of two-bridge knots or links lift. It would, however be interesting to find a characterization more directly in terms of the rational number $\frac{p}{q}$ (maybe something involving continued fraction expansion of $\frac{p}{q}$, or the up-down graph [28]). Recall that a two-bridge knot can have at most one (non-trivial) tricoloring, up to conjugation; and in fact it follows from the above discussion that when a two-bridge knot admits a simple simple B_3 coloring, it is unique, up to conjugation.

Among the tricolorable two-bridge knots in Rolfsen's knot table [64], the following admits a simple simple B_3 coloring:

$$3_1, 9_1, 9_6, 9_{23}, 10_5, 10_9, 10_{32}, 10_{40};$$

and the following do not:

$$6_1, 7_4, 7_7, 8_{11}, 9_2, 9_4, 9_{10}, 9_{11}, 9_{15}, 9_{17}, 10_4, 10_{10}, 10_{19}, 10_{21}, 10_{29}, 10_{31}, 10_{36}, 10_{42}.$$

9.4 Homomorphism of link groups

In this section, let us discuss some generalities about having homomorphisms from a link group $\pi_1(S^3 \setminus L)$ to some group G.

Let H be a subgroup of G contained in the center $\mathcal{Z}(G)$ of G. So given any homomorphism $\phi : \pi_1(S^3 \setminus L) \to G$, we get a group homomorphism from $\psi : \pi_1(S^3 \setminus L) \to G/H$ by composing with the natural projection $G \to G/H$. We will show that the converse is also true.

We know that $\pi_1(S^3 \setminus L)$ has a Wirtinger presentation $\langle x_1, ..., x_k | r_1, ..., r_k \rangle$, so given any group homomorphism $\psi : \pi_1(S^3 \setminus L) \to G/H$, let us pick any element g_1 in G which projects to $\psi(x_1)$. The Wirtinger relation $x_j = x_i x_1 x_i^{-1}$ will determine where x_j has to go, as follows. Pick any g_i lifting $\psi(x_i)$, and we are forced to send x_j to $g_i g_1 g_i^{-1}$. The reader should note that if we picked another lift g_i' then $g_i' = g_i z$ for some central element z, and consequently $g_i g_1 g_i^{-1} = g_i' g_1 {g'}_i^{-1}$. Hence, if we choose meridians, one for each of the component of the link, and lift for the images under ψ each of those meridians, the Wirtinger relations give us a lift ϕ of ψ, as required.

Let us focus on the case of $G = B_3$ and $H = Z(G)$, which is known to be generated by the square of the Garside element $\Delta^2 = (\sigma_1 \sigma_2 \sigma_1)^2$. It is well known that the quotient G/H is the modular group $PSL(2, \mathbb{Z}) \cong \mathbb{Z}_2 * \mathbb{Z}_3$. The above result means given any homomorphism $\psi : \pi_1(S^3 \setminus L) \to PSL(2, \mathbb{Z})$ then it lifts to a homomorphism $\phi : \pi_1(S^3 \setminus L) \to B_3$, i.e. $p \circ \phi = \psi$, where $p : B_3 \to PSL(2, \mathbb{Z})$ denotes the quotient map[2]. Consequently, it follows that lifting an S_3-coloring of a link to a B_3-coloring is equivalent to whether it lifts to an $PSL(2, \mathbb{Z})$-coloring (or $SL(2, \mathbb{Z})$-coloring). The reader should note that the natural projection $B_3 \to S_3$ factors through $SL(2, \mathbb{Z})$ and $PSL(2, \mathbb{Z})$, and so it makes sense to talk about the lifting problem in that context. Also, we see that admissible B_3-colorings correspond to admissible $PSL(2, \mathbb{Z})$-coloring (or admissible $SL(2, \mathbb{Z})$-coloring).

[2] and of course we get similar statement if we replace $PSL(2, \mathbb{Z})$ with $SL(2, \mathbb{Z})$.

Now if we were considering an epimorphism (= surjective homomorphism) $\psi : \pi_1(S^3 \setminus L) \to PSL(2,\mathbb{Z})$ sending meridians to standard generators (standard transvections), then we see that we can lift it to an epimorphism $\phi : \pi_1(S^3 \setminus L) \to B_3$, as follows. Observe that, up to conjugation, we can choose to send via ϕ a meridian $\mu \in \pi_1(S^3 \setminus L)$ to σ_1 (which the lift of a standard transvection), and since we know ψ is surjective we know there is an element $\alpha \in \pi_1(S^3 \setminus L)$ so that $\psi(\alpha) = p(\sigma_2)$. Then for the lift ϕ we have $\phi(\alpha\mu\alpha^{-1}) = \sigma_2\sigma_1\sigma_2^{-1}$. Since by the braid relation

$$\sigma_2 = \sigma_1\sigma_2\sigma_1\sigma_2^{-1}\sigma_1^{-1} = \phi(\mu\alpha\mu\alpha^{-1}\mu^{-1}),$$

the image of ϕ contains both σ_1 and σ_2, an so ϕ is surjective.

If we have a homomorphism $\psi : \pi_1(S^3 \setminus L) \to PSL(2,\mathbb{Z})$, then the image of ψ is a subgroup of $PSL(2,\mathbb{Z})$; and by Kurosh subgroup theorem, will be abstractly isomorphic to a free product of $\mathbb{Z}$, $\mathbb{Z}_2$ and $\mathbb{Z}_3$'s.

9.5 Tricolorings of knots

If we are considering the image of a knot group, then we know that the abelianization has to be cyclic, so the only possible images in $PSL(2,\mathbb{Z})$ are isomorphic to $\{1\}$, $\mathbb{Z}$, $\mathbb{Z}_2$, $\mathbb{Z}_3$ and $\mathbb{Z}_2 * \mathbb{Z}_3$. If we are considering such a ψ coming from a non-trivial simple B_3-coloring, then the only possibility is $\mathbb{Z}_2 * \mathbb{Z}_3$ because:

- The subgroup generated by the coset of half twist is isomorphic to the integers (rules out $\{1\}$, $\mathbb{Z}_2$, $\mathbb{Z}_3$)

- Two distinct half twists in B_3 cannot commute (as one of the endpoints has to be the same); and this continues to be true in the quotient, which rules out $\mathbb{Z}_2$. In fact it is known that two half twists in B_3 either satisfy no relations, or satisfy the braid relation.

Now the group $PSL(2,\mathbb{Z})$ is not co-Hopfian, meaning there are proper subgroups isomorphic to it, and thus cannot directly use our observation about lifting epimorphisms.

Suppose we have any epimorphism[3] $\psi : \pi_1(S^3 \setminus K) \to PSL(2,\mathbb{Z})$, and we will show that it has to lift to an epimorphism $\phi : \pi_1(S^3 \setminus K) \to B_3$, as follows. For any meridian $\mu \in \pi_1(S^3 \setminus K)$, if $\psi(\mu)$ has exponent sum in $\mathbb{Z}_6$ (exponent sum from B_3 is well defined to the integers, and since we get $PSL(2,\mathbb{Z})$ by quotienting by an element of exponent sum 6, we see that exponent sum descends to a well defined homomorphism $\varepsilon : PSL(2,\mathbb{Z}) \to \mathbb{Z}_6$, and by abuse of terminology we will still call it exponent sum) not equal to ± 1, then the exponent sum is in $\{2,3,4\}$, which would imply the exponent sum of the entire image of ψ is a proper subset of $\mathbb{Z}_6$, which contradicts the fact that ψ is surjective. Changing orientation of K if necessary, let us assume that the exponent sum of $\psi(\mu)$ is $1 \in \mathbb{Z}_6$.

Let us choose the lift $\tau \in B_3$ of $\psi(\mu)$, with exponent sum of τ being 1 (the various choices for τ differ up to a central element, $(\sigma_1\sigma_2\sigma_1)^{2n}$ where n is some integer). As we saw earlier, there is a unique lift $\phi : \pi_1(S^3 \setminus K) \to B_3$ of ψ sending μ to τ. Moreover we see by using the surjectivity of ψ, that for $i = 1, 2$ there are elements $\alpha_i \in \pi_1(S^3 \setminus K)$ so that $\psi(\alpha_i) = p(\sigma_i)$ and α_1 is conjugate to α_2. We must have $\phi(\alpha_i) = \sigma_i(\Delta^2)^n$ where n is some integer.

If we write τ as a word in σ_1 and σ_2; and we write out the same word in α_1 and α_2, we see that element will map under ϕ to $\tau(\Delta^2)^n$. Thus $(\Delta^2)^n$ is in the image of ϕ, and hence so are σ_1 and σ_2 and consequently ϕ is surjective. Hence, we have

Theorem 9.5.1. *If K is a knot which has a simple B_3 coloring, then there is an epimorphism from the knot group $\pi_1(S^3 \setminus K)$ to B_3.*

The advantage of promoting the existence of a homomorphism to the existence

[3]we do not assume here it sends meridians to standard transvections, unlike the previous subsection

an epimorphism is that there are known obstructions to such epimorphism. For example, Fox [19] showed that if there is any epimorphism between knot groups (or groups like knot groups, where Alexander polynomials are defined) then the Alexander polynomial of the target space has to divide the Alexander polynomial of the source space. This obstruction was upgraded to obstruction coming from twisted Alexander polynomials [54], and these tools have been used to study partial orders on the set of knots [53]. As a consequence, there are lots of tricolorable knots, for which the tricoloring does not lift to a simple B_3-coloring.

Theorem 9.5.2. *Suppose K is any tricolorable knot so that $1 - t + t^2$ does not divide the Alexander polynomial of K (or an analogous statement with the twisted Alexander polynomials), then no tricoloring of K lifts to a simple B_3-coloring.*

This theorem let's us answer for each knot in Rolfsen's knot table, if a knot admits a simple B_3-coloring. In Rolfsen's table the bridge index of each knot is at most three, and we already know the answer for two-bridge knots, so it remains to answer it for the three-bridge knots in the table. The three-bridge tricolorable in Rolfsen's knot table which have a simple braid coloring (see [53] for explicit homomorphisms) are:

$$8_5, 8_{10}, 8_{15}, 8_{18}, 8_{19}, 8_{20}, 8_{21}, 9_{16}, 9_{24}, 9_{28}, 9_{40}, 10_{61}, 10_{62}, 10_{63}, 10_{64}, 10_{65}, 10_{66},$$

$$10_{76}, 10_{77}, 10_{78}, 10_{82}, 10_{84}, 10_{85}, 10_{87}, 10_{98}, 10_{99}, 10_{103}, 10_{106}, 10_{112}, 10_{114},$$

$$10_{139}, 10_{140}, 10_{141}, 10_{142}, 10_{143}, 10_{144}, 10_{159}, 10_{164};$$

and those knots which does not have a simple braid coloring are:

$$9_{29}, 9_{34}, 9_{35}, 9_{37}, 9_{38}, 9_{46}, 9_{47}, 9_{48}, 10_{59}, 10_{67}, 10_{68}, 10_{69}, 10_{74}, 10_{75}, 10_{89}, 10_{96}, 10_{97}, 10_{107},$$

$$10_{108}, 10_{113}, 10_{120}, 10_{122}, 10_{136}, 10_{145}, 10_{146}, 10_{147}, 10_{158}, 10_{160}, 10_{163}, 10_{165}.$$

The above statement is about existence of a simple B_3-coloring on a knot, not about whether a given tricoloring lifts. More precisely, we can ask:

Question 9.5.3. Is there a prime knot K with two tricolorings, one of which lifts to a simple B_3-coloring, and the other does not?

If we did not include the hypothesis that K is prime, then the answer is easily seen to be "Yes". For we can take a connect sum of a knot K_1 which has a non-trivial simple B_3-coloring (for example the trefoil, 3_1), and a tricolorable knot which does not have a non-trivial simple B_3-coloring (for example the 6_1 knot) and consider two tricolorings of $K_1 \# K_2$, one which is non-trivial on K_1 and trivial on K_2, and another which is non-trivial on both K_1 and K_2.

Let us digress for a moment and discuss of colorings for a connect sum of knots, and we see that the lifting problem for a connect sum reduces to a lifting problem for each of the components.

Proposition 9.5.4. *Suppose K is a connect sum of two knots K_1, K_2 in S^3. Then for any G-coloring on K, the colors on the two strands on the boundary of the band corresponding to the connect sum are the same (where we choose consistently oriented meridians for each of the strands). Consequently, by cutting the two strands and joining them to each component, we get G- colorings on K_1 and K_2 respectively.*

Proof. Consider a splitting sphere S or for the connect sum which intersects $K_1 \# K_2$ in exactly two points. Let us choose the basepoint for the knot complement on S, and by choosing an orientation on K, we get oriented meridians for the two strands of $K_1 \# K_2$ intersecting S. We can homotope the meridians to lie on the sphere S punctured at two points (we remove from S the two points of intersection). We know see the meridians are the homotopic in the twice punctured sphere, and hence in the knot complement. The result follows since any homomorphism must preserve equalities in the domain. □

Remark 9.5.5. We note that the analogue of the above result also holds for analogues of connect sum of links (by which we mean we can pick any two components of either link and perform a band attachment). While the resulting link will depend (in general) on the choice of the components and the band, any G-coloring on it will canonically give rise to G-colorings on each of the original links. We also remark that similar result holds for codimension two links in higher dimensional spheres, with exactly the same proof.

It follows from the above Proposition that a tricoloring on a connected sum of knots lift if and only if the corresponding tricolorings on each of the individual knots lift.

Returning to our example, we can conclude the first tricoloring on $K_1 \# K_2$ lifts to a braid coloring and the second does not.

Note that for two-bridge knots there is only one tricoloring up to conjugation, and so in this case whether a given tricoloring lifts is the same question as whether the underlying knot has a simple B_3 coloring. The answer to the above question is still "Yes", and this means the question about lifting tricolorings is something pertaining to a branched covering map (corresponding to permutation coloring), not just about what the underlying branch set is (or the branched covering manifold upstairs).

To answer Question 9.5.3, we need to gain a better understanding of types of relations about more than two Dehn twists. The author was able to show (see [44]) subgroups in B_3 generated by three half twists (equivalently subgroups in $S_{1,1}$ generated by three Dehn twists) is either free (of rank at most 3), or the entire braid group. This implies any simple braid coloring of a three bridge knot must actually be surjective. However this does not immediately answer the question about whether a tricoloring on a 3-bridge knot lifts to a braid coloring, it still appears to be an infinite check.

However, by building upon ideas from there, we will answer the question for a family of 3-strand pretzel knots. Let us first make the observation that the epimorphism $\pi : B_3 \to S_3$ factors through $SL_2(\mathbb{Z})$, the mapping class group of the torus. $B_3 \cong \langle a, b | aba = bab \rangle$ is the mapping class group of the once holed torus, and from there we can get the mapping class group of the torus by capping off the boundary component, which corresponds to adding the relation $(ab)^6 = 1$. Recall that we get the presentation of the symmetric group S_3 by adding the relations $a^2 = 1$ and $b^2 = 1$. Note the relation $(ab)^6 = 1$ holds in the symmetric group since:

$$(ab)^6 = (ababab)^2 = (abaaba)^2 = (ab^2a)^2 = (a^2)^2 = 1.$$

Thus, we see that π factors through[4] $SL_2(\mathbb{Z})$, i.e. there are homomorphisms $\tau : B_3 \to SL_2(\mathbb{Z})$ and $\rho : SL_2(\mathbb{Z}) \to S_3$ so that $\pi = \rho \circ \tau$. We observe that π_1 sends half twists in the braid group to Dehn twists in the mapping class group of the torus (this is exactly the Dehn twist about the curve in the double branched cover which is a lift of the arc corresponding to the half twist, except that we have capped off the boundary component). Recall simple closed curves (and Dehn twists about them) in the torus are in one to one correspondence of projectivised[5] primitive vectors in the first homology $H_1(\mathbb{T}^2) \cong \mathbb{Z}^2$. So given a primitive vector $\vec{x} = \begin{pmatrix} p \\ q \end{pmatrix}$, let us first discuss how to find the image of T_x under ρ.

Claim 9.5.6. *The image under ρ of any Dehn twist T_x only depends on the congruence class of $\vec{x}$ (with either orientation) modulo 2. More specifically,*

- *if* $\vec{x} \equiv \begin{pmatrix} 1 \\ 0 \end{pmatrix} \pmod 2$, *then* $\rho(T_x) = (12)$,

[4] In fact π factors also through $PSL_2(\mathbb{Z})$ as we actually showed $(ab)^3 = 1$ in S_3.
[5] up to a sign (for orientation)

- *if* $\vec{x} \equiv \begin{pmatrix} 0 \\ 1 \end{pmatrix} \pmod 2$, *then* $\rho(T_x) = (23)$,

- *if* $\vec{x} \equiv \begin{pmatrix} 1 \\ 1 \end{pmatrix} \pmod 2$, *then* $\rho(T_x) = (13)$.

Proof. By definition (or by convention) we have that $\rho(T_x) = (12), \rho(T_y) = (23), \rho(T_z) = (13)$, where $\vec{x} = \begin{pmatrix} 1 \\ 0 \end{pmatrix}, \vec{y} = \begin{pmatrix} 0 \\ 1 \end{pmatrix}, \vec{z} = \begin{pmatrix} 1 \\ 1 \end{pmatrix}$ respectively. By the proof of [44, Remark 7.4], we see that given any primitive vector $\vec{u}$, there is another primitive vector $\vec{v} \in \{\pm\vec{x}, \pm\vec{y}, \pm\vec{z}\}$, and a word w in T_x^2, T_y^2 and T_z^2 so that $w\vec{v} = \vec{u}$. It follows that $T_u = wT_vw^{-1}$. Since $\rho(T_x^2) = \rho(T_y^2) = \rho(T_z^2) = 1$, it follows that $\rho(T_u) = \rho(T_v)$, and hence the claim holds.

□

Let us record the following consequence of the above claim for future use.

Claim 9.5.7. *If $\vec{u}$ and $\vec{v}$ are primitive vectors in $\mathbb{Z}^2$, then $\rho(T_u) = \rho(T_v)$ if and only if the algebraic intersection number $\langle \vec{u}, \vec{v} \rangle$ is even.*

Proof. Recall the algebraic intersection number $\langle \vec{u}, \vec{v} \rangle$ is equal to the determinant of the matrix with columns $\vec{u}$ and $\vec{v}$ (in that order). To find the parity of the determinant (i.e. reduce the determinant modulo 2), we may equivalently reduce $\vec{u}$ and $\vec{v}$ modulo 2, and then find the determinant. For a primitive vector modulo 2, there are exactly three choices, and the result now follows from the previous claim. □

9.6 Labellings in a twist region

Suppose we have a twist region with m half twists (m can be positive or negative) both strands oriented bottom to top[6]. Let the bottom left and bottom right merid-

[6]Even if the natural orientation of the strands coming from the knot or link goes the other way, we can take the inverse of the meridian and carry out the computations assuming the strands are oriented from bottom to top in the twist region

ians in the fundamental group be a and b, and we denote by A and B the inverses of a and b respectively.

If $m = 2n$ is even, by Wirtinger relations the top left and top right meridians are $a^{(ba)^n}$ and $b^{(ba)^n}$ (which equals $b^{(ab)^{n-1}a}$) respectively. If $m = 2n+1$ is odd, by Wirtinger relations the top left and top right meridians are $b^{a(ba)^n}$ and $a^{a(ba)^n}$ (which equals $a^{(ba)^n}$) respectively.

Figure 9.8 illustrates these formulas with twist regions with four positive and negative crossings respectively.

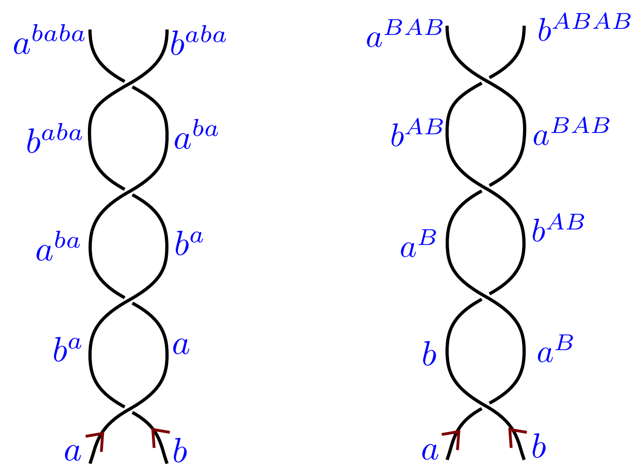

Figure 9.8: Meridians in twist regions using the Wirtinger presentation, if we start with meridians a, b in the bottom; and A and B denote their inverses.

Consider a braid coloring of the twist region with the meridians mapping to half twists, and let us further send it to the corresponding Dehn twist in the double branched cover, and call this coloring ϕ.

Note that for Dehn twists we have $T_{f(x)} = f \circ T_x \circ f^{-1}$, so if $\phi(a) = T_x$ and $\phi(b) = T_y$, then by Wirtinger relation $c = a^{-1}ba$ (respectively $c = aba^{-1}$) we have $\phi(c) = T_x \circ T_y$ (respectively $\phi(c) = T_x^{-1} \circ T_y$).

We see that

$$\phi(a^{(ba)^n}) = T_{(T_xT_y)^n(x)} \quad \phi(b^{(ba)^n}) = T_{(T_xT_y)^n(y)}$$

$$\phi(b^{a(ba)^n}) = T_{(T_xT_y)^n(T_x(y))} \quad \phi(a^{(ba)^n}) = T_{(T_xT_y)^n(x)}$$

Instead of labeling the strands with a left or right handed Dehn twist, we could just label by the vector in homology corresponding to the simple closed curve (there is a sign ambiguity when we make initial choices for the bottom left and bottom right) about which the Dehn twists are taking place. We make the following observation:

Claim 9.6.1. *A simple B_3 coloring on a link in S^3 is equivalent to having a labelling on the strands by projectivised primitive vectors in $\mathbb{Z}^2$, such that at each crossing the associated Dehn twists satisfy the Wirtinger relations.*

Let us now rewrite the labellings on the strands in a twist region with m half twists with this convention. Suppose the bottom left strand is labelled with $\vec{x}$ and the bottom right strand is labelled with $\vec{y}$. If $m = 2n$ is even, the labelling on the top left and top right strands are $(T_xT_y)^n(\vec{x})$ and $(T_xT_y)^n(\vec{y})$ respectively. If $m = 2n+1$ is odd, the labelling on the top left and top right strands are $(T_xT_y)^n(T_x(\vec{y}))$ and $(T_xT_y)^n(\vec{x})$ respectively. Let us try to understand how these experssions look as a linear combination of $\vec{x}$ and $\vec{y}$.

Let $k = \langle \vec{x}, \vec{y} \rangle$, the by definition we have $T_y(\vec{x}) = \vec{x} - k\vec{y}$, and hence we obtain

$$T_x \circ T_y(\vec{x}) = T_x(T_y(\vec{x})) = \vec{x} - k\vec{y} + \langle \vec{x}, \vec{x} - k\vec{y} \rangle \vec{x} = \vec{x} - k\vec{y} - k\langle \vec{x}, \vec{y} \rangle \vec{x} = (1-k^2)\vec{x} - k\vec{y}$$

More generally, we inductively have for any natural number n:

$$(T_x \circ T_y)^n(\vec{x}) = [1 - k^2 A_n(k)]\vec{x} - kB_n(k)\vec{y},$$

as justified below for some integer valued functions A_n, B_n of k.

We note that

$$T_y \circ (T_x \circ T_y)^n(\vec{x}) = T_y((T_x \circ T_y)^n(\vec{x})) = T_x \circ T_y([1 - k^2 A_n(k)]\vec{x} - kB_n(k)\vec{y})$$

$$= [1 - k^2 A_n(k)][\vec{x} - k\vec{y}] - kB_n(k)\vec{y} = [1 - k^2 A_n(k)]\vec{x} - k[B_n(k) + 1 - k^2 A_n(k)]\vec{y}$$

Hence we have

$$(T_x \circ T_y)^{n+1}(\vec{x}) = T_x([1 - k^2 A_n(k)]\vec{x} - k[B_n(k) + 1 - k^2 A_n(k)]\vec{y})$$

$$= [1 - k^2 A_n(k)]\vec{x} - k[B_n(k) + 1 - k^2 A_n(k)][\vec{y} + k\vec{x}]$$

$$= [1 - k^2[(1 - k^2)A_n(k) + B_n(k) + 1]]\vec{x} - k[B_n(k) + 1 - k^2 A_n(k)]\vec{y}$$

Hence we have the recursive formulas

$$A_{n+1}(k) = (1 - k^2)A_n(k) + B_n(k) + 1, \text{ and} \tag{9.1}$$

$$B_{n+1}(k) = B_n(k) + 1 - k^2 A_n(k), \tag{9.2}$$

with the initial conditions $A_1(k) = 1 = B_1(k)$.

Since we only see quadratic terms in k, it follows that $A_n(-k) = A_n(k)$ and $B_n(-k) = B_n(k)$. By interchanging the roles of x and y (and remembering that $\langle \vec{y}, \vec{x} \rangle = -\langle \vec{x}, \vec{y} \rangle = -k$) we see that

$$(T_y \circ T_x)^n(\vec{y}) = kB_n(k)\vec{x} + (1 - k^2 A_n(k))\vec{y}$$

Along the way we also have found formulas for the other labels appearing at the end of the twist regions:

$$T_y \circ (T_x \circ T_y)^n(\vec{x}) = [1 - k^2 A_n(k)]\vec{x} - kB_{n+1}(k)\vec{y}$$

and (once again by interchanging x and y)

$$T_x \circ (T_y \circ T_x)^n(\vec{y}) = [1 - k^2 A_n(k)]\vec{y} + kB_{n+1}(k)\vec{x}$$

In a similar fashion we may calculate

$$(T_x^{-1} \circ T_y^{-1})^n(\vec{x}) = [1 - k^2 A_n(k)]\vec{x} - kB_n(k)\vec{y},$$

$$T_y^{-1}(T_x^{-1} \circ T_y^{-1})^n(\vec{x}) = [1 - k^2 A_n(k)]\vec{x} - kB_{n+1}(k)\vec{y},$$

One similarly has functions C_n, D_n of k so that we have the following formulas for composition of left and right handed Dehn twists:

$$(T_x \circ T_y^{-1})^n(\vec{x}) = [1 + k^2 C_n(k)]\vec{x} + kD_n(k)\vec{y},$$

$$T_y^{-1}(T_x \circ T_y^{-1})^n(\vec{x}) = [1 + k^2 C_n(k)]\vec{x} + kD_{n+1}(k)\vec{y},$$

$$(T_x^{-1} \circ T_y)^n(\vec{x}) = [1 + k^2 C_n(k)]\vec{x} - kD_n(k)\vec{y},$$

$$T_y(T_x^{-1} \circ T_y)^n(\vec{x}) = [1 + k^2 C_n(k)]\vec{x} - kD_{n+1}(k)\vec{y}.$$

We have similar recursive formulas for C_n and D_n, just like the ones for A_n and B_n

$$C_{n+1}(k) = (1 + k^2)C_n(k) + D_n(k) + 1, \text{ and} \tag{9.3}$$

$$D_{n+1}(k) = D_n(k) + 1 + k^2 C_n(k), \tag{9.4}$$

with the initial conditions $C_1(k) = 1 = D_1(k)$.

In fact, we can directly relate the functions C_n and D_n to the functions A_n and B_n as follows:

$$C_n(k) = A_n(ik), \text{ and } D_n(k) = B_n(ik),$$

where i is a square root of -1. An alternate (and probably less mysterious) way of making the same statement is as follows. Recall that A_n, B_n, C_n and D_n are polynomial functions of k, where only even degree terms appear. Consequently, we can think of them as polynomials in k^2. We get the polynomial C_n (respectively D_n) by substituting all occurrences of k^2 in A_n (respectively B_n) by $-k^2$, and vice versa.

We illustrate using recurrence formulas by finding the labellings in a twist regions with three positive half twists, with the bottom strands colored by the Dehn twists $T_x^{\pm 1}$ and $T_y^{\pm 1}$, and we pick some orientation of x and y, and let k denote the algebraic intersection number between x and y. Depending on the sign of the exponents, we have four cases to deal with, in Figure 9.9 (see Remark 9.6.2) we consider the two cases that the two Dehn twists are similar handed (i.e. both right handed or both left handed); while in Figure 9.10 (see Remark 9.6.3) we consider the two cases that the two Dehn twists are different handed.

We can also do a similar calculation and see what the labellings would turn out to be if we had a negative twist region. With the same choices as above, if the labellings after n positive half twists are $a\vec{x} + b\vec{y}$ and $c\vec{x} + d\vec{y}$ (read from left to right), then the labellings after n positive half twists are $(-1)^n(d\vec{x} - b\vec{y})$ and $(-1)^n(-c\vec{x} + a\vec{y})$. One way to think about this is think of the input colors as a basis, and the output colors as the image of a linear map. The linear maps corresponding to positive and negative twist regions (with the same number of half twists) should be inverses of each other, and everything boils down to the formula of the inverse of a 2×2 matrix:

$$\begin{pmatrix} a & b \\ c & d \end{pmatrix}^{-1} = \frac{1}{ad-bc}\begin{pmatrix} d & -b \\ -c & a \end{pmatrix}.$$

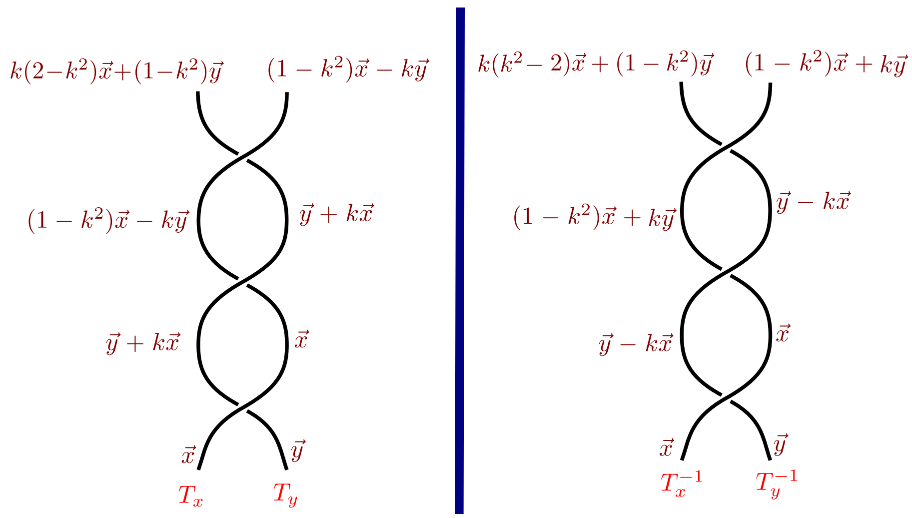

Figure 9.9: Labellings of twist region with homology vectors corresponding to similar handed Dehn twists

Remark 9.6.2. We discuss the case the two Dehn twists same handed, and this case is illustrated by Figure 9.9.

If there are an even number of half twists, the labelling on the top left and top right strands are of the form $(1-k^2a)\vec{x}+kb\vec{y}$ and $-kb\vec{x}+(1-k^2c)\vec{y}$ respectively for some integers a, b, c. Moreover we have $a+c=\mp b$, where the sign is same as the sign of the twist region, times the exponent sum of the bottom left coloring.

If there are an odd number of half twists, the labelling on the top left and top right strands are of the form $kb\vec{x}+(1-k^2a)\vec{y}$ and $(1-k^2a)\vec{x}+kc\vec{y}$ respectively for some integers a, b, c. Moreover we have $b+c=\pm(1-k^2a)$, where the sign is same as the sign of the twist region, times the exponent sum of the bottom left coloring.

Remark 9.6.3. We now discuss the case of opposite handed Dehn twists, see Figure 9.10.

If there are an even number of half twists, the labelling on the top left and top

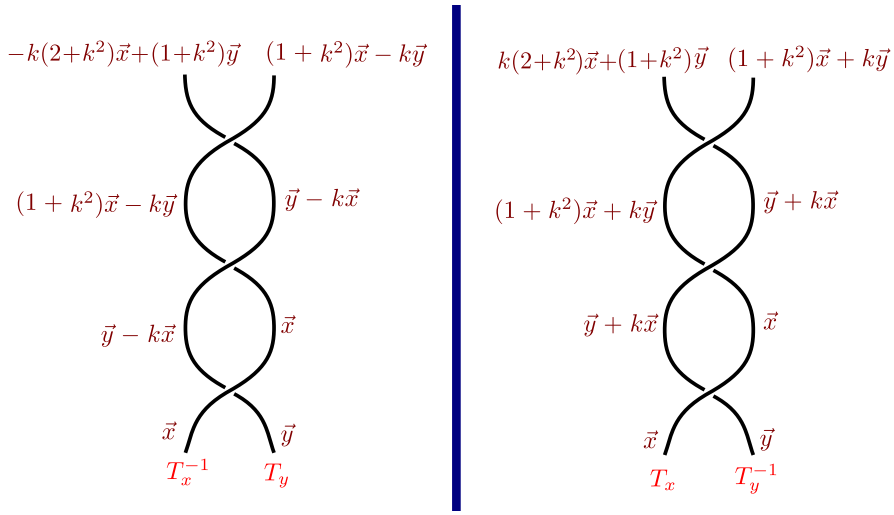

Figure 9.10: Labellings of twist region with homology vectors corresponding to different handed Dehn twists

right strands are of the form $(1+k^2a)\vec{x}+kb\vec{y}$ and $kb\vec{x}+(1+k^2c)\vec{y}$ respectively for some integers a, b, c. Moreover we have $a-c=\pm b$, where the sign is same as the sign of the twist region, times the exponent sum of the bottom left coloring.

If there are an odd number of half twists, the labelling on the top left and top right strands are of the form $kb\vec{x}+(1+k^2a)\vec{y}$ and $(1+k^2a)\vec{x}+kc\vec{y}$ respectively for some integers a, b, c. Moreover we have $b-c=\pm(1+k^2a)$, where the sign is same as the sign of the twist region, times the exponent sum of the bottom left coloring.

Note that in this case if the number of half twists increase, then so do these coefficients a, b and c. This is because the functions $C_n(k)$ and $D_n(k)$ are strictly increasing for $k \neq 0$, by the recurrence relations.

Remark 9.6.4. Consider $\vec{x}$ and $\vec{y}$ to have algebraic intersection number 1, and consider the two situations in Figure 9.9. We see the labellings on the top strands are $\vec{x}$ and $-\vec{y}$ for the sub figure on the left (corresponding to two right handed Dehn twists), and $-\vec{x}$ and $\vec{y}$ for the sub-figure on the right (corresponding to two left handed Dehn twists). We see the labellings at the top and bottom match up only if we allow the sign ambiguity. However, if we close up the twist region, we get a trefoil, with the standard non-trivial braid coloring. This example is to illustrate that it is necessary that we allow the sign ambiguity when we are dealing with labellings.

9.7 Pretzel Knots: Introduction

A pretzel link $P(q_1, q_2, ..., q_m)$ has a diagram with m twist regions joined up as illustrated in Figure 9.11, where there are q_i (which can be both positive and negative and zero) is the number of half-twists in the i-th region.

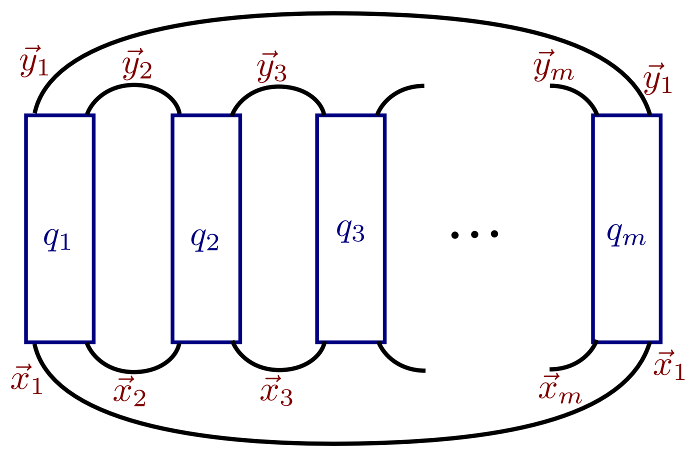

Figure 9.11: A pretzel link $P(q_1, q_2, ..., q_m)$.

Fact 9.7.1. *We recall some basic facts about pretzel links.*

- $P(q_1, q_2, ..., q_m)$ *is isotopic to* $P(q_2, ..., q_m, q_1)$.
- $P(q_1, q_2, ..., q_m)$ *is a knot if and only if either exactly one of the* q_i *is even, or all the* q_i*'s and* m *are odd.*
- *For a pretzel knot, if we pick any orientation on the knot, then one of the following possibilities occur:*
    1. *in every twist region the strands go in opposite directions (this happens if and only if all the* q_i*'s and* m *are odd);*

2. *in every twist region the strands go in same directions (this happens if and only if exactly one of the q_i is even and m is even);*
3. *in exactly one twist region the strands go in opposite direction (this happens if and only if exactly one of the q_i is even and m is odd).*

Claim 9.7.2. *If we have any G-coloring on a pretzel link, and suppose that for some twist region the colors on the bottom left (respectively right) strand is the same as the colors on the top left (respectively right) strand, where we look at the color individually on each twist region orienting the strands from bottom to top. Then same holds in any twist region, i.e. the colors on the bottom strands is the same as the colors on the top strands (in the same order).*

Proof. In any twist region, the products of the meridians we have around the top two strands is the same as that around the bottom two strands, since a loop enclosing the bottom two strands is homotopic to the loop bounding the top two strands. Alternately, this can be deduced by repeated application of the Wirtinger relations, notice that the Wirtinger relation is precisely the statement in the previous sentence if the twist region has one crossing. If we are given that the G-coloring fixes the colors on the left strand (which is equivalent to both left and right strand), we see the same has to be true for the rightmost strand of the twist region to the left, and we get the result by repeating this observation. □

Proposition 9.7.3. *Suppose we have a non-trivial simple B_3-coloring, so that the associated labelling by primitive vectors in $\mathbb{Z}^2$ on two strands on the bottom of a twist region in any pretzel knot $P(q_1, ..., q_m)$ are the linearly dependent (i.e. same or negatives of each other). Then in every twist region where the coloring is non-constant must have the strands gong the same way, and the number of half twists must be a multiple of 3, and we have the pattern from Remark 9.3.2 repeated in each such a twist region.*

Proof. As we have a non-trivial braid coloring, so there must be two twist regions, say T_1 and T_2 next to each other with say T_1 on the left having the same labellings, and T_2 on the right different labellings. We note that this twist region with different labellings must go in the same direction, as otherwise we cannot get the same label (since the functions $C_n(k)$ and $D_n(k)$ are monotonically increasing by Remark 9.6.3).

Since we have the strands going the same way in the twist region on the right, we know that the exponent sums of the coloring top left and bottom left strands on T_2 must be the same, and hence it follows that the same should be true for the exponent sums of the coloring top right and bottom left strands on T_2. In particular, for the twist region T_2 the colorings on the top left strand is the same as the colorings of the bottom left strand, and now the result follows from the previous claim and Remark 9.6.2. □

As a consequence of the above proposition, when we are analyzing simple B_3-colorings on pretzel knots, we may assume the associated labellings in each twist regions are distinct, since otherwise we understand the coloring extremely well by the above proposition.

Remark 9.7.4. We introduce some notation for future use. Suppose we label the strands at the bottom and top with the labels $\vec{x}_1$,...,$\vec{x}_m$ and $\vec{y}_1$,...,$\vec{y}_m$ as illustrated in Figure **??**.

Let us denote by k_i the algebraic intersection number $\langle \vec{x}_i, \vec{x}_{i+1} \rangle$.

Since we assume for all i, $\vec{x}_{i-1}$ and $\vec{x}_i$ are linearly independent we can express each x_{i+1} as a rational linear combination of x_{i-1} and x_i,

$$\vec{x}_{i+1} = \alpha_i \vec{x}_{i-1} + \beta_i \vec{x}_i \text{ for some } \alpha_i, \beta_i \in \mathbb{Q}.$$

Notice that we have:

$$k_i = \langle \vec{x}_i, \vec{x}_{i+1} \rangle = \langle \vec{x}_i, \alpha_i \vec{x}_{i-1} + \beta_i \vec{x}_i \rangle = \alpha_i \langle \vec{x}_i, \vec{x}_{i-1} \rangle = -\alpha_i k_{i-1}, \text{ and} \tag{9.5}$$

$$\langle \vec{x}_{i-1}, \vec{x}_{i+1} \rangle = \langle \vec{x}_{i-1}, \alpha_i \vec{x}_{i-1} + \beta_i \vec{x}_i \rangle = \beta_i \langle \vec{x}_{i-1}, \vec{x}_i \rangle = \beta_i k_{i-1}. \tag{9.6}$$

9.8 Three strand Pretzel knots I: all odd

Let us consider the pretzel knot $P(p,q,r)$ with p,q,r all odd. The Alexander polynomial of this knot is [55, Example 6.9]

$$\Delta_{P(p,q,r)}(t) = \frac{1}{4}((pq+qr+rp)(t^2-2t+1)+t^2+2t+1)).$$

In particular the determinant of such a pretzel knot is $\Delta_{P(p,q,r)}(-1) = pq+qr+rp$ (this formula for the determinant is true for more general pretzel knots, see [43, Section 8]) and so pretzel knots $P(p,q,r)$ is tricolorable if and only if 3 divides $pq+qr+rp$.

It is easy to see that $\Delta_{P(p,q,r)}(t)$ is divisible by $1-t+t^2$, the Alexander polynomial of the trefoil knot (which is a pretzel knot $P(1,1,1)$ or $P(-1,-1,-1)$ depending on the handedness) if and only if $pq+qr+rp=3$. It follows from Theorem 9.5.2 that if the determinant $pq+qr+rp$ is any multiple of three different from three, then any associated tricoloring does not lift to a simple B_3-coloring. In this section we will show that the only such pretzel knots which admit a simple B_3-coloring are the left and right handed trefoils.

We remark that the knot group of the trefoil (recall the knot groups of any knot in S^3 and it's mirror are isomorphic) is isomorphic to the braid group B_3 on three strands, and this isomorphism sends meridians to half-twist, and gives us the desired braid coloring.

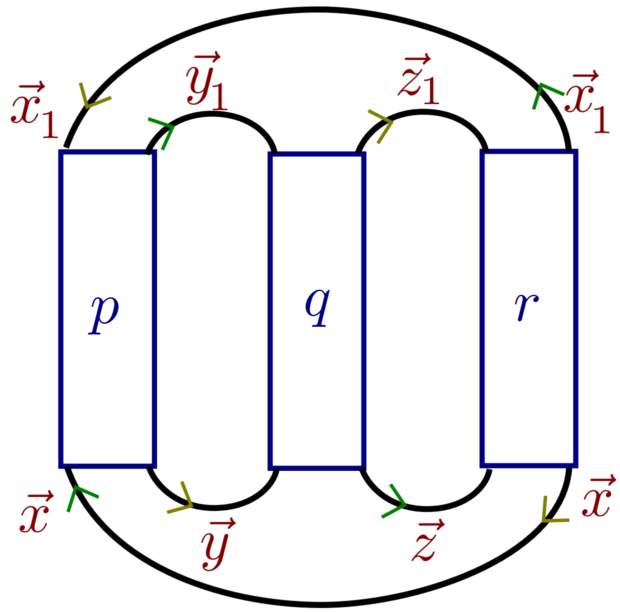

Figure 9.12: A three strand pretzel knot with p, q and r are all odd. The arrows (in different colors) indicate an orientation of the knot in each twist region.

Suppose we have a pretzel knot $P(p, q, r)$, with the strands in the bottom labelled by $\vec{x}, \vec{y}, \vec{z}$ and the three strands on top labelled by $\vec{x}_1, \vec{y}_1, \vec{z}_1$, as illustrated in Figure 9.12 , and let us suppose $\langle \vec{x}, \vec{y} \rangle = k$, $\langle \vec{y}, \vec{z} \rangle = l$ and $\langle \vec{z}, \vec{x} \rangle = m$.

By our discussion in the last section, from the leftmost twist region we get:

$$\pm \vec{x}_1 = (1 + k^2 a)\vec{y} + kb\vec{x} \text{ and } \pm \vec{y}_1 = (1 + k^2 a)\vec{x} + kc\vec{y}.$$

From the middle twist region we get:

$$\pm \vec{y}_1 = (1 + l^2 d)\vec{z} + le\vec{y} \text{ and } \pm \vec{z}_1 = (1 + l^2 d)\vec{y} + lf\vec{z}.$$

From the rightmost twist region we get:

$$\pm \vec{z}_1 = (1 + m^2 g)\vec{x} + mh\vec{z} \text{ and } \pm \vec{x}_1 = (1 + m^2 g)\vec{z} + mi\vec{x}.$$

In case any two of $\vec{x}$, $\vec{y}$ and $\vec{z}$ are linearly dependent, any braid coloring has to be trivial by Proposition 9.7.3. So we may assume that we are in the non trivial case of $\vec{x}$ and $\vec{y}$ are linearly independent in $H_1(S_{1,1}) \cong \mathbb{Z}^2$, and thus forms a basis for $\mathbb{Q}^2$ over the rationals, and thus we can express $\vec{z}$ as a rational linear combination of $\vec{x}$ and $\vec{y}$, $\vec{z} = \alpha\vec{x} + \beta\vec{y}$.

Note that $l = \langle \vec{y}, \vec{z} \rangle = \alpha\langle \vec{y}, \vec{x} \rangle = -\alpha k$ and $m = \langle \vec{z}, \vec{x} \rangle = \beta\langle \vec{y}, \vec{x} \rangle = -\beta k$.

Comparing coefficients in the expansion of $\vec{x}_1$, for some $\eta_1 \in \{\pm 1\}$ we obtain:

$$\eta_1(1 + k^2 a) = \beta(1 + m^2 g); \quad \eta_1 k b = \alpha(1 + m^2 g) + mi \tag{9.7}$$

Similarly, comparing coefficients in the expansion of $\vec{y}_1$, for some $\eta_2 \in \{\pm 1\}$ we get:

$$\eta_2(1 + k^2 a) = \alpha(1 + l^2 d); \quad \eta_2 k c = \beta(1 + l^2 d) + le \tag{9.8}$$

Finally, comparing coefficients in the expansion of $\vec{z}_1$, for some $\eta_3 \in \{\pm 1\}$ we have:

$$\eta_3 l f \alpha = (1 + m^2 g) + mh\alpha; \quad \eta_3(l f \beta + (1 + l^2 d)) = mh\beta$$

Equivalently, we obtain:

$$1 + m^2 g = \alpha(\eta_3 l f - mh); \quad 1 + l^2 d = \beta(\eta_3 mh - lf) = -\eta_3\beta(\eta_3 l f - mh) \tag{9.9}$$

From the equalities in the left of (9.7) and (9.8) we obtain:

$$|k|(1+k^2a) = |l|(1+l^2d) = |m|(1+m^2g) \tag{9.10}$$

Claim 9.8.1. *The integers k, l and m are pairwise coprime.*

Proof. Suppose not, say $\gcd(k,l) > 1$ (a similar argument works for other pairs). From the second equality in Equation (9.8) we get $\eta_2 k^2 c = -m(1+l^2d) + kle$. It follows that $\gcd(k,l)^2$ divides $m(1+l^2d)$, and hence $\gcd(k,l)^2$ divides m. From Equation (9.10), it follows that $\gcd(k,l)^2$ divides $k(1+k^2a)$ and $l(1+l^2d)$, and consequently it divides k and l. Thus, $\gcd(k,l)^2$ must divide $\gcd(k,l)$, a contradiction. □

Thus k and l are coprime integers both dividing $1+m^2g$, and we must have for some integer θ, $1+m^2g = kl\theta$. Note that by Equation (9.10), θ must be coprime to k, l and m. Suppose we set $\Delta = \eta_3 lf - mh$, then we note that $\Delta = -k^2\theta$. We see by using Equations (9.7), (9.8) and (9.9) that

$$\frac{\eta_1\alpha}{\eta_2\beta} = \frac{1+m^2g}{1+l^2d} = -\frac{\alpha\Delta}{\eta_3\beta\Delta} = -\frac{\alpha}{\eta_3\beta},$$

and hence we have $\eta_1\eta_3 = -\eta_2$. Now we see

$$kb + kc = \eta_1\alpha(1+m^2g) + \eta_1 mi + \eta_2\beta(1+l^2d) + \eta_2 le$$

Since we know that $\eta_1\eta_3 = -\eta_2$ we have

$$kb + kc = \eta_1(\alpha(1+m^2g) + mi - \eta_3\beta(1+l^2d) - \eta_3 le))$$

Now taking η_1 to the other side and substituting

$$\eta_1(kb+kc) = \alpha(1+m^2g) + mi - \eta_3\beta(1+l^2d) - \eta_3 le = (\alpha^2+\beta^2)\Delta + mi - \eta_3 le$$

$$= (\alpha^2+\beta^2)\Delta - \Delta + m(i-h) - \eta_3 l(e-f)$$

$$= (\alpha^2+\beta^2)\Delta - \Delta \pm m(1+m^2g) \pm l(1+l^2d)$$

$$= \Delta(\alpha^2+\beta^2-1 \pm \alpha m \pm \beta l) = -\theta(l^2+m^2-k^2 \pm \gamma klm)$$

Thus θ divides $kb+kc$ and $kb-kc = \pm k(1+k^2a)$. Consequently θ divides $2kb$ and $1+k^2a$, and since $\vec{x}_1$ is primitive, it must be the case that $\theta \in \{\pm 1, \pm 2\}$. Thus we have:

$$1+k^2a = |\theta lm|, \quad 1+l^2d = |\theta km|, \quad 1+m^2g = |\theta kl| \tag{9.11}$$

Note that one of a, d or g is 0 if and only if p, q or r equals ± 1, respectively. If that happens, then we claim that must have $P(p,q,r)$ is a (left or right handed) trefoil.

For instance, if $a = 0$ (the argument holds similarly for d or g being 0), then $1 = |\theta lm|$, which means $|\theta| = |l| = |m| = 1$, and so $|k| = 1+d = 1+g$. Since $a = 0$, one of b or c must be 0 as well. Thus by Equations (9.7) or (9.8), we see that one of e or i has to be 1, which in turn implies one of d or g has to be 0 or 1. Since we know $|k| = 1+d = 1+g$, $|k|$ must be either equal to 1 or 2. We now have the case $|p| = 1$, and since $d = g$, we must have $|q| = |r|$, which must lie in $\{1,3\}$, with $|k| \in \{1,2\}$, and $|l| = |m| = 1$. One can check[7] that we get non-trivial colorings only on the trefoils, $\pm P(1,1,1)$ and $\pm P(3,3,-1)$.

[7]This can be done either directly, by trying to find solution to the system of equations, or by using the Alexander polynomial criterion, or by using Theorem 9.3.1. For the last method, observe that $\pm P(1,3,-3)$ is isotopic to the $\pm 6_1$ knot, and $\pm P(1,3,3)$ is isotopic to the $\pm 7_4$ knot, and clearly $\pm P(1,-1,1)$ is the unknot.

Without loss of generality assume $|k| \leq |l| \leq m$. Let us now suppose all of a, d, g are at least 1. It cannot be the case that $|\theta| = 1$, since otherwise $1 + m^2 g$ will not strictly bigger than $|kl|$.

Thus $\theta = \pm 2$, and it follows that k, l, m and a, d, g are odd. If $g > 1$, we again see that we cannot have $1 + m^2 g = 2|kl|$, hence $g = 1$.

If $|m| = 1$, it implies $|k| = |l| = 1$. Thus by Equation (9.11) we have $a = d = g = 1$, and so $|p| = |q| = |r| = 3$. In this case 9 divides the determinant of $P(p, q, r)$, and consequently there cannot be a non-trivial simple B_3 coloring. If $|m| = 3,$ then $1 + m^2 g = 10 = 2|kl|$, which implies either $|k|$ or $|l|$ has to be at least 5, contradicting the maximality of $|m|$. Thus $|m| > 4$, and so $2|kl| = 1 + m^2 g = 1 + m^2 > 4|m|$, i.e $|m| \leq \frac{|kl|}{2}$. In particular this implies $|k| \geq 2$, and thus we also have the inequalities $|l| \leq \frac{|km|}{2}$ and $|k| \leq \frac{|lm|}{2}$. Thus $\vec{x}, \vec{y}$ and $\vec{z}$ are 1-proportional, and hence by [44, Theorem 1.1], there cannot be any relations between T_x, T_y and T_z. Hence, we have shown:

Theorem 9.8.2. *Consider the three strand pretzel knot $P(p, q, r)$ with p, q, r odd. Then a non-trivial tricoloring on $P(p, q, r)$ lifts if and only if*

$$\pm(p, q, r) \in \{(1, 1, 1), (3, 3, -1), (3, -1, 3), (-1, 3, 3)\}.$$

Recall $P(p, q, r)$ is tricolorable if and only if 3 divides $pq + qr + rp$, and so the above proposition gives infinitely many tricolrings of three strand odd pretzel knots which do not lift to braid colorings.

Remark 9.8.3. It follows from the discussion above that the only odd three stranded pretzel knots which is isotopic to the trefoil are the four in the statement of the proposition above.

We are yet to see an example of a knot with two distinct tricolorings, one of which lift to B_3 and the other do not. In the next section we will see such examples using similar techniques as our discussion above.

9.9 Three strand Pretzel knots II: one even

Let us consider the pretzel knot $P(p,q,r)$ with p even and q,r odd. Suppose we have a diagram of $P(p,q,r)$ with the strands in the bottom labelled by $\vec{x},\vec{y},\vec{z}$ and the three strands on top labelled by $\vec{x}_1,\vec{y}_1,\vec{z}_1$, as illustrated in Figure 9.13,

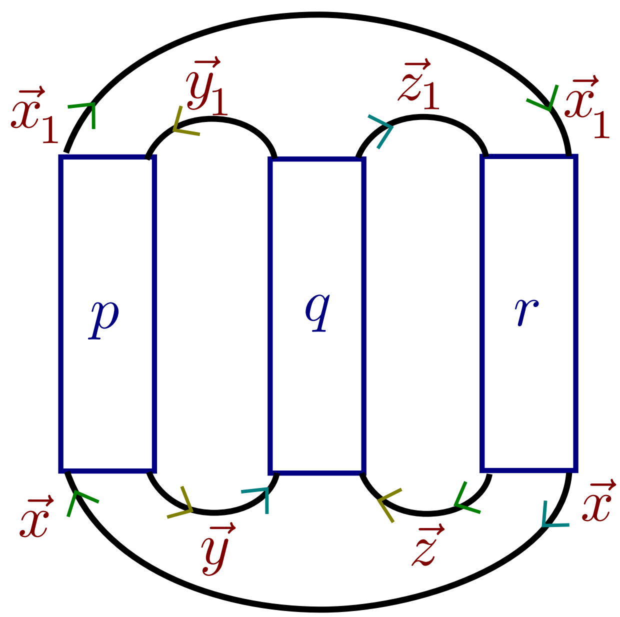

Figure 9.13: A three strand pretzel knot with p even and q and r are odd, together with labellings on strands.

and let us suppose $\langle\vec{x},\vec{y}\rangle = k$, $\langle\vec{y},\vec{z}\rangle = l$ and $\langle\vec{z},\vec{x}\rangle = m$.

In the leftmost twist region we get:

$$\pm\vec{x}_1 = (1+k^2a)\vec{x} + kb\vec{y} \text{ and } \pm\vec{y}_1 = kb\vec{x} + (1+k^2c)\vec{y}.$$

From the middle twist region we get:

$$\pm\vec{y}_1 = (1-l^2d)\vec{z} + le\vec{y} \text{ and } \pm\vec{z}_1 = (1-l^2d)\vec{y} + lf\vec{z}.$$

From the rightmost twist region we get:

$$\pm\vec{z}_1 = (1 - m^2 g)\vec{x} + mh\vec{z} \text{ and } \pm\vec{x}_1 = (1 - m^2 g)\vec{z} + mi\vec{x}.$$

In case any two of $\vec{x}$, $\vec{y}$ and $\vec{z}$ are linearly dependent, any braid coloring has to be trivial by Proposition 9.7.3 or constant on the leftmost twist region. So we may assume that we are in the non trivial case of $\vec{x}$ and $\vec{y}$ are linearly independent in $H_1(S_{1,1}) \cong \mathbb{Z}^2$, and thus forms a basis for $\mathbb{Q}^2$ over the rationals, and thus we can express $\vec{z}$ as a rational linear combination of $\vec{x}$ and $\vec{y}$, $\vec{z} = \alpha\vec{x} + \beta\vec{y}$.

Note that $l = \langle\vec{y}, \vec{z}\rangle = \alpha\langle\vec{y}, \vec{x}\rangle = -\alpha k$ and $m = \langle\vec{z}, \vec{x}\rangle = \beta\langle\vec{y}, \vec{x}\rangle = -\beta k$. Comparing coefficients in the expansion of $\vec{x}_1$, for some $\eta_1 \in \{\pm 1\}$ we obtain:

$$\eta_1(1 + k^2 a) = \alpha(1 - m^2 g) + mi; \quad \eta_1 kb = \beta(1 - m^2 g) \tag{9.12}$$

Similarly, comparing coefficients in the expansion of $\vec{y}_1$, for some $\eta_2 \in \{\pm 1\}$ we get:

$$\eta_2 kb = \alpha(1 - l^2 d); \quad \eta_2(1 + k^2 c) = \beta(1 - l^2 d) + le \tag{9.13}$$

Finally, comparing coefficients in the expansion of $\vec{z}_1$, for some $\eta_3 \in \{\pm 1\}$ we have:

$$\eta_3 lf\alpha = (1 - m^2 g) + mh\alpha; \quad \eta_3(lf\beta + (1 - l^2 d)) = mh\beta$$

Equivalently, we obtain:

$$1 - m^2 g = \alpha(\eta_3 lf - mh); \quad 1 - l^2 d = \beta(\eta_3 mh - lf) = -\eta_3\beta(\eta_3 lf - mh) \tag{9.14}$$

From the equalities in the right of Equation (9.12) and left of Equation (9.13) we obtain:

$$k^2 b = |l(1 - l^2 d)| = |m(1 - m^2 g)| \tag{9.15}$$

Claim 9.9.1. *The integers k, l and m are pairwise coprime.*

Proof. From Equation (9.15) we see that $\gcd(k,l)^2$ divides l and $\gcd(k,m)^2$ divides m. Now, we observe that from Equation (9.14) that $k(1 - m^2 g) = -l(\eta_3 l f - mh)$, and consequently $\gcd(l,m)^2$ divides k.

Suppose now $\gcd(l,m) > 1$, and suppose x is a prime power exactly dividing $\gcd(l,m)$, and so x^2 divides k. Without loss of generality, assume x exactly divides l, and consequently x divides $\gcd(k,l)$, and hence x^2 divides l, a contradiction. Thus $\gcd(l,m) = 1$.

From Equation (9.12), we see that $\alpha(1 - m^2 g)$ and $\beta(1 - m^2 g)$, and consequently k divides $l(1 - m^2 g)$ and $m(1 - m^2 g)$. Since $\gcd(l,m) = 1$, it follows that k divides $1 - m^2 g$, and thus $\gcd(k,m) = 1$. A similar argument shows $\gcd(k,l) = 1$. $\square$

Thus k^2 and l are coprime integers both dividing $1 - m^2 g$, thus we must have for some integer θ, $1 - m^2 g = k^2 l \theta$. Hence, from Equation (9.14), we see that $l(1 - l^2 d) = -\eta_3 m(1 - m^2 g) = -\eta_3 k^2 l m \theta$, and so $1 - l^2 d = -\eta_3 k^2 m \theta$. Similarly, from Equation (9.12), we see $k^2 b = -\eta_1 k^2 l m \theta$.

Note that by Equation (9.15), θ must be coprime to l and m. From Equations (9.12), (9.13) and (9.14) we see that:

$$\frac{\eta_1}{\eta_2} = \frac{\beta(1 - m^2 g)}{\alpha(1 - l^2 d)} = \frac{m(1 - m^2 g)}{l(1 - l^2 d)} = -\frac{1}{\eta_3}.$$

and hence $\eta_1 \eta_2 \eta_3 = -1$. From Equations (9.12) and (9.13) we get:

$$1 + k^2a + 1 + k^2c = \eta_1\alpha(1 - m^2g) + \eta_1 mi + \eta_2\beta(1 - l^2d) + \eta_2 le$$

$$= \eta_1\alpha(1 - m^2g) + \eta_1(mi - mh) + \eta_1 mh + \eta_2\beta(1 - l^2d) + \eta_2 l(e - f) + \eta_2 lf$$

$$= \eta_1\alpha(1-m^2g) - \eta_1 \operatorname{sgn}(r) m(1-m^2g) + \eta_2\beta(1-l^2d) + \eta_2 \operatorname{sgn}(q) l(1-l^2d) + \eta_2(lf - \eta_3 mh)$$

We note that each summand on the right hand side is an integer divisible by $k\theta$, by using the formulas $1-m^2g = k^2l\theta$, $1-l^2d = \eta_3k^2m\theta$, and $k(1-m^2g) = -l(\eta_3lf - mh)$.

Since $k\theta$ divides the sum and difference of $1+k^2a$ and $1+k^2c$, and $\vec{x}_1$ is primitive; it follows that $|k\theta|$ has to be either 0, 1 or 2.

Let us consider various cases:

1. $m(1 - m^2g) = 0$ (Note that by Equation (9.15), this contains the case $|k\theta| = 0$): Since $m(1 - m^2g) = 0$, we see that either $m = 0$, or $1 - m^2g = 0$, which implies $|m| = 1$. In either case, the coloring by Dehn twists on the right twist region starts and ends with the same colors, hence by Proposition 9.7.3, the same must be true for all the twist regions. This means $k = 0$, and $|m|, |l|$ can be either 0 or 1. The braid coloring is non-trivial if one of m and l is non-zero, which means the other has to be as well. We see that all non-trivial braid colorings we get in this case which are constant in the leftmost twist region, and non-constant in the middle and right twist regions (but the coloring matches at the ends of either twist regions). In particular this can happen only when q and r are odd multiples of 3.

2. $|k| = 1$ and $|\theta| = 1$: we see then $|1-m^2g| = |l|$ and $|1-l^2d| = |m|$. We consider the subcases:

   - $dg = 0$: Without loss of generality let us assume $d = 0$, which implies then $|m| = 1$, and hence $|l| = |1 - g|$. Since $|m| = 1$, and the strands are going in the same direction in the rightmost twist region, we know the pattern repeats every three half twists, we can assume $r \in \{\pm 1, \pm 3\}$. Consequently the possible values of g are 0 and 1. Hence $|l|$ has to be 1 or 0 (which we already dealt with). So $b = 1$, and hence $p = \pm 2$. let us assume $p = 2$, by mirroring the pretzel knot if necessary. Note that $P(2, -1, -1)$, is the trefoil, and has a tricoloring which lifts to a simple B_3 coloring. Hence, by adding multiples of 6 to the right and middle twist regions, we obtain simple B_3-colorings[8] on $\pm P(2, 6q_0 - 1, 6r_0 - 1)$, for any integers q_0, r_0; and we see that no other pretzel knot has a non-trivial simple B_3 coloring of this type.

- $dg \neq 0$: If $d \neq 1$, then we see $|m| = |1 - l^2 d| > |l|$, and similarly if $g \neq 1$, then $|l| = |1 - m^2 g| > |m|$. Since we cannot simultaneously have $|l| > |m|$ and $|m| > |l|$, it must be that one of d or g is 1. If $d = 1$, we must have $|l| > 1$ (otherwise $m = 0$, a case we saw earlier), so $|m| = |l^2 - 1| > |l|$. Similarly if $g = 1$, then either $|m| = 1$ (which implies $l = 0$, which we saw earlier), or $|l| = |1 - m^2 g| > |m|$. Hence, we do not come across any new braid colorings in this subcase.

3. $|k| = 1$ and $|\theta| = 2$: we see then $|1 - m^2 g| = 2|l|$ and $|1 - l^2 d| = 2|m|$. Thus, m, g, l and d have to be odd. If $g = 1$, then $1 - m^2 g = (1 - m)(1 + m)$ is divisible by 4, since m is odd. But this means l is even, since $|1 - m^2 g| = 2|l|$, which contradicts that l is odd. We get a similar contradiction if $d = 1$. If $g \neq 1$, then $2|l| = |1 - m^2 g| > m^2$, and so either $|l| > |m|$ or $|l| = |m| = 1$. Similarly, if $d \neq 1$, then either $|m| > |l|$, or $|l| = |m| = 1$. Thus, we have to have $|l| = |m| = 1$, since we cannot simultaneously have $|l| > |m|$ and $|m| > |l|$. In case $|l| = |m| = 1$, by Figure 9.9 (and the fact that the labellings

[8] Note that for these knots the determinant is ± 3, and so there is only one tricoloring (up to conjugation), which lifts to a unique (up to conjugation) simple B_3-coloring.

repeat after six half twists) the possible values of d and g are 0, 1 and 2, which leads to a contradiction, as we saw above. Thus, we do not come across any new braid colorings in this case.

4. $|k| = 2$ and $|\theta| = 1$: we see then $|1 - m^2 g| = 4|l|$ and $|1 - l^2 d| = 4|m|$. Hence d, g, l and m are odd. Without loss of generality, let us assume $|l| \leq |m|$. First suppose $|l| = 1$, we know by Remark 9.3.2 (since the braid coloring repeats) and Figure 9.9; the only possible values of d are 0, 1 and 2. Since d has to be odd, we have $d = 1$, and so $4|m| = |1 - l^2 d| = 0$, a contradiction. If $|l| \neq 1$, then $|l| \geq 3$, and so $|m| \geq |l| + 2$ since $|m|$ has to be an odd integer coprime to $|l|$. Consequently, $4|l| = |m^2 g - 1| \geq |m^2 - 1| \geq (|l| + 2)^2 - 1 > 4|l|$, a contradiction. Thus, we do not obtain any new braid colorings in this case.

By combining our discussion of the various cases (and using that $P(p, q, r)$ is isotopic to $P(q, r, p)$), we have proved:

Proposition 9.9.2. *Suppose we have a three strand pretzel knot $P(p, q, r)$ with one of p, q or r even. Then, any tricoloring on $P(p, q, r)$ lifts to a simple B_3-coloring if and only if the tricoloring is constant on the twist region with an even number of half twists. Moreover, there is unique (up to conjugation) lift to B_3, when the tricoloring does lift.*

We know [43, Section 8] that if p, q, r are all multiples of 3, then there are four inequivalent tricolorings, depending on how many twist regions have non-constant tricolorings. We illustrate this with the four colorings on the pretzel knot $P(3, 3, 6)$, see Figure 9.14.

By the Proposition above, we see that three of these tricolorings do not lift, while the fourth does. More generally, we have:

Proposition 9.9.3. *Consider the pretzel knot $P(p, q, r)$ with two of p, q, r odd multiples of 3, and the third a multiple of 6. Then exactly one among the four inequivalent tricolorings of $P(p, q, r)$ lift to a simple B_3-coloring.*

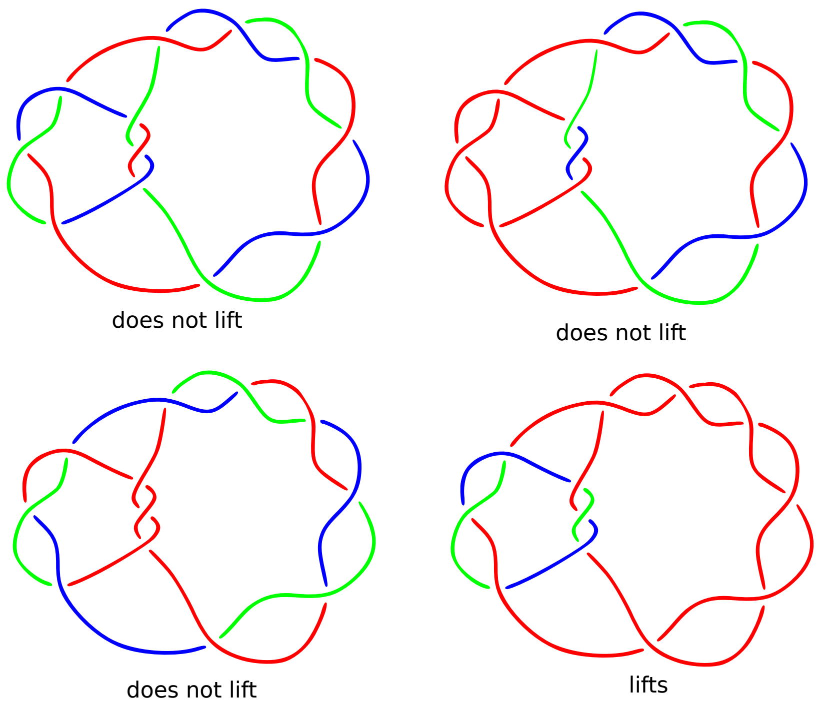

Figure 9.14: Four tricolorings of $P(3,3,6)$, of which only the last one lifts to a simple B_3-coloring.

Thus we see that the answer to Question 9.5.3 is "Yes", and in fact there are infinitely many such examples.

CHAPTER 10

LIFTING BRANCHED COVERINGS IN HIGHER DIMENSIONS

10.1 Lifting coverings of manifolds in dimension bigger than four

It turns out that liftings of coverings of manifolds of dimension bigger than four is essentially a question about algebra. This is because any finitely presented group is the fundamental group of a compact manifold of any dimension greater than or equal to four. For, given any finite presentation, we can attach one handles for each of the generators and one two handle for each of the relations, that winds around the one handles according to the relation. If dimension is bigger than four, we can make sure these one handles are disjoint, and hence we obtain a manifold. This stands in marked contrast with fundamental groups of two and three dimensional manifolds, where the dimension restricts the type of fundamental groups we can come across.

10.2 Lifting branched coverings over higher dimensional spheres

10.2.1 Colorings of Fox's Example 12

In Example 12 in [26], Ralph Fox proved a conjecture of Morton Curtis, by showing that there is a 2-knot (i.e. smoothly knotted 2-sphere in S^4) for which the knot group has torsion.

See Figure 10.1 for a motion picture description of the 2-knot. It has knot group

$$G = \langle x, a \mid xa^2 = ax, a^2x = xa \rangle.$$

Note that in G we have $a^2(xa^2) = a^2(ax)$, and so $a^2(xa) = a^3x$, thus $a^3 = 1$, whence

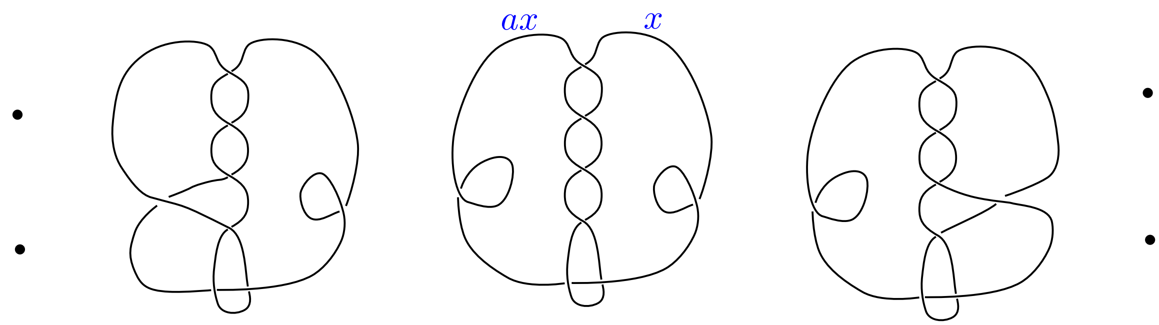

Figure 10.1: Fox's Example 12: A motion picture description of a 2-knot. Starting with the equatorial cross section (the middle picture), note that the result of attaching a band gives rise to two component unlinks, which can be then capped off.

there is torsion in G. Given ths relation, the two relations in the presentation of G become equivalent to $axa = x$. Thus we have

$$G = \langle x, a \mid a^3 = 1, axa = x \rangle.$$

Consider the tricoloring in Figure 10.2, of Fox's example 12 defined by (observe that all meridians are conjugate to x)

$$a \mapsto (123), \quad x \mapsto (23).$$

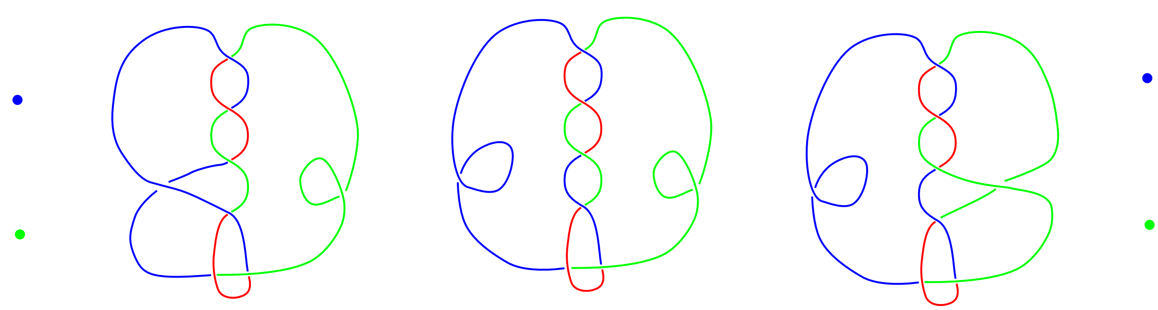

Figure 10.2: A tricoloring on Fox's Example 12.

Since a is torsion in G, we see that this tricoloring does not lift to a B_3-coloring, by Claim 6.1.4. Note that we do not need to add the constraint that the braid coloring be simple, meaning the branched cover associated to this coloring does not lift to any (even possibly non-locally flat topological) braided embedding.

10.3 Non-liftable branched covers in dimension bigger than 4

As there are other 2-knot groups with torsion [36, Section 15.4], and n-knot groups with $n \geq 3$ (Kervaire characterization) with torsion, we have lots of branched covers over S^n, with $n \geq 4$, which do not lift to braided embeddings. Once we find a non-liftable branched cover, we can get such families in all higher dimension, using Artin's spinning construction [6], as explained below.

Recall that given any codimension 2 embedded connected submanifold K in $\mathbb{R}^n$ (equivalently S^n), we can delete a standard ball (B^n, B^{n-2}) pair from $(\mathbb{R}^n, K)$ and we end up with a properly embedded submanifold K_1 with boundary in the right half plane $\mathbb{R}^n_+$. By spinning this half plane about an axis we get $\mathbb{R}^{n+1}$, and K_1 sweeps out a submanifold $S(K)$, called the spun knot of K. $S(K)$ is a knot (in the same category as the original knot K) with the same knot group as K.

Since the knot groups are isomorphic, there is a canonical bijection between colorings on these knots, and thus a branched coring on a knot lifts to a braided embedding if and only if the corresponding branched cover on the spun knot lifts to a braided embedding. Hence if we start with any non-liftable branched cover over a surface knot K in S^4 (for instance the one coming from the tricoloring in Fox's example 12 mentioned in the previous section), we see that for any $m \in \mathbb{N}$, there is a branched cover (coming from the corresponding coloring) on the spun knot $S_m(K)$ in S^{4+m} which does not lift to a braided embedding.

CHAPTER 11

CONCLUSION AND FUTURE DIRECTIONS

In this final chapter we will briefly discuss how the topics related to braided embeddings developed in this thesis can be interacts contact geomtery, and how these ideas can help us prove purely topological results such as non-existence of specific kinds of branched coverings. As an illustration of the latter, we will first go over how a closely related topic of braided immersions can be used to show non-existence of nice branched covers.

11.1 Braided immersions and non-existence of nice branched covers

In light of Theorem 2.7.1, a natural question is to construct branched coverings of a closed oriented manifold over the sphere with the simplest possible branch locus, or to figure out obstructions. Let us say a branched covering is nice if it is a map and branch locus is a submanifold with trivial normal bundle. The following result gives an obstruction to existence of nice branched coverings.

Proposition 11.1.1. *[21, Theorem 3.7] Any nice branched cover lifts to a codimension two braided immersion.*

By a braided immersion $f : M \to M \times D^2$ here we will mean an immersion so that the the projection $pr_1 \circ f$ is a branched covering [1] Etnyre and Furukawa [21, Section 3.2] used this result with characteristic class obstructions to existence of immersions to show that:

1. For $k > 1$, $\mathbb{C}P^k$ cannot be a nice branched cover over S^{2k},

[1]This is the natural analogue of braided embeddings in codimension two we have been studying, where we replaced embedding with an immersion.

2. For $k > 7$, $\mathbb{R}P^k$ cannot be a nice branched cover over S^k.

11.2 Branched coverings of S^5

We will show a similar non-existence of branched covering result, using contact geometry (specifically [21]), together with the following upgraded version of Theorem 5.1.1, which is work in progress.

Theorem 11.2.1. *(in progress) Any piecewise linear embedded closed oriented three manifold in $\mathbb{R}^5$ (or equivalently S^5) can be isotoped to be a closed braid, where the associated branch covering of the three manifold over S^3 is simple, and the branch locus a submanifold.*

Theorem 11.2.2. *Any smooth closed oriented five manifold which is a branched cover over S^5, branched over a smoothly (or piecewise linear locally flatly) embedded orientable three manifold must admit a contact structure.*

Proof. Any smooth embedding has a piecewise linear approximation, and thus it suffices we are in the case of the branch locus B being piecewise linear locally flatly embedded. By Theorem 11.2.1 above, we see that we can isotope B to be a closed braid with the associated branch locus being simple. We can look at the monodromy defined by this braided embedding; and we note that we can now construct a smooth braided embedding with this data. This is because we saw in Chapter 7 that for simple branch covers, the criterion for extending a braided embedding over the branch locus coincide in the smooth and piecewise linear categories. Now we can conclude that same smooth closed oriented five manifold a branched cover over S^5, branched over a smoothly braided embedded three manifold in S^5. By [21, Theorem 1.27], we can now isotope this branch locus to be transversly embedded, and hence we can pull back the standard contact structure on S^5 to obtain a contact structure in M. $\square$

It is known that smooth closed oriented five manifolds have two cobordism classes, one containing S^5 and the other containing the Wu manifold. The former class admits contact structures while the latter do not. It therefore follows that:

Proposition 11.2.3. *Any closed oriented five manifold cannot be a brached cover over the 5-sphere, branched over a smoothly (or p.l. locally flatly) embedded orientable three manifold.*

The above discussion strongly suggests we may be able to improve Theorem 5.1.1 in the smooth category, and further study is needed to understand where the smooth and piecewise linear categories behave similarly (or differently) for embeddings of manifolds. It is also interesting to investigate if there are obstructions to existence of a braided embedding if we know an embedding exists.

Appendices

APPENDIX A

MATHEMATICA CODE FOR BRAIDED TORUS

The following Mathematica code was used to generate the images of projections the braided torus used in Chapter 1.

```
ST = Graphics3D[{Black, Sphere[{0, 0, .5}, 0.1],
   Yellow, Opacity[.2],
   Polygon[{{1, 1, 0}, {2, 2, 0}, {2, -2, 0}, {1, -1, 0}}],
   Yellow, Opacity[.2],
   Polygon[{{1, 1, 0}, {2, 2, 0}, {-2, 2, 0}, {-1, 1, 0}}],
   Yellow, Opacity[.2],
   Polygon[{{-1, -1, 0}, {-2, -2, 0}, {2, -2, 0}, {1, -1, 0}}],
   Yellow, Opacity[.2],
   Polygon[{{-1, -1, 0}, {-2, -2, 0}, {-2, 2, 0}, {-1, 1, 0}}],
   Yellow, Opacity[.2],
   Polygon[{{1, 1, 1}, {2, 2, 1}, {2, -2, 1}, {1, -1, 1}}],
   Yellow, Opacity[.2],
   Polygon[{{1, 1, 1}, {2, 2, 1}, {-2, 2, 1}, {-1, 1, 1}}],
   Yellow, Opacity[.2],
   Polygon[{{-1, -1, 1}, {-2, -2, 1}, {2, -2, 1}, {1, -1, 1}}],
   Yellow, Opacity[.2],
   Polygon[{{-1, -1, 1}, {-2, -2, 1}, {-2, 2, 1}, {-1, 1, 1}}],
   Yellow, Opacity[.2],
   Polygon[{{2, 2, 0}, {2, 2, 1}, {2, -2, 1}, {2, -2, 0}}],
   Yellow, Opacity[.2],
   Polygon[{{2, 2, 0}, {2, 2, 1}, {-2, 2, 1}, {-2, 2, 0}}],
```

```
    Yellow, Opacity[.2],
    Polygon[{{-2, -2, 0}, {-2, -2, 1}, {2, -2, 1}, {2, -2, 0}}],
    Yellow, Opacity[.2],
    Polygon[{{-2, -2, 0}, {-2, -2, 1}, {-2, 2, 1}, {-2, 2, 0}}],
    Blue, Opacity[.3],
    Polygon[{{1, 1, 0}, {1, 1, 1}, {1, -1, 1}, {1, -1, 0}}],
    Blue, Opacity[.3],
    Polygon[{{1, 1, 0}, {1, 1, 1}, {-1, 1, 1}, {-1, 1, 0}}],
    Blue, Opacity[.3],
    Polygon[{{-1, -1, 0}, {-1, -1, 1}, {1, -1, 1}, {1, -1, 0}}],
    Blue, Opacity[.3],
    Polygon[{{-1, -1, 0}, {-1, -1, 1}, {-1, 1, 1}, {-1, 1, 0}}],
    }]

TST = Graphics3D[{Black, Sphere[{1.5, 0, .5}, 0.1],
    Yellow, Opacity[.2],
    Polygon[{{1, 1, 0}, {2, 2, 0}, {2, -2, 0}, {1, -1, 0}}],
    Yellow, Opacity[.2],
    Polygon[{{1, 1, 0}, {2, 2, 0}, {-2, 2, 0}, {-1, 1, 0}}],
    Yellow, Opacity[.2],
    Polygon[{{-1, -1, 0}, {-2, -2, 0}, {2, -2, 0}, {1, -1, 0}}],
    Yellow, Opacity[.2],
    Polygon[{{-1, -1, 0}, {-2, -2, 0}, {-2, 2, 0}, {-1, 1, 0}}],
    Yellow, Opacity[.2],
    Polygon[{{1, 1, 1}, {2, 2, 1}, {2, -2, 1}, {1, -1, 1}}],
    Yellow, Opacity[.2],
    Polygon[{{1, 1, 1}, {2, 2, 1}, {-2, 2, 1}, {-1, 1, 1}}],
```

```
    Yellow, Opacity[.2],
    Polygon[{{-1, -1, 1}, {-2, -2, 1}, {2, -2, 1}, {1, -1, 1}}],
    Yellow, Opacity[.2],
    Polygon[{{-1, -1, 1}, {-2, -2, 1}, {-2, 2, 1}, {-1, 1, 1}}],
    Yellow, Opacity[.2],
    Polygon[{{2, 2, 0}, {2, 2, 1}, {2, -2, 1}, {2, -2, 0}}],
    Yellow, Opacity[.2],
    Polygon[{{2, 2, 0}, {2, 2, 1}, {-2, 2, 1}, {-2, 2, 0}}],
    Yellow, Opacity[.2],
    Polygon[{{-2, -2, 0}, {-2, -2, 1}, {2, -2, 1}, {2, -2, 0}}],
    Yellow, Opacity[.2],
    Polygon[{{-2, -2, 0}, {-2, -2, 1}, {-2, 2, 1}, {-2, 2, 0}}],
    Yellow, Opacity[.5],
    Polygon[{{1, 1, 0}, {1, 1, 1}, {1, -1, 1}, {1, -1, 0}}],
    Blue, Opacity[.3],
    Polygon[{{1, 1, 0}, {1, 1, 1}, {-1, 1, 1}, {-1, 1, 0}}],
    Blue, Opacity[.3],
    Polygon[{{-1, -1, 0}, {-1, -1, 1}, {1, -1, 1}, {1, -1, 0}}],
    Blue, Opacity[.3],
    Polygon[{{-1, -1, 0}, {-1, -1, 1}, {-1, 1, 1}, {-1, 1, 0}}]
    }]

CM=Graphics3D[{Black, Sphere[{1.5, 0, .5}, 0.1],
  Green, Opacity[.5],
  Polygon[{{1, 1, 0}, {-1, 1, 0}, {-1, -1, 0}, {1, -1, 0}}],
  Green, Opacity[.5],
  Polygon[{{1, 1, 1}, {-1, 1, 1}, {-1, -1, 1}, {1, -1, 1}}],
```

```
  Blue, Opacity[.5],
  Polygon[{{1, 1, 0}, {1, 1, 1}, {-1, 1, 1}, {-1, 1, 0}}],
  Blue, Opacity[.5],
  Polygon[{{-1, -1, 0}, {-1, -1, 1}, {1, -1, 1}, {1, -1, 0}}],
  Blue, Opacity[.5],
  Polygon[{{-1, -1, 0}, {-1, -1, 1}, {-1, 1, 1}, {-1, 1, 0}}],
  Green, Opacity[.5], Polygon[{{1, 1, 0}, {1, 1, 1}, {1.9, 0, .5}}],
  Green, Opacity[.5],
  Polygon[{{1, -1, 0}, {1, -1, 1}, {1.9, 0, .5}}],
  Green, Opacity[.5], Polygon[{{1, 1, 0}, {1, -1, 0}, {1.9, 0, .5}}],
  Green, Opacity[.5], Polygon[{{1, 1, 1}, {1, -1, 1}, {1.9, 0, .5}}]
  }]

BT=Graphics3D[{Black, Sphere[{1.5, 0, .5}, 0.05],
  Yellow, Opacity[.2],
  Polygon[{{1, 1, 0}, {2, 2, 0}, {2, -2, 0}, {1, -1, 0}}],
  Yellow, Opacity[.2],
  Polygon[{{1, 1, 0}, {2, 2, 0}, {-2, 2, 0}, {-1, 1, 0}}],
  Yellow, Opacity[.2],
  Polygon[{{-1, -1, 0}, {-2, -2, 0}, {2, -2, 0}, {1, -1, 0}}],
  Yellow, Opacity[.2],
  Polygon[{{-1, -1, 0}, {-2, -2, 0}, {-2, 2, 0}, {-1, 1, 0}}],
  Yellow, Opacity[.2],
  Polygon[{{1, 1, 1}, {2, 2, 1}, {2, -2, 1}, {1, -1, 1}}],
  Yellow, Opacity[.2],
  Polygon[{{1, 1, 1}, {2, 2, 1}, {-2, 2, 1}, {-1, 1, 1}}],
  Yellow, Opacity[.2],
```

```
Polygon[{{-1, -1, 1}, {-2, -2, 1}, {2, -2, 1}, {1, -1, 1}}],
Yellow, Opacity[.2],
Polygon[{{-1, -1, 1}, {-2, -2, 1}, {-2, 2, 1}, {-1, 1, 1}}],
Yellow, Opacity[.2],
Polygon[{{2, 2, 0}, {2, 2, 1}, {2, -2, 1}, {2, -2, 0}}],
Yellow, Opacity[.2],
Polygon[{{2, 2, 0}, {2, 2, 1}, {-2, 2, 1}, {-2, 2, 0}}],
Yellow, Opacity[.2],
Polygon[{{-2, -2, 0}, {-2, -2, 1}, {2, -2, 1}, {2, -2, 0}}],
Yellow, Opacity[.2],
Polygon[{{-2, -2, 0}, {-2, -2, 1}, {-2, 2, 1}, {-2, 2, 0}}],
Yellow, Opacity[.7],
Polygon[{{1, 1, 0}, {1, 1, 1}, {1, -1, 1}, {1, -1, 0}}],
Green, Opacity[.3],
Polygon[{{1, 1, 0}, {-1, 1, 0}, {-1, -1, 0}, {1, -1, 0}}],
Green, Opacity[.3],
Polygon[{{1, 1, 1}, {-1, 1, 1}, {-1, -1, 1}, {1, -1, 1}}],
Green, Opacity[.3], Polygon[{{1, 1, 0}, {1, 1, 1}, {1.9, 0, .5}}],
Green, Opacity[.3],
Polygon[{{1, -1, 0}, {1, -1, 1}, {1.9, 0, .5}}],
Green, Opacity[.3], Polygon[{{1, 1, 0}, {1, -1, 0}, {1.9, 0, .5}}],
Green, Opacity[.3], Polygon[{{1, 1, 1}, {1, -1, 1}, {1.9, 0, .5}}]
}]
```

REFERENCES

[1] C. Adams. The Knot book. *American Mathematical Soc.*, 2004.

[2] J.W. Alexander. Note on Riemann spaces. *Bull. Amer. Math. Soc.* , 26:370-372, 1920.

[3] J.W. Alexander. A lemma on systems of knotted curves. *Proc. Nat. Acad. Sci. USA*, 9:93–95, 1923.

[4] E. Artin. Theorie der Zopfe. *Hamburg Abh.* 4:47-72, 1925.

[5] E. Artin. Theory of Braids. *Annals of Mathematics*, 48 (1): 101-126, 1947.

[6] E. Artin. Zur Isotopie zweidimensionalen Flachen in R_4. *Abh. Math. Sem.*, Univ. Hamburg, 4:174-177, 1926.

[7] I. Berstein and A. L. Edmonds. The degree and branch set of a branched covering. *Inventiones Mathematicae.*, 45, no. 3: 213-220, 1978.

[8] I. Berstein and A. L. Edmonds. On the classification of generic branched coverings of surfaces. *Illinois J. Math.*, 28, no. 1: 64-82, 1984.

[9] Bessis, D., Digne, F., and Michel, J. Springer theory in braid groups and the Birman-Ko-Lee monoid. *Pacific J. Math.* , 205, 287-309, 2000.

[10] J.S. Birman. Braids, Links, and Mapping Class Groups. *Annals of Mathematics Studies*, Princeton University Press, 1974.

[11] J. S. Birman and T. Brendle. Braids: A Survey. *Handbook of Knot Theory*, Chapter 2, Pages 19-103, 2005.

[12] J. S. Birman and H. M. Hilden. On the mapping class groups of closed surfaces as covering spaces. *Ann. of Math. Studies*, No. 66, 81-115, 1971.

[13] K. Borsuk. Drei Satze uber die n-dimensionale euklidische Sphare. *Fundamenta Mathematicae*, 20: 177190, 1933.

[14] A. Breiland, L. Oesper and L. Taalman. p-Coloring classes of torus knots. pdf link, 2004.

[15] N. Caplinger and S. Kolay. Simple colorings of pretzel knots. In preparation.

[16] J.S. Carter and S. Kamada. How to Fold a Manifold. *New Ideas in Low Dimensional Topology*, ed. Kauffman and Manturov, 2014.

[17] A. Clebsch. Zur Theorie der Riemann'schen Fläche. *Math. Ann.*, 6: 216-230, 1873.

[18] A. Constantin and B. Kolev. The theorem of Kerékjártó on periodic homeomorphisms of the disc and the sphere. *Enseign. Math (2) 40 No 3-4*, 193-204, 1994.

[19] R.H. Crowell and R.H. Fox Introduction to knot theory. *Graduate texts 57*, *Springer-Verlag*, New York, 1977.

[20] S. Eilenberg. Sur les transformations périodiques de la surfacede sphère, Fund. Math. 22 (1934), 2841.

[21] J. B. Etnyre and R. Furukawa. Braided Embeddings of Contact 3-manifolds in the standard Contact 5-sphere, *Journal of Topology*, 2017.

[22] A. Fathi, F. Laudenbach, and V. Poénaru, editors. Travaux de Thurston sur les surfaces. *Astérisque volume 66*, Société Mathématique de France, Paris, 1979. Séminaire Orsay, with an English summary.

[23] E. Fadell. and L.Neuwirth. Configuration Spaces. *Mathematica Scandinavica*, 10: 111118, 1962.

[24] R.H. Fox. and L.Neuwirth. The braid groups. *Mathematica Scandinavica*, 10: 119126, 1962.

[25] R.H. Fox. Covering spaces with singularities. *Algebraic Geometry and Topology: A Symposium in Honor of S. Lefschetz* pp. 243-257, 1957.

[26] R.H. Fox. A Quick Trip through Knot Theory. *Topology of 3-Manifolds and Related Topics, Prentice Hall*, 1962.

[27] R.H. Fox. A note on branched cyclic coverings of spheres. *Rev. math. Hisp.-Amer.*, 32: 158-162 , 1972.

[28] R. Gaebler. Alexander Polynomials of Two-Bridge Knots and Links. Undergraduate Thesis, 2004.

[29] F.A. Garside. The braid group and other groups *Quarterly Journal of Mathematics*, Oxford II. Ser., 20: 235254, 1969.

[30] J Gonzlez-Meneses. The nth root of a braid is unique up to conjugacy. *Algebraic & Geometric Topology* 3 (2), 1103-1118, 2003.

[31] J. Gonzalez-Meneses and B Wiest. On the structure of the centralizer of a braid. *Annales scientifiques de l'Ecole*, 2004.

[32] V.L. Hansen. Embedding finite covering spaces into trivial bundles. *Math. Ann.*, 36, 3:239-243, 1978.

[33] A. Hatcher. Algebraic Topology. *Cambridge University Press*, 2002.

[34] H.M. Hilden. Three-Fold Branched Coverings of S^3. *American Journal of Mathematics*, Vol. 98, No. 4, pp. 989-997, 1976.

[35] H.M. Hilden, M.T. Lozano and J. Montesinos. All three-manifolds are pull-backs of a branched covering S^3 to S^3, *Trans. Amer. Math. Soc.*, 279(2):729-735, 1983.

[36] J. Hillman. Four-manifolds, geometries and knots. Geometry and Topology Monographs, vol 5, 2002.

[37] M.W. Hirsch. On imbedding differentiable manifolds in euclidean space. *Ann. of Math.*, (2) , 73:566-571,v1961.

[38] U. Hirsch. Uber offene Abbildungen auf die -sphere. *Math Z.*, 140: 203-230, 1974.

[39] A. Hurwitz. Ueber Riemann'sche Flächen mit gegebenen Verzweigungspunkten. *Math. Ann.*, 39: 1-60, 1891.

[40] Atsushi Ishida. The structure of subgroup of mapping class groups *Proc. Japan Acad. Ser. A Math. Sci.*, 72(10):240241, 1996.

[41] Nikolai V Ivanov, John D McCarthy. On injective homomorphisms between Teichmuller modular groups. I *Invent. Math.*, 135:425486, 1999.

[42] V.F.R. Jones. Hecke algebra representation of braid groups and link polynomials. *Annals of Mathematics*, 126:335-388, 1987.

[43] S. Kamada. A characterization of groups of closed orientable surfaces 4-space. *Topology*, 33:113–122, 1994.

[44] S. Kamada. Braid and Knot Theory in Dimension Four. *American Mathematical Society*, 2002.

[45] S. Kamada, S. Satoh and M. Takabayashi. The Braid Index Is Not Additive for the Connected Sum of 2-Knots, *Transactions of the American Mathematical Society* Vol. 358, No. 12 (Dec., 2006), pp. 5425-5439.

[46] B. de Kerékjártó. Uber die periodischen Transformationen der Kreisscheibe undder Kugelflache. *Math. Annalen*, 80:3-7, 1919.

[47] S. Kolay. Piecewise Linear Genaralized Alexander's Theorem in dimension at most 5. `arXiv:1703.08588` [math.GT], 2017.

[48] S. Kolay. Subgroups of the mapping class group of the torus generated by powers of Dehn twists. `arXiv:1909.07360` [math.GT], 2019.

[49] S. Kolay. Lifting Branched Covers to Braided Embeddings. `Pre-print`.

[50] S. Kolay. Knot Colorings: Coloring and Goeritz matrices. In preparation.

[51] K. Kordek, D. Margalit. Homomorphisms of commutator subgroups of braid groups. `arXiv:1910.06941` [math.GT], 2019.

[52] R. C. Kirby. The topology of 4-manifolds, volume 1374 of Lecture Notes in Mathematics. *Springer-Verlag*, Berlin, 1989.

[53] T. Kitano, M. Suzuki. A partial order in the knot table. *Experimental Math*, 2005.

[54] T. Kitano, M. Suzuki and M. Wada. Twisted Alexander polynomials and surjectivity of a group homomorphism *Alg. Geo. Top.*, 2005.

[55] W. B. R. Lickorish. A finite set of generators for the homeotopy group of a 2-manifold. *Proc. Cambridge Philos. Soc.* , 60:769778, 1964.

[56] W. B. R. Lickorish An Introduction to Knot Theory. *Springer*, 1997.

[57] A. Loi and R. Piergallini. Compact Stein surfaces with boundary as branched covers of B^4. *Invent. Math.*, February 2001, Volume 143, Issue 2, pp 325348.

[58] S.A. Melikhov. Transverse fundamental group and projected embeddings. *Proc. Steklov Inst. Math.*, 290, 155165 (2015).

[59] A. Markov. Uber die freie Aquivqlenz geschlossener Zopfe. *Recueil Math*, 1935.

[60] J.M. Montesinos. A representation of closed orientable 3-manifolds as 3-fold branched coverings of S^3. *Bulletin of the American Mathematical Society*, 80 no. 5: 845-846,1974.

[61] J.R. Munkres. Topology; a First Course. *Prentice-Hall*, 1974.

[62] P. Petersen. Fatness of covers. *J. Reine Angew. Math.* 403:154165, 1990.

[63] R. Piergallini. Four-manifolds as 4-fold branched covers of S^4. *Topology*, 34, no. 3: 497-508, 1995.

[64] D. Rolfsen. Knots and Links. *Mathematics Lecture Series 7*, Publish or Perish, 1976.

[65] C.P. Rourke and B.J. Sanderson. Introduction to Piecewise Linear Topology. *Springer-Verlag*, 1972.

[66] L. Rudolph. Braided surfaces and Seifert ribbons for closed braids. *Comment. Math. Helv.*, 58(1):137, 1983.

[67] A. Skopenkov. Embedding and knotting of manifolds in Euclidean spaces., *Surveys in Contemporary Mathematics* (London Mathematical Society Lecture Note Series, pp. 248-342). Cambridge University Press, 2007.

[68] A. Fathi, F. Laudenbach, and V. Poénaru, editors. Travaux de Thurston sur les surfaces. *Astérisque volume 66*, Société Mathéematique de France, Paris, 1979. Séminaire Orsay, with an English summary.

[69] W. P. Thurston, H. Winkelnkemper. On the existence of contact forms. *Proc. Amer. Math. Soc.*, 52 (1975), 345347.

[70] R. F. Williams. The braid index of generalized cables. *Pacific J. Math.* , Volume 155, Number 2 (1992), 369-375.

[71] E. C. Zeeman, Unknotting spheres. *Ann. of Math.* (2) 72, 350-360, 1960.